CONFIDENTIAL

NACA

RESEARCH MEMORANDUM

THE EFFECT OF END PLATES, END STRUTS, AND DEPTH OF SUBMERGENCE ON THE CHARACTERISTICS OF A HYDROFOIL

By Kenneth L. Wadlin, Rudolph E. Fontana,
and Charles L. Shuford, Jr.

Langley Aeronautical Laboratory
Langley Field, Va.

NATIONAL ADVISORY COMMITTEE FOR AERONAUTICS

WASHINGTON
April 12, 1951

CONFIDENTIAL

NACA RM L51B13

NATIONAL ADVISORY COMMITTEE FOR AERONAUTICS

RESEARCH MEMORANDUM

THE EFFECT OF END PLATES, END STRUTS, AND DEPTH OF SUBMERGENCE ON THE CHARACTERISTICS OF A HYDROFOIL

By Kenneth L. Wadlin, Rudolph E. Fontana, and Charles L. Shuford, Jr.

SUMMARY

An investigation was made in Langley tank no. 2 of the effect of end plates and end-mounted struts on the lift-drag ratios of a hydrofoil. The hydrofoil had an aspect ratio of 4. The tests were made at various depths below the water surface at speeds from 15 to 35 feet per second corresponding to Reynolds numbers from 0.873×10^6 to 2.04×10^6. These speeds were all above the limiting speed of wave propagation (13.9 fps) for the 6-foot water depth used and below the range at which cavitation occurs.

Only small improvements were found in the maximum lift-drag ratios by the addition of end plates and these improvements occurred only at low lift coefficients with small end plates. As the lift coefficient was increased above the value for maximum lift-drag ratio the optimum end-plate size increased; however, the absolute value of lift-drag ratio decreased. The detrimental effect of the drag of the additional strut for a hydrofoil using end struts in contrast to a single central strut was greater than any beneficial effects due to the end-plate effect of the end struts. The ratio of the effective aspect ratio to the geometric aspect ratio varied with end-plate size approximately as predicted by aerodynamic theory (Von Kármán and Burgers). Although the hydrodynamic data obtained with the end plates were slightly higher than the theoretical curve, the agreement was good when the accuracy to which such data could be obtained is considered. An approximate theoretical solution of the effect of depth on the lift of a hydrofoil was developed. The agreement of the experimental results with the results given by this solution was good.

INTRODUCTION

The use of end plates as a means of increasing the effective aspect ratio of airfoils and thereby increasing lift-drag ratios has been investigated at various times. In general, these investigations have not led to the use of end plates on airplane wings. End plates have been used on tail surfaces where the necessity for having two surfaces at right angles to each other enables the end plates to serve two functions. Because hydrofoils normally will be supported by one or more struts extending through the water surface, it is possible to use the struts for a dual purpose by placing them at the ends of the hydrofoil where they also serve as end plates. This possibility, together with other considerations, such as structural and stability considerations, that might result in the desirability of using end plates on hydrofoils has led to the present investigation of the effect of end plates and end struts on the lift and drag characteristics of a hydrofoil.

Another problem considered in the present investigation is that of determining the effect of depth of submergence below the water surface on the characteristics of a hydrofoil. There is a great amount of aerodynamic data available for use in hydrofoil problems but, in general, these data are for a fluid without boundaries, whereas hydrofoils may operate close to the boundary formed by the water surface. In order to extend the usefulness of these existing data, an approximate theoretical solution for the effect of depth of submergence on the lift of a hydrofoil is developed.

Experimental data obtained with a hydrofoil of aspect ratio 4 at various depths of submersion at speeds from 15 to 35 feet per second (Reynolds numbers from 0.873×10^6 to 2.04×10^6) and at angles of attack from -3.5° to 4.0°, with and without end plates and end struts, are presented. The investigation was conducted at speeds above the limiting speed of wave propagation (13.9 fps) for the 6-foot water depth of Langley tank no. 2. These experimental data are correlated with existing theory giving the effect of end plates on effective aspect ratio and with the developed theory giving the effect of depth of submergence on lift.

The method for obtaining a theoretical solution of the effect of depth on lift was suggested by Mr. Thomas A. Toll of the Langley Stability Research Division.

SYMBOLS

L	lift, pounds
D	drag, pounds

[redacted]

C_L	lift coefficient (L/qS)
C_D	drag coefficient (D/qS)
C_{D_i}	induced drag coefficient
c_{d_o}	section drag coefficient
S	area of hydrofoil, square feet
q	free-stream dynamic pressure, pounds per square foot $\left(\frac{1}{2}\rho V^2\right)$
V	velocity, feet per second
ρ	mass density, slugs per cubic foot
c_l	section lift coefficient at finite depth of hydrofoil submersion
c_{l_o}	section lift coefficient at infinite depth of hydrofoil submersion
α	angle of attack, degrees
C_{L_α}	finite lift-curve slope at finite depth of hydrofoil submersion
c_{l_α}	section lift-curve slope at finite depth of hydrofoil submergence
$c_{l_{\alpha_o}}$	section lift-curve slope at infinite depth of hydrofoil submersion
L/D	lift-drag ratio
$(L/D)_{max}$	maximum lift-drag ratio
$C_{L_{(L/D)_{max}}}$	lift coefficient for maximum lift-drag ratio
Γ	circulation strength of vortex
w_1	downwash at three-quarter-chord point due to hydrofoil vortex, feet per second
w_2	downwash at three-quarter-chord point due to hydrofoil vortex image, feet per second

[redacted]

h	depth of hydrofoil submersion below free water surface, feet
c	chord of hydrofoil, feet
b	span of hydrofoil, feet
h'	area of one end plate, excluding hydrofoil section area, divided by chord of hydrofoil
R	geometric aspect ratio (b^2/S)
σ	aspect-ratio correction factor for rectangular wings
R_e	effective aspect ratio
E_e	effective edge-velocity correction factor for lift

DESCRIPTION OF MODEL

Various end plates and end-mounted struts were attached to an 8-inch-chord hydrofoil having an aspect ratio of 4. Photographs of all the configurations tested are shown in figure 1. The hydrofoil, struts, and end plates were made of stainless steel. They were polished to a smooth finish consistent with current wind-tunnel practice.

The sections for the hydrofoil and end struts were the same as those used in reference 1. The hydrofoil had an NACA 64_1A412 section which differs from the NACA 64_1-412 section only by elimination of the trailing-edge cusp; the section characteristics of these two are essentially the same (see reference 2). The struts had an NACA 66_1-012 section. Figure 2 gives the ordinates for the hydrofoil and strut sections as computed from references 2 and 3.

The five end plates tested consisted of $\frac{1}{4}$-inch-thick flat plates with elliptical edges. Three of the end plates were designed to cover various amounts of the two-dimensional pressure field about the hydrofoil computed at an angle of attack of 0°, which was expected to be close to the angle for maximum lift-drag ratio. The coverage was such that the static pressure at the boundaries of the end plates would deviate approximately 20, 10, and 5 percent from the free-stream static pressure. The details of these end plates are given in figure 3. The pressure fields were computed by the method used in reference 4 and are shown by the dashed lines in figure 3.

[redacted]

The other end plates were rectangular and the details of these end plates are given in figure 4.

APPARATUS AND PROCEDURE

The tests were made by using the main carriage of Langley tank no. 2. A sting support was used to reduce interference effects. Figure 5 shows a view of the test setup with the hydrofoil, supporting sting, and balance attached to the support structure on the carriage.

The details of the supporting-sting arrangement are shown in figure 6. The sting was supported by an 8-inch-chord strut having an NACA 66_1-012 section. The spacing between the strut and the hydrofoil was such (1.5 chords) that the influence of the strut on the flow at the hydrofoil should be negligible (reference 5).

The hydrofoil was moved vertically by means of a motor-driven jacking screw which moved the balance and hydrofoil as a unit. Change in angle of attack was obtained at the plate attaching the strut to the balance.

Measurements of lift and drag were made by means of electrical strain gages. The force measurements were made at constant speed, angle of attack, and depth of submersion. The depth of submersion is defined as the distance from the water surface to the point of the hydrofoil nearest the water surface. A range of submersions from 0.5 chord (4 in.) to 4 chords (32 in.), of speeds from 15 to 35 feet per second, and of angles of attack from -3.5° to 4.0° was covered. Submersions where the end plates protruded through the water surface were omitted. The maximum angle of attack was limited to 4.0° since the maximum lift-drag ratios were expected to occur below this angle of attack. The change in angle of attack due to structural deflection caused by the lift and drag forces on the hydrofoil was obtained during the calibration of the balance and the test data were adjusted accordingly.

The supporting sting and strut were run alone at the same range of speeds, depths, and angles as when the hydrofoil was installed. For these tests the end of the sting was fitted with a faired cap. The tares thus obtained were deducted from the test data to give the net forces.

The net forces were converted to the usual aerodynamic lift and drag coefficients by using a measured value of ρ of 1.966 slugs per cubic foot corresponding to a water temperature during the tests of 70° F. All coefficients were based on the area of the hydrofoil, 1.78 square feet.

[redacted]

The correction for the ground effect of the bottom of the tank determined by the method described in reference 6 was only 0.7 percent of the induced drag at the maximum depth of submersion (4 chords) and 0.1 percent at the minimum depth (0.5 chord). The correction to the angle of attack was even less. The corrections therefore were considered negligible.

RESULTS AND DISCUSSION

The results of the tests are presented in figures 7 to 13. In these figures lift and drag are plotted against angle of attack with speed and depth as the parameters. The fairings appearing in these figures were made by using cross fairings against speed and depth so the data are faired as a whole and not for individual speeds or depths. This same method of fairing was carried out in all subsequent figures. The data, converted to coefficients, are presented in figures 14 to 20 in the usual form for aerodynamic data.

The present tests were made principally to investigate the effect of end plates, end struts, and depth of submergence on hydrofoil characteristics. The scope of the investigation was not sufficient to evaluate completely the effects of Froude number, Reynolds number, cavitation, and the possible effects of limiting speed of wave propagation in the towing tank. Care, therefore, must be taken in making specific applications of the results.

Lift coefficient did not vary with speed but the drag coefficient decreased with increasing speed. The variation of drag coefficient with speed was, however, very small at the higher speeds. The slopes of the lift curves increased with increasing depth, but at depths greater than 2 chords the increase in slope was very small.

Lift-Drag Ratio

The variation of lift-drag ratio with lift coefficient for the hydrofoil with and without end plates is shown in figure 21 for a depth of 4 chords and a speed of 35 feet per second. It can be seen that the smallest end plate gave the highest maximum lift-drag ratio. Further increases in the size of the end plate reduced the maximum lift-drag ratio and increased the lift coefficient at which it occurred. Only a small increase in lift-drag ratio can be obtained in the region of maximum lift-drag ratio and this increase can only be obtained with small end plates. However, at high lift coefficients even the larger end plates improve the lift-drag ratio, though at lower absolute values than

at the lower lift coefficients. As the lift coefficient is increased above the value for maximum lift-drag ratio the optimum end-plate size increases.

Figure 22 shows the variation with depth and speed of the maximum lift-drag ratios and the lift coefficients at which they occur. Without end plates the variation with depth was negligible at depths greater than 1.5 chords. As the size of the end plate was increased the effect of depth persisted to greater depths. As the speed was increased the maximum lift-drag ratio increased and the lift coefficient at which it occurred decreased; these effects of speed decreased with increasing speed. The effect of speed on the lift coefficient for maximum lift-drag ratio varied with end-plate size. With no end plates the variation with speed appeared to be negligible but it increased with end-plate size.

The variation of lift-drag ratio with lift coefficient for the hydrofoil with the end struts is shown in figure 23. These curves are for several depths and a speed of 35 feet per second. As the depth is increased the maximum lift-drag ratio decreased and the lift coefficient at which it occurred increased. Apparently the strut drag impaired the lift-drag ratio to a greater extent than the end-plate effect improved it.

The effect of end-plate size on the maximum lift-drag ratio and the lift coefficient at which it occurs are shown in figure 24 for the range of depths and speeds covered. The parameter for end-plate size is h'/b where h' is the area of one end plate, excluding the hydrofoil section area, divided by the chord of the hydrofoil and b is the span of the hydrofoil. The increase in maximum lift-drag ratio by the addition of small end plates is again shown. This increase, however, disappears as the speed is decreased and indicates that the reduction in drag coefficient due to the addition of end plates is of the same order as the reduction in profile drag coefficient obtained by increasing speed over this range.

Since the end struts provide for support of the hydrofoil and the end plates do not, a comparison of t'e lift-drag ratios does not give an adequate measure of their relative merits for a practical application. Figure 25 shows the maximum lift-drag ratio that would be obtained if the drag of a single strut (from reference 1) were added to the hydrofoil alone, or to the hydrofoil-end-plate arrangement that gave the highest lift-drag ratio. The curve for the end-strut configuration is shown for comparison. Both the hydrofoil and hydrofoil-end-plate arrangement with a single strut had higher lift-drag ratios over the range of depths covered than the hydrofoil-end-strut arrangement.

Effective Aspect Ratio

Though the maximum lift-drag ratio was not improved to any great extent by the addition of end plates, the effect of the end plates in increasing the effective aspect ratio is of fundamental interest. The effective aspect ratio was obtained both from the slopes of the lift curves and from the slopes of plots of drag coefficient against lift coefficient squared. By using the lift-curve slopes the effective aspect ratio was obtained by using figure 26. This figure was calculated from the formula

$$C_{L_\alpha} = \frac{Rc_{l_\alpha}}{RE_e + \frac{57.3c_{l_\alpha}}{\pi}}$$

(see reference 7) where C_{L_α} is the slope of the lift curve as determined in the tests, R is the aspect ratio, c_{l_α} is the section lift-curve slope, and E_e is an effective edge-velocity correction. Numerical values of E_e are given in reference 8.

The section lift-curve slope for the hydrofoil of aspect ratio 4 was obtained from the upper plot by using the finite lift-curve slope obtained in the tests. Since the finite slopes changed with depth, this change was reflected in the section slopes. For corresponding depths of submersion the finite slopes obtained at an aspect ratio of 10 (reference 1) gave the same section slopes. In view of the agreement in section lift-curve slopes for the two hydrofoils at corresponding depths, it may then be assumed that the depth of submersion affects only the section lift-curve slope and not the relation between finite lift-curve slope and aspect ratio. The lower plot is based on this assumption and was used to determine effective aspect ratios at the various depths of the configurations incorporating end plates and end struts. By using the drag data the slopes of the plot of the drag coefficient against the lift coefficient squared were considered to be $1/\pi R_e(1 + \sigma)$ where R_e is the effective aspect ratio and σ is a correction, derived by Glauert for rectangular wings, dependent on aspect ratio.

The effective aspect ratios obtained from both lift and drag data are shown in the upper plot of figure 27. The faired lines drawn in this figure are based primarily on the lift data because these data gave more consistent results than the drag data. The effective aspect ratio increased with increasing end-plate size and depth of submersion. The ratio of effective aspect ratio to the geometric aspect ratio R_e/R

was obtained from this plot and are presented in the lower plot of the same figure. The ratio R_e/R increased with end-plate size h'/b in much the same manner as predicted by Von Kármán and Burgers in reference 9 though it was higher in the tank tests, the deviation being larger at the larger depths. Considering the accuracy to which such data can be obtained the agreement is good. The tank data for both the curved and rectangular end plates fell together, indicating no appreciable effect of end-plate shape for the shapes tested.

Also included in this figure is the variation of the ratio R_e/R with h'/b where h' is the immersed depth of the end struts. The end struts were not as effective as the end plates in increasing the effective aspect ratio. This reduction in effectiveness could be expected since the effectiveness of the end plates was reduced as they approached the water surface and the end struts actually intersect this surface. In the case of the end struts the ratio R_e/R was lower than that predicted in reference 9.

Wind-tunnel data for end plates A, B, C, and D have been obtained in the Langley stability tunnel. The ratio R_e/R obtained from both the wind-tunnel lift and drag data for end plates A, B, C, and D is also presented in figure 27. The agreement between the tank and wind-tunnel data is good.

APPLICATION OF AERODYNAMIC DATA TO HYDROFOILS

For comparison with airfoil data, the drag coefficients for the hydrofoil alone were corrected to infinite aspect ratio by the usual equation

$$C_{D_i} = \frac{C_L^2}{\pi R}(1 + \sigma)$$

where R is the aspect ratio and σ is a correction for rectangular wings dependent on aspect ratio. For an aspect ratio of 4 the value of σ is 0.032. The slope of the lift curve was corrected to infinite aspect ratio by using the method previously discussed.

Figure 28 is a plot of the data at a speed of 35 feet per second (Reynolds number of 2.04×10^6) after converting to infinite aspect ratio by this method. The aerodynamic data at a Reynolds number of 2.0×10^6 for the NACA 64_1-412 section (see reference 10) are also included in this figure. The slope of the lift curve increased with

[redacted]

increasing depth. At depths of 2 chords and greater the agreement with aerodynamic data is good. The drag coefficients fall slightly above the aerodynamic data for the smooth condition. The variation due to depth was very small compared to the possible effects due to roughness. During the tests the surface of the model was slightly pitted by the salt water in the tank and was possibly rougher than in the aerodynamic tests.

There is a mass of aerodynamic data available on airfoils suitable for use as hydrofoils. The present tests together with those of reference 1 show that at immersion depths of 2 chords and greater these aerodynamic data are directly applicable to hydrofoils within the limitations imposed by Froude number, Reynolds number, cavitation effects, and the effects of the low limiting speed of wave propagation for the towing tank. At lesser depths the method of determining the induced drag is apparently not strictly correct as evidenced by the large deviation at the depth of 0.5 chord (see fig. 28) from aerodynamic data. However, at the depths considered the drag data are applicable with an accuracy of the same order as the allowance that must be made for practical roughness of the hydrofoil surface. This error in determining the induced drag may be considerably larger at depths less than 0.5 chord.

At shallow depths it is, however, necessary to alter the aerodynamic lift coefficients to take into account the reduction caused by the proximity of the free water surface. One method is to establish the ratio of the lift-curve slopes at shallow depths to the slope at great depths.

Estimation of the Effect of Depth on Lift

A complete theoretical solution of the lift of a hydrofoil at various depths of submersion does not seem to have been obtained, although several approaches to the problem have been made (as examples, see references 11 and 12). The physical conditions that need to be satisfied in such a solution are rather complex; however, the phenomena can be at least partially understood by considering the similarity to the case of a wing placed near the jet boundary in an open-throat wind tunnel. The boundary condition to be satisfied is that of constant pressure along the boundary streamlines. If distortion of the boundary can be neglected (an assumption which on the basis of experimental observation seems permissible, except possibly at very shallow depths), this boundary condition is essentially equivalent to that of constant longitudinal velocity and can be satisfied by introducing a system of vortices above the surface which have the same distribution and direction of rotation as those which represent the loading on the hydrofoil. As a first approximation to the two-dimensional problem, a single-image vortex can represent the load on the hydrofoil if located at a height above the fluid surface equal to the depth of the center of pressure of the hydrofoil.

[redacted]

The presence of the image vortex does not change the incidence of the flow relative to the hydrofoil chord line in the vicinity of the center of pressure, but it does tend to curve the streamlines relative to the hydrofoil chord line and to introduce a forward component of fluid velocity at the hydrofoil. The curvature effect is equivalent to introducing camber of the hydrofoil in such a manner as to produce a negative lift increment. The significance of the forward component of fluid velocity due to the image vortex is not clear, although a first thought might be that this condition amounts to a reduction in dynamic pressure which should cause a reduction in lift in addition to the loss due to streamline curvature. This interpretation is, in fact, the proper one in the case of the biplane problem, as pointed out in reference 13. For the case of the hydrofoil approaching the planing condition, it is evident that, although the forward component of fluid velocity exists, this forward component results directly from the action of the lower hydrofoil surface, which tends to displace the fluid forward and downward. The reaction due to this displacement or acceleration of the fluid is responsible for the lift carried by the hydrofoil in the planing condition, and, as pointed out in reference 12, amounts to about one-half the lift carried by the hydrofoil at the same angle of attack but at infinite depth.

Since the arrangement of the streamlines of the flow below the planing hydrofoil probably is not greatly different from the arrangement of streamlines below the hydrofoil when at infinite depth, it would seem that a reasonably close approximation to the effect of depth could be obtained by simply evaluating the effect of streamline curvature. To accomplish this, a technique frequently used in approximate solutions of aerodynamic problems may be employed (see reference 14). This involves determination of the circulation Γ required to produce a downwash velocity $w_1 + w_2$ at the three-quarter-chord location, which, when combined with the free-stream velocity V produces a flow tangent to the mean camber line of the hydrofoil. Thus, if geometric camber is neglected, the hydrofoil angle of attack α is equal to the sum of the angles at the three-quarter-chord point induced by the hydrofoil vortex (assumed to be located at the quarter-chord point of the hydrofoil) and its image located at a distance $2h$ directly above the hydrofoil (see following sketch):

[redacted]

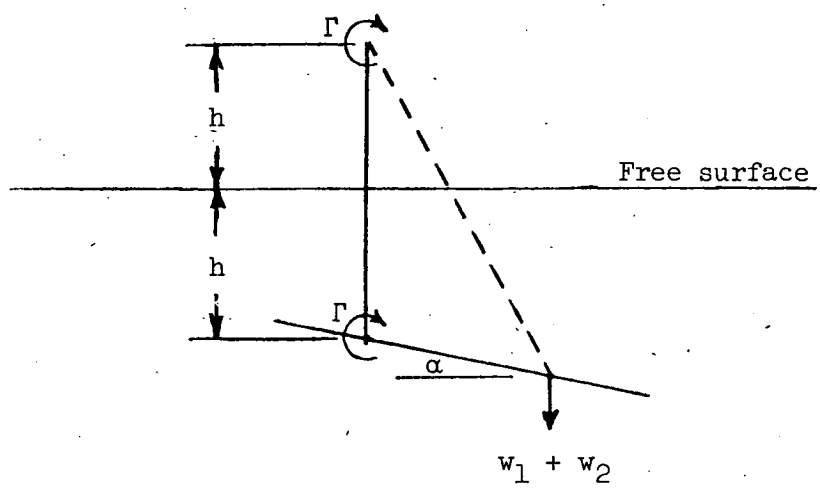

that is (for small angles),

$$\alpha = \frac{w_1}{V} + \frac{w_2}{V}$$

where

$$w_1 = \frac{\Gamma}{\pi c} \cos \alpha$$

and

$$w_2 = \frac{\Gamma}{2\pi\sqrt{\left(2h + \frac{c}{2}\sin\alpha\right)^2 + \left(\frac{c}{2}\cos\alpha\right)^2}} \frac{\frac{c}{2}\cos\alpha}{\sqrt{\left(2h + \frac{c}{2}\sin\alpha\right)^2 + \left(\frac{c}{2}\cos\alpha\right)^2}}$$

The symbol c is the hydrofoil chord and h is the depth of submergence. Therefore,

$$\alpha = \frac{\Gamma \cos\alpha}{\pi V c}\left[1 + \frac{1}{\left(4\frac{h}{c} + \sin\alpha\right)^2 + \left(\frac{c}{2}\cos\alpha\right)^2}\right]$$

where

$$\Gamma = \frac{cc_l V}{2}$$

Γ = circulation strength

The angle of attack α, which, when given in radian measure, is approximately equal to $\sin \alpha$, can be expressed in terms of the lift coefficient at infinite depth; that is,

$$\alpha = \frac{c_{l_o}}{2\pi}$$

Therefore, by taking $\cos \alpha = 1$, the ratio of lift coefficient at finite depth to lift coefficient at infinite depth is,

$$\frac{c_l}{c_{l_o}} = \frac{\left(4\frac{h}{c} + \frac{c_{l_o}}{2\pi}\right)^2 + 1}{\left(4\frac{h}{c} + \frac{c_{l_o}}{2\pi}\right)^2 + 2}$$

For all practical purposes, the term $c_{l_o}/2\pi$ in this equation has an insignificant effect on the results at all depths, and when this term is dropped, an equation, which can be interpreted as the ratio of lift-curve slope at finite depth to lift-curve slope at infinite depth, is obtained; that is,

$$\frac{c_{l_\alpha}}{c_{l_{\alpha_o}}} = \frac{\left(4\frac{h}{c}\right)^2 + 1}{\left(4\frac{h}{c}\right)^2 + 2}$$

Comparison of Theory and Experiment

Results calculated by this method are compared in figure 29 with the present experimental results for a hydrofoil of aspect ratio 4 and with the experimental results given in reference 1 for a hydrofoil of aspect ratio 10 after conversion of both sets of data to infinite aspect

[redacted]

ratio by the method previously discussed. Results calculated by the method of reference 11 which shows a strong influence of speed (not indicated by the present tests or those of reference 1) also are shown in figure 29. No comparison has been made with results predicted by the method of reference 12, since that method suggests that the variation of lift coefficient with depth depends rather strongly on the value of the lift coefficient at great depth - an effect not noted in the experimental investigations.

The agreement of the experimental results with results given by the equation developed herein is good. Although the assumptions made in the derivation certainly do not allow a complete presentation of the known physical conditions, the simplicity of the final equation and the good agreement with experiment for aspect ratios of 4 and 10 should justify use of the equation for certain applications. One possible application might be in connection with the calculation of the dynamic stability of hydrofoil systems. For such a problem, consideration may have to be given to possible variations with time of the depth of one or more members of the system, and it would, therefore, be convenient to express the variation of lift with depth by a simple equation.

CONCLUSIONS

The results of the tank tests of the hydrofoil with aspect ratio 4 with and without end plates and end-mounted struts may be summarized as follows:

1. Only small improvements were found in the maximum lift-drag ratios by the addition of end plates. These improvements occurred only at low lift coefficients and with small end plates.

2. At values of lift coefficient above the value for maximum lift-drag ratio, optimum end-plate size increased with lift coefficient and considerable improvement was obtained.

3. The detrimental effect of the drag of the additional strut for a configuration having end struts in contrast to a single central strut was greater than the beneficial effects due to the end-plate effect of the end struts.

4. The ratio of the effective aspect ratio with end plates to the geometric aspect ratio varied with end-plate size approximately as predicted by aerodynamic theory (Von Kármán and Burgers). Although the hydrodynamic data were slightly higher than the theoretical curve, the agreement was good when the accuracy to which such data could be obtained is considered.

[redacted]

5. The agreement of the experimental results with the results given by the approximate theoretical equation developed herein for the effect of depth on the lift of a hydrofoil was good.

Langley Aeronautical Laboratory
National Advisory Committee for Aeronautics
Langley Field, Va.

[redacted]

REFERENCES

1. Wadlin, Kenneth L., Ramsen, John A., and McGehee, John R.: Tank Tests at Subcavitation Speeds of an Aspect-Ratio-10 Hydrofoil with a Single Strut. NACA RM L9K14a, 1950.

2. Loftin, Laurence K., Jr.: Theoretical and Experimental Data for a Number of NACA 6A-Series Airfoil Sections. NACA Rep. 903, 1948.

3. Abbott, Ira H., Von Doenhoff, Albert E., and Stivers, Louis S., Jr.: Summary of Airfoil Data. NACA Rep. 824, 1945.

4. Daley, Bernard N., and Hanna, Lillian E.: Subsonic Two-Dimensional-Flow Conditions near an Airfoil Determined by Static Pressures Measured at the Tunnel Wall. NACA TN 1873, 1949.

5. Lindsey, W. F.: Effect of Mach Number on Position Error as Applied to a Pitot-Static Tube Located 0.55 Chord ahead of an Airplane Wing. NACA CB L4E29, 1944.

6. Reid, Elliott G.: Applied Wing Theory. First ed., McGraw-Hill Book Co., Inc., 1932, pp. 166-176.

7. Swanson, Robert S., and Crandall, Stewart M.: Lifting-Surface-Theory Aspect-Ratio Corrections to the Lift and Hinge-Moment Parameters for Full-Span Elevators on Horizontal Tail Surfaces. NACA Rep. 911, 1948.

8. Swanson, Robert S., and Priddy, E. LaVerne: Lifting-Surface-Theory Values of the Damping in Roll and of the Parameter Used in Estimating Aileron Stick Forces. NACA ARR L5F23, 1945.

9. Von Kármán, Th., and Burgers, J. M.: General Aerodynamic Theory - Perfect Fluids. Airfoils and Airfoil Systems of Finite Span. Vol. II of Aerodynamic Theory, div. E, ch. IV, sec. 19, W. F. Durand, ed., Julius Springer (Berlin), 1935, pp. 211-212.

10. Loftin, Laurence K., Jr., and Smith, Hamilton A.: Aerodynamic Characteristics of 15 NACA Airfoil Sections at Seven Reynolds Numbers from 0.7×10^6 to 9.0×10^6. NACA TN 1945, 1949.

11. Keldish, M., and Lavrentiev, M.: The Motion of an Aerofoil below the Surface of a Heavy Fluid. Transactions of the Conference on the Theory of Wave Resistance, U.S.S.R. (Moscow), 1937. British A.R.C., March 17, 1938. (Translated by A.I.(T), Air Ministry.)

[redacted]

12. Weinig, F.: On the Theory of Hydrofoils and Planing Surfaces. NACA TM 845, 1938.

13. Glauert, H.: The Elements of Aerofoil and Airscrew Theory. Second ed., Cambridge Univ. Press, 1948.

14. Wieghardt, Karl: Chordwise Load Distribution of a Simple Rectangular Wing. NACA TM 963, 1940.

[redacted]

Page intentionally left blank

Page intentionally left blank

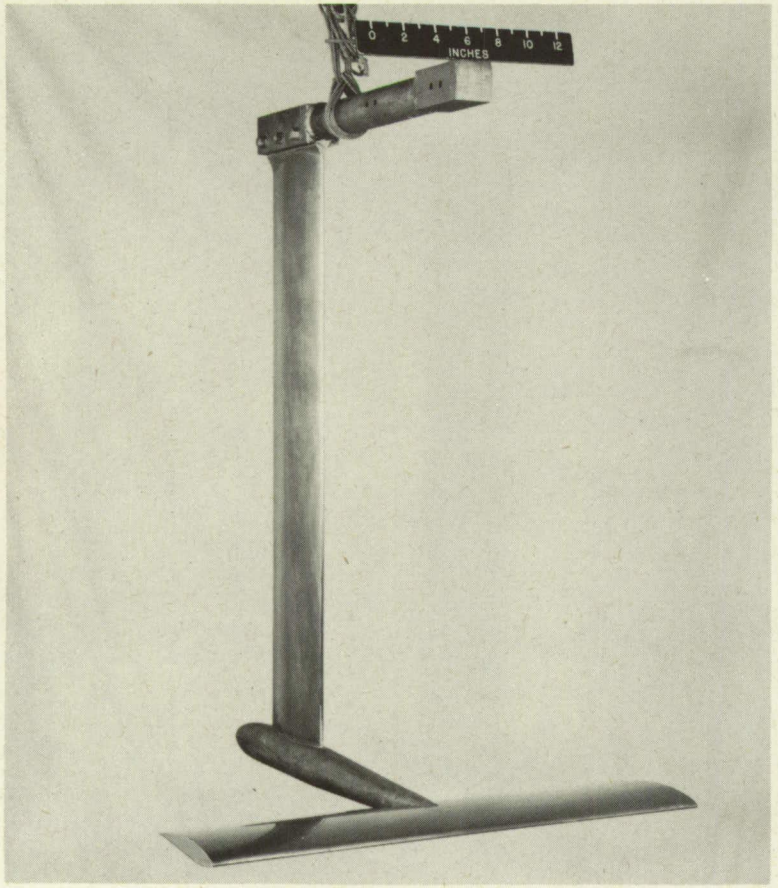

(a) Without end plate.

(b) End plate A.

NACA
L-68428

Figure 1.- Photographs of the hydrofoil-end-plate arrangements investigated.

Page intentionally left blank

Page intentionally left blank

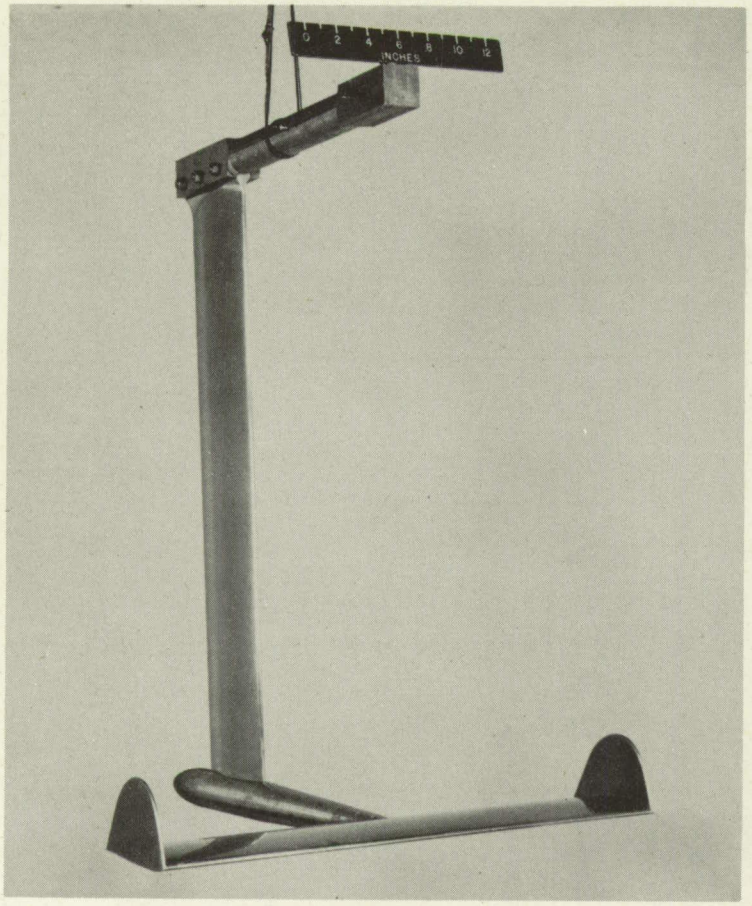

(c) End plate B.

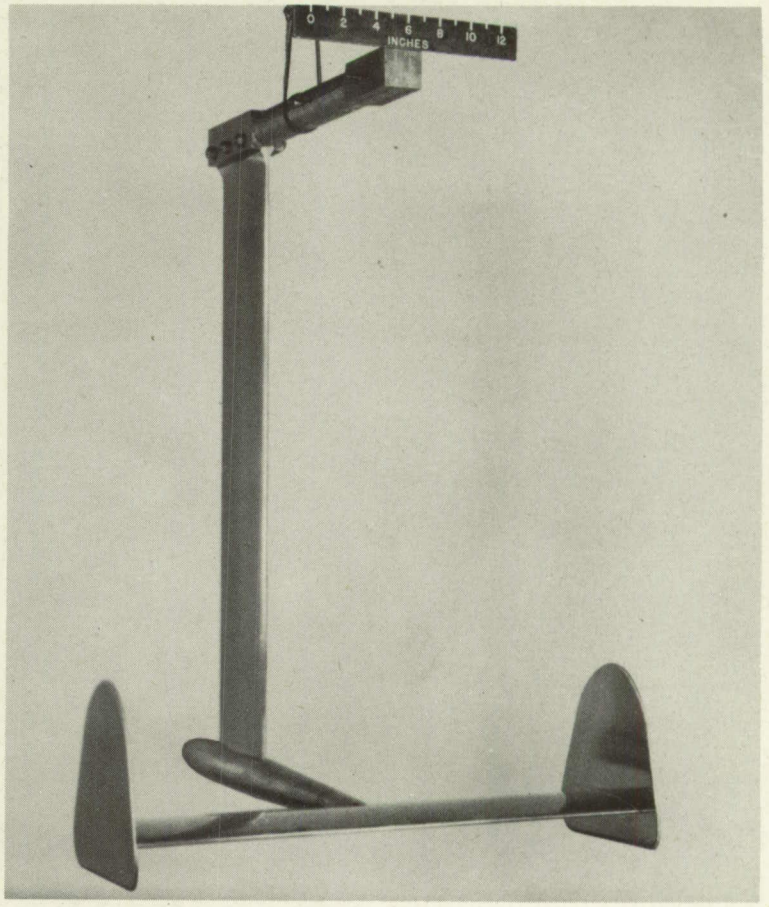

(d) End plate C.

NACA
L-68429

Figure 1.- Continued.

Page intentionally left blank

Page intentionally left blank

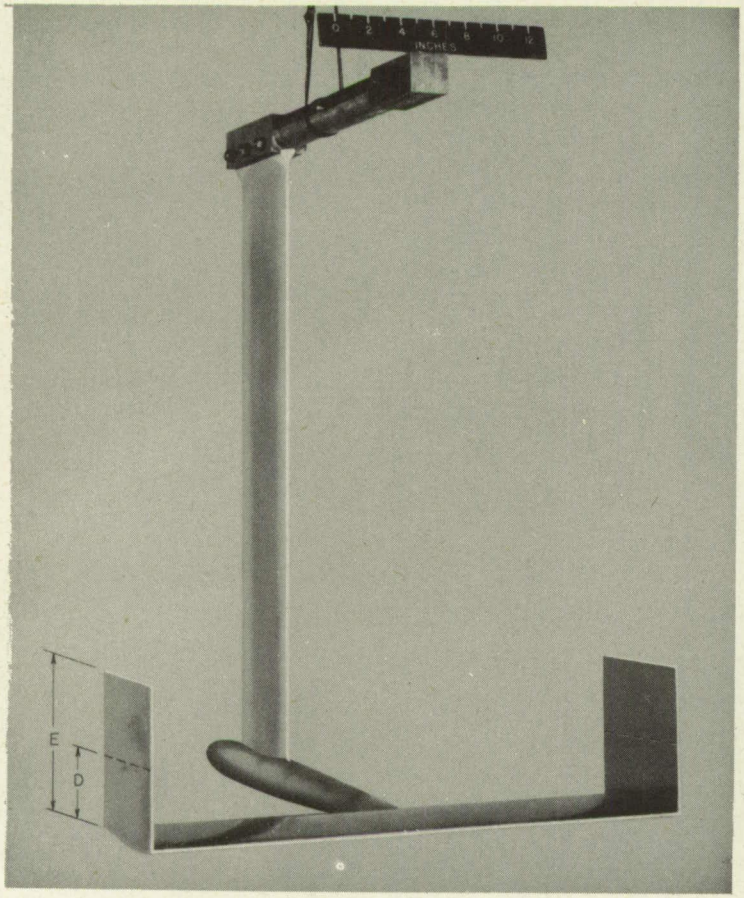

(e) End plates D and E.

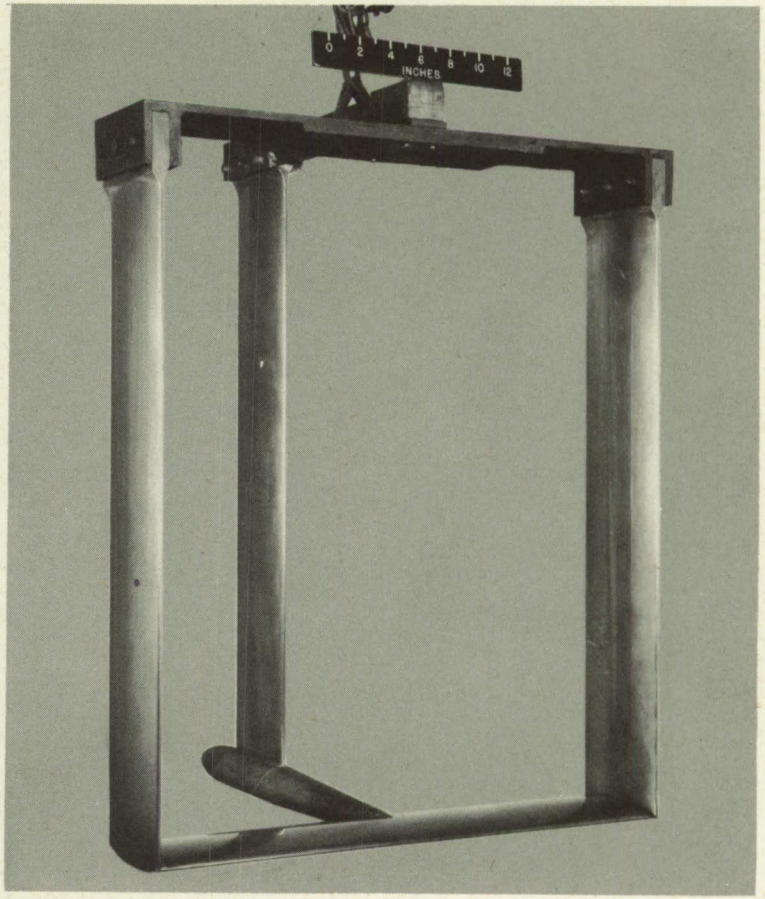

(f) End struts.

NACA

L-68430

Figure 1.- Concluded.

Page intentionally left blank

Page intentionally left blank

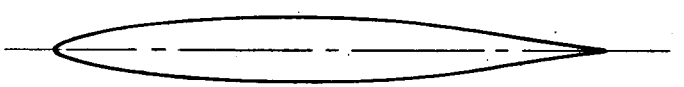

Strut, NACA 66_1-012

Station	Ordinate
0	0
.040	.072
.060	.087
.100	.109
.200	.145
.400	.200
.600	.243
.800	.280
1.200	.339
1.600	.384
2.000	.419
2.400	.445
2.800	.464
3.200	.476
3.600	.480
4.000	.477
4.400	.467
4.800	.447
5.200	.411
5.600	.361
6.000	.301
6.400	.236
6.800	.167
7.200	.099
7.600	.038
8.000	0
L.E. radius: 0.076	

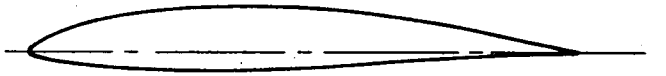

Hydrofoil, NACA 64_1A412

Upper surface		Lower surface	
Station	Ordinate	Station	Ordinate
0.026	0.084	0.054	-0.067
.044	.104	.076	-.079
.082	.135	.118	-.096
.178	.194	.221	-.126
.376	.279	.424	-.164
.575	.346	.625	-.190
.790	.401	.810	-.211
1.176	.490	1.224	-.241
1.578	.559	1.622	-.261
1.981	.611	2.019	-.274
2.384	.648	2.416	-.281
2.788	.673	2.812	-.281
3.192	.684	3.208	-.275
3.595	.679	3.605	-.259
3.999	.661	4.001	-.236
4.398	.632	4.402	-.207
4.795	.592	4.805	-.176
5.192	.544	5.208	-.142
5.590	.487	5.610	-.108
5.988	.422	6.012	-.076
6.386	.349	6.414	-.050
6.786	.265	6.814	-.034
7.190	.179	7.210	-.022
7.595	.090	7.605	-.012
8.000	.002	8.000	-.002
L.E. radius: 0.083			
Slope of radius through L.E.: 0.168			

Figure 2.- Ordinates of strut and hydrofoil in inches.

SSP = stream static pressure

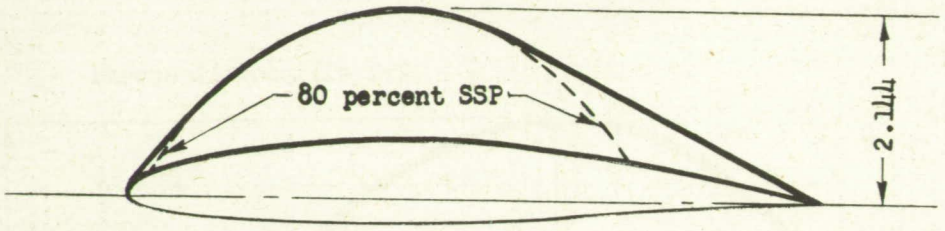

End plate A.

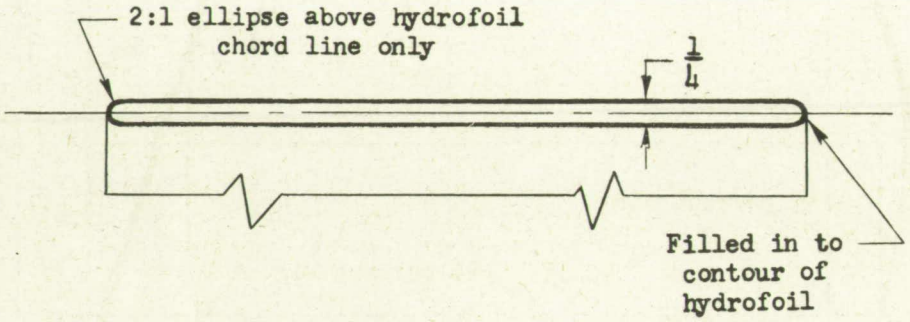

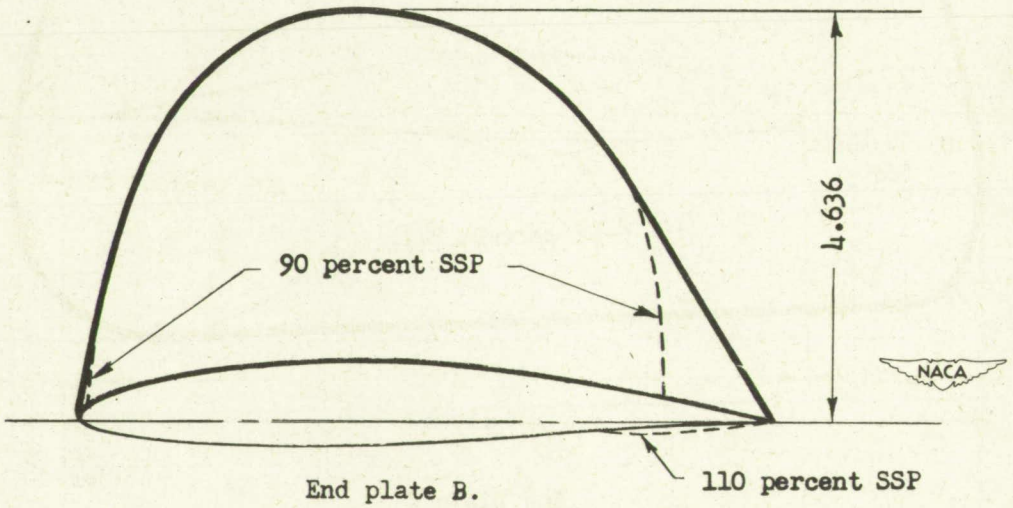

End plate B.

Area of end plate A (excluding sectional area of hydrofoil) = 6.63 sq. in.
Area of end plate B (excluding sectional area of hydrofoil) = 22.48 sq. in.
Sectional area of hydrofoil = 5.12 sq. in.

Figure 3.- Details of pressure field end plates A, B, and C. All dimensions are in inches.

SSP = stream static pressure

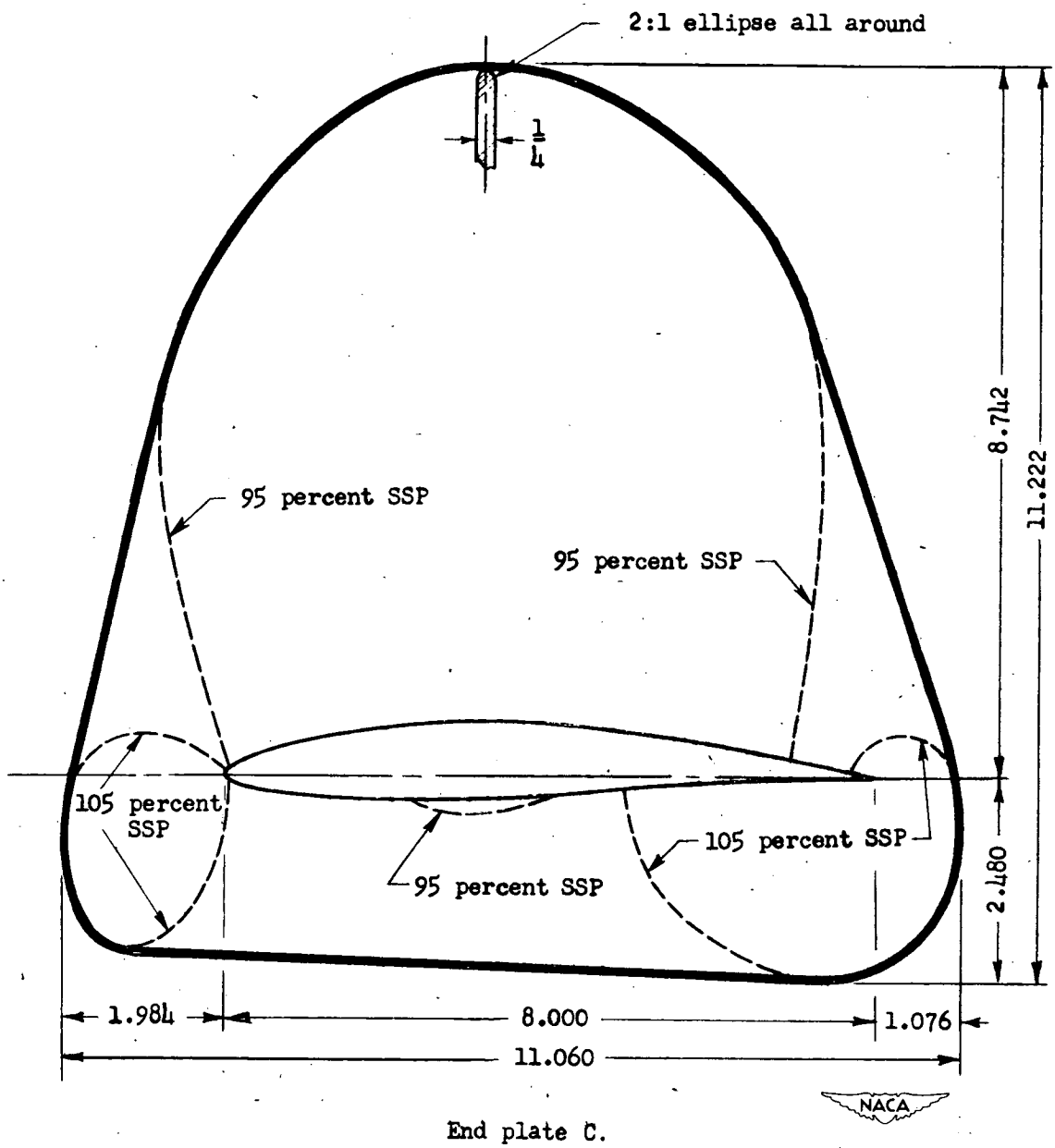

End plate C.

Area of end plate (excluding sectional area of hydrofoil) = 89.1 sq. in.
Sectional area of hydrofoil = 5.12 sq. in.

Figure 3.- Concluded.

[redacted]

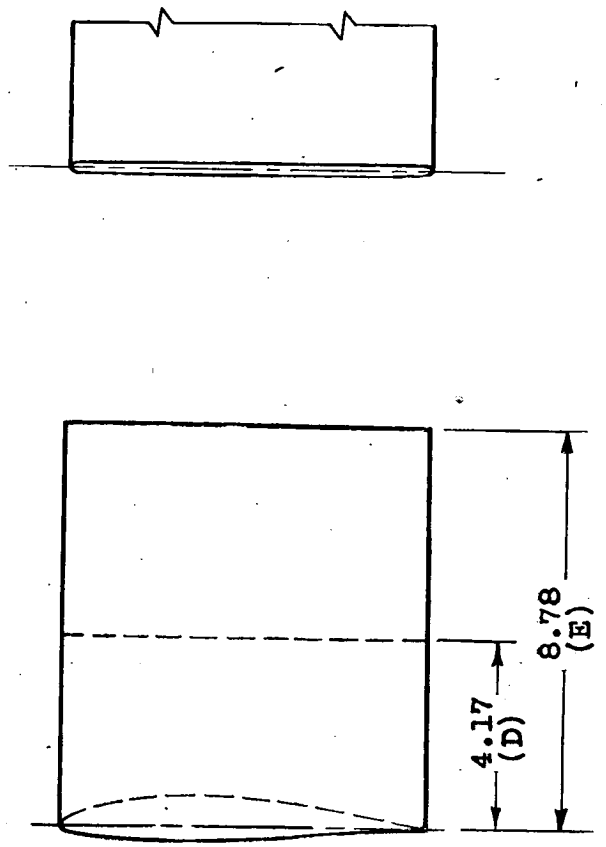

Area of end plate D (excluding sectional area of hydrofoil) = 29.59 sq. in.
Area of end plate E (excluding sectional area of hydrofoil) = 66.48 sq. in.
Sectional area of hydrofoil = 5.12 sq. in.

Figure 4.- Details of end plates D and E. All dimensions are in inches.

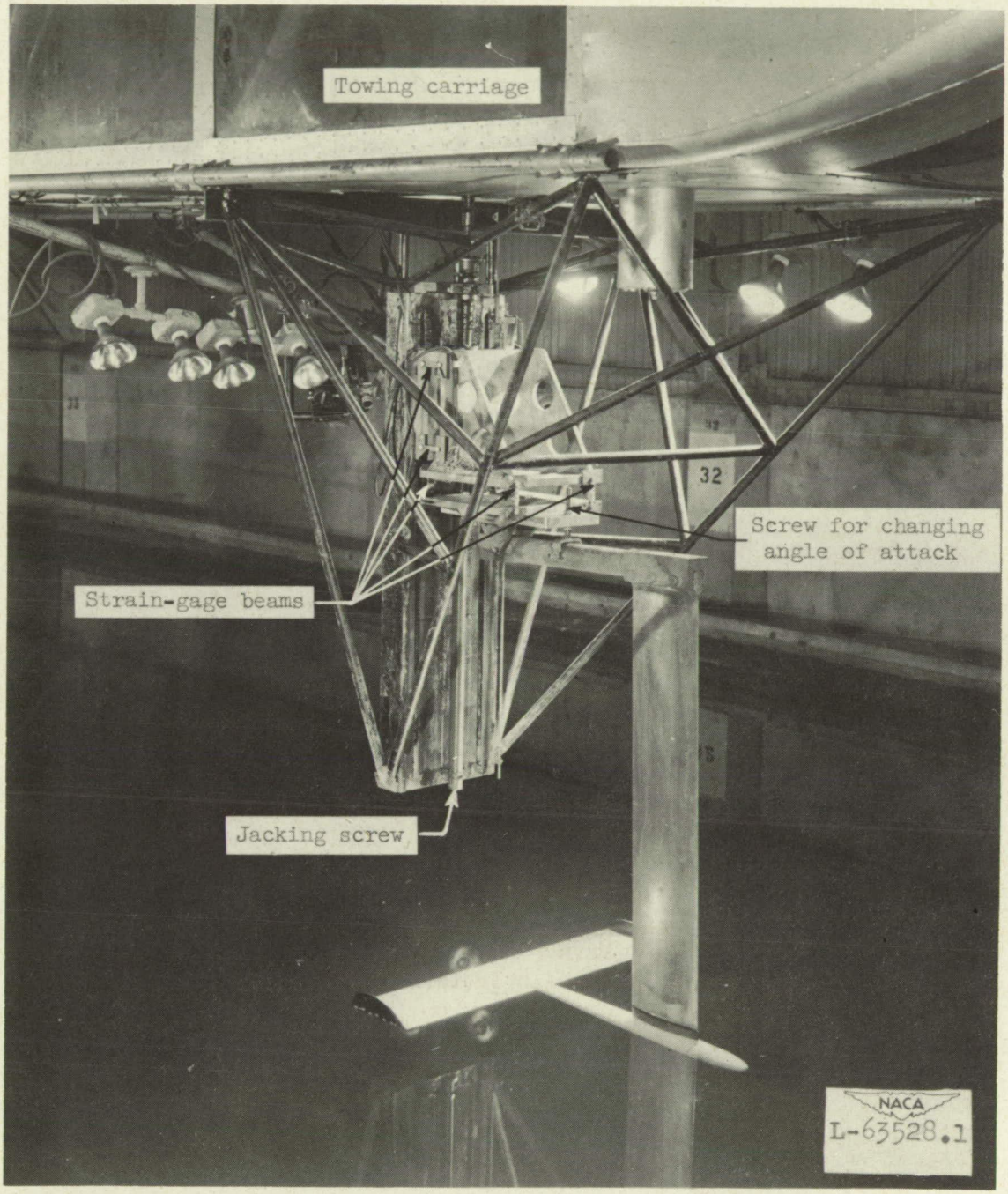

Figure 5.- Test setup showing hydrofoil suspended from balance attached to towing carriage.

Page intentionally left blank

Page intentionally left blank

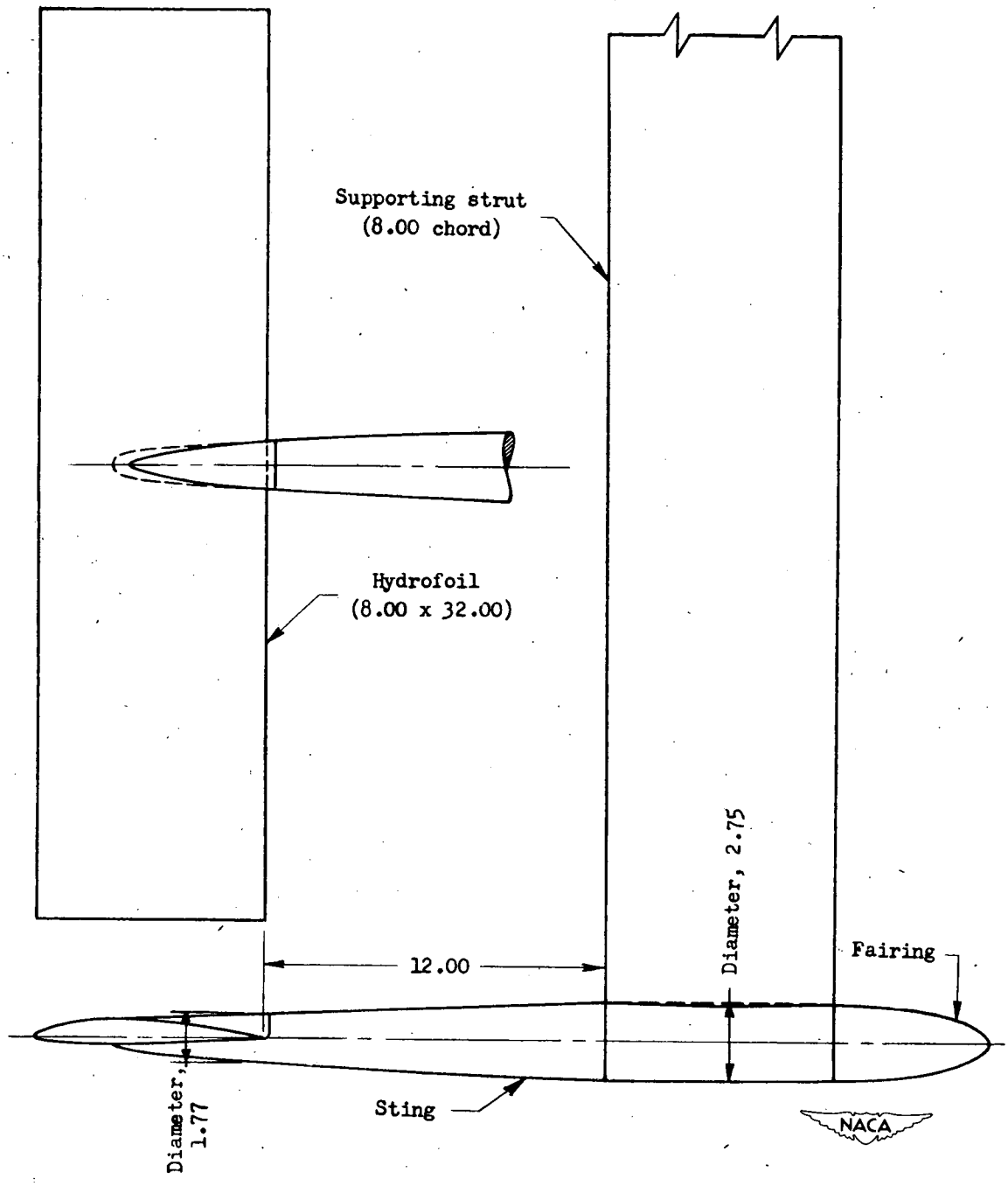

Figure 6.- Details of hydrofoil-support arrangement. All dimensions are in inches.

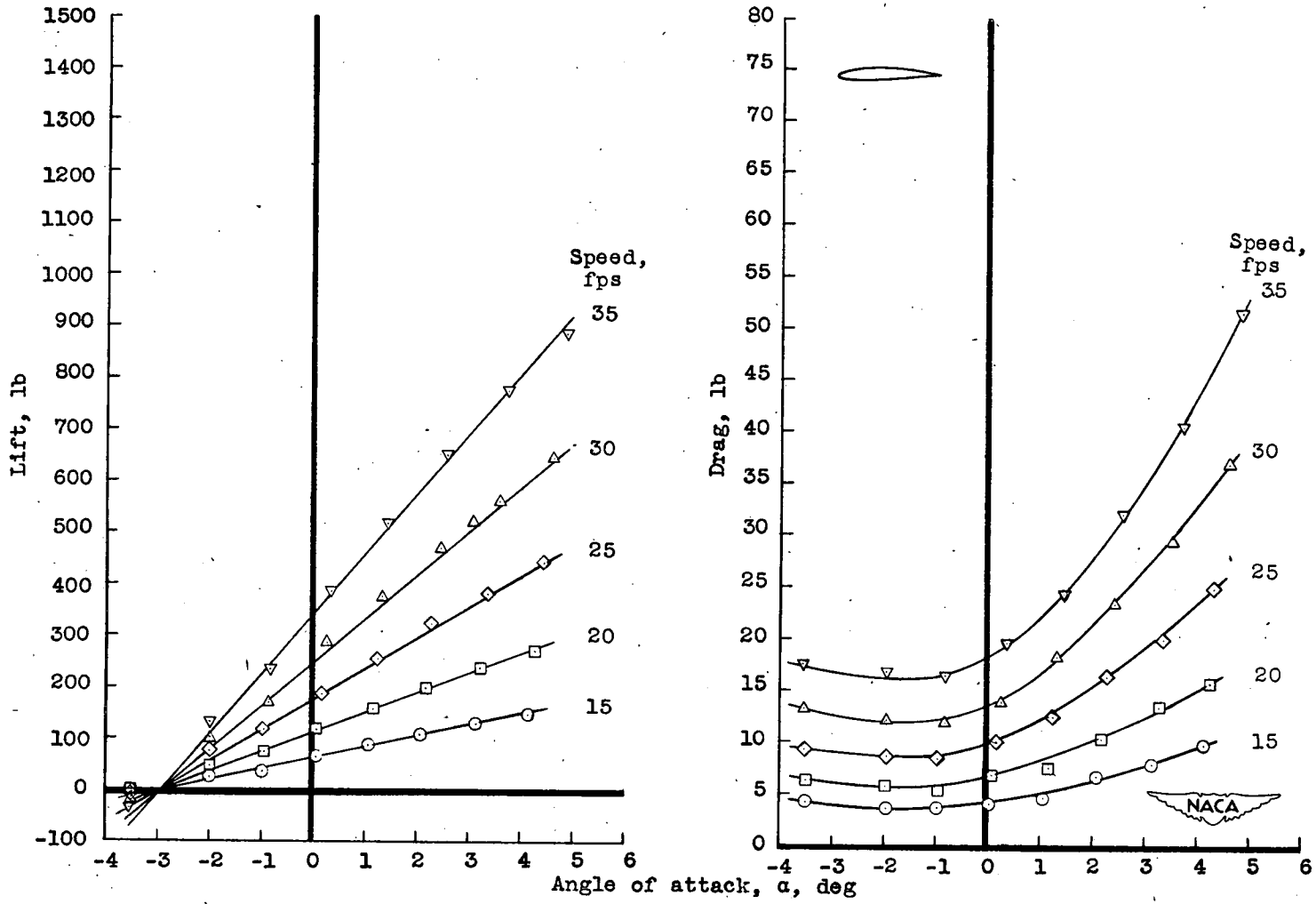

(a) Depth, 0.5 chords.

Figure 7.- Lift and drag of hydrofoil without end plates.

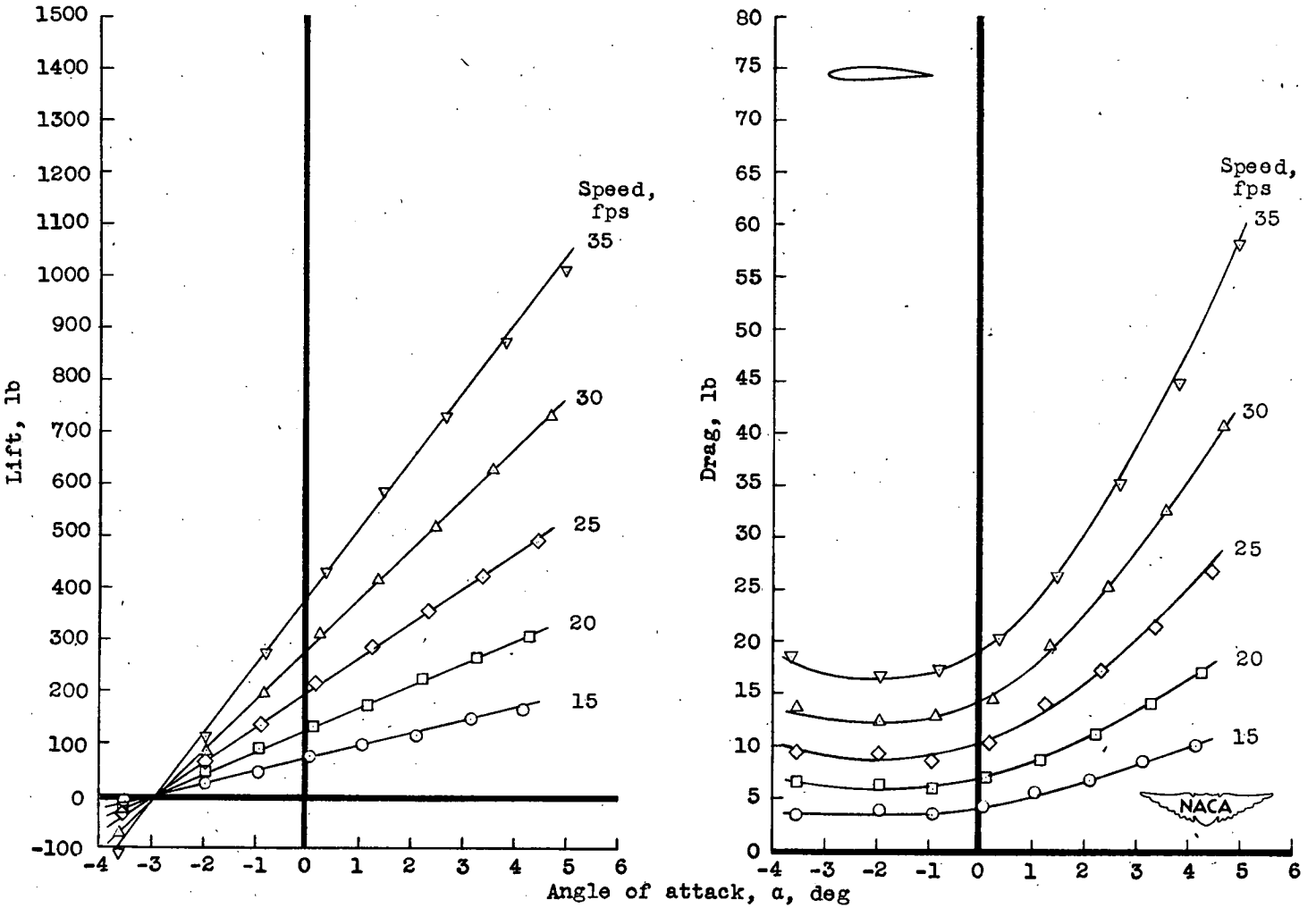

(b) Depth, 1.0 chord.

Figure 7.- Continued.

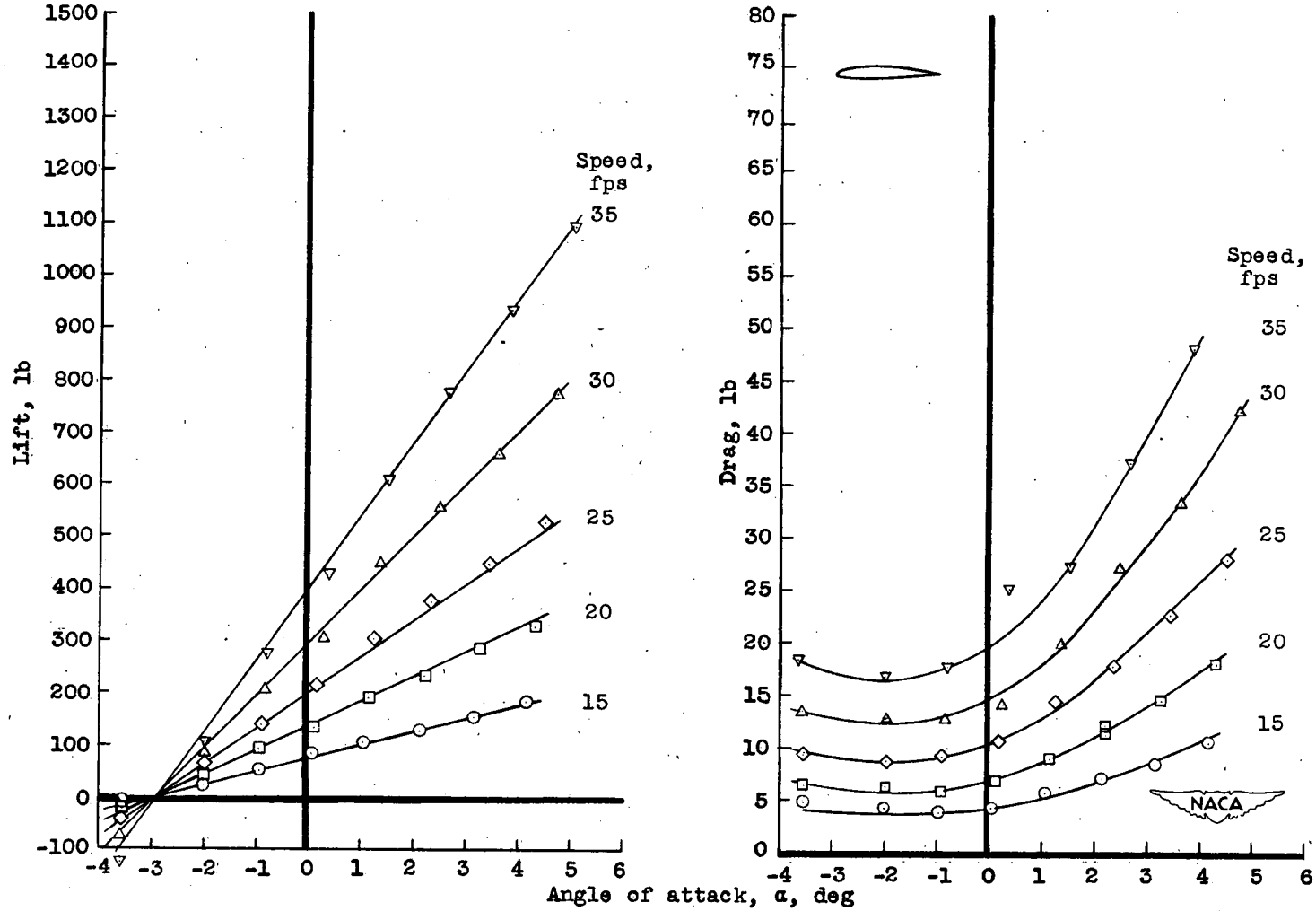

(c) Depth, 2.0 chords.

Figure 7.- Continued.

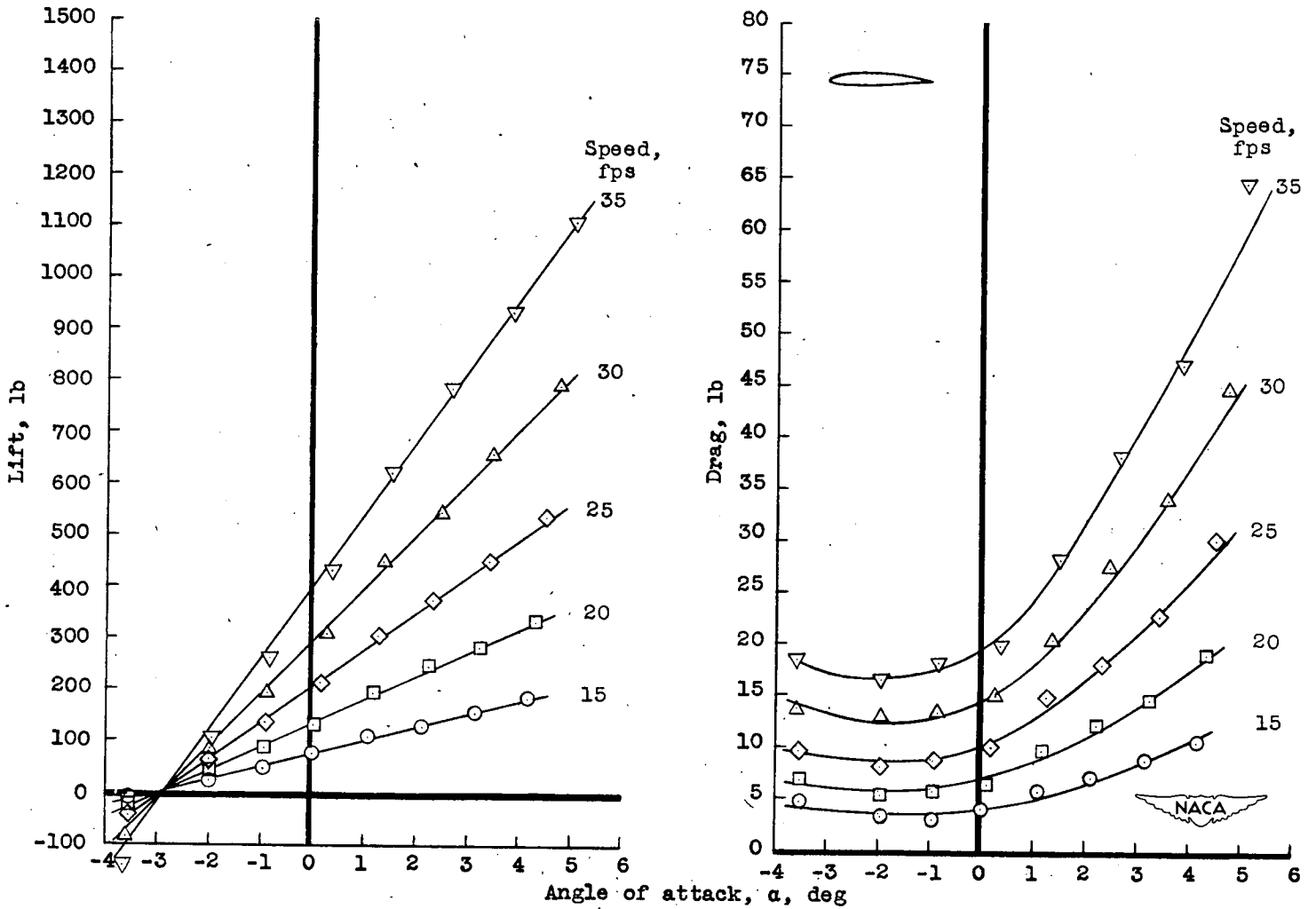

(d) Depth, 3.0 chords.

Figure 7.- Continued.

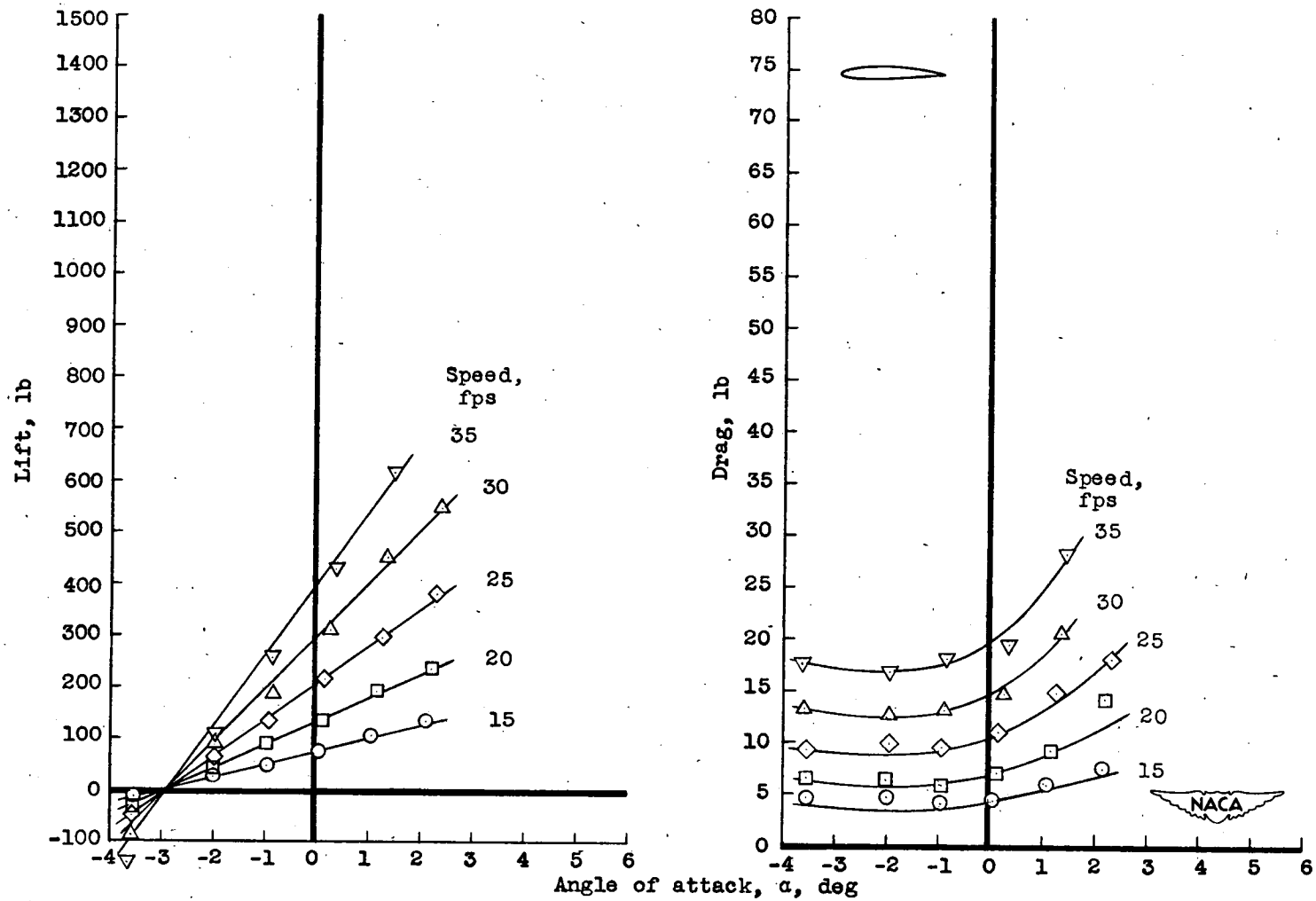

(e) Depth, 4.0 chords.

Figure 7.- Concluded.

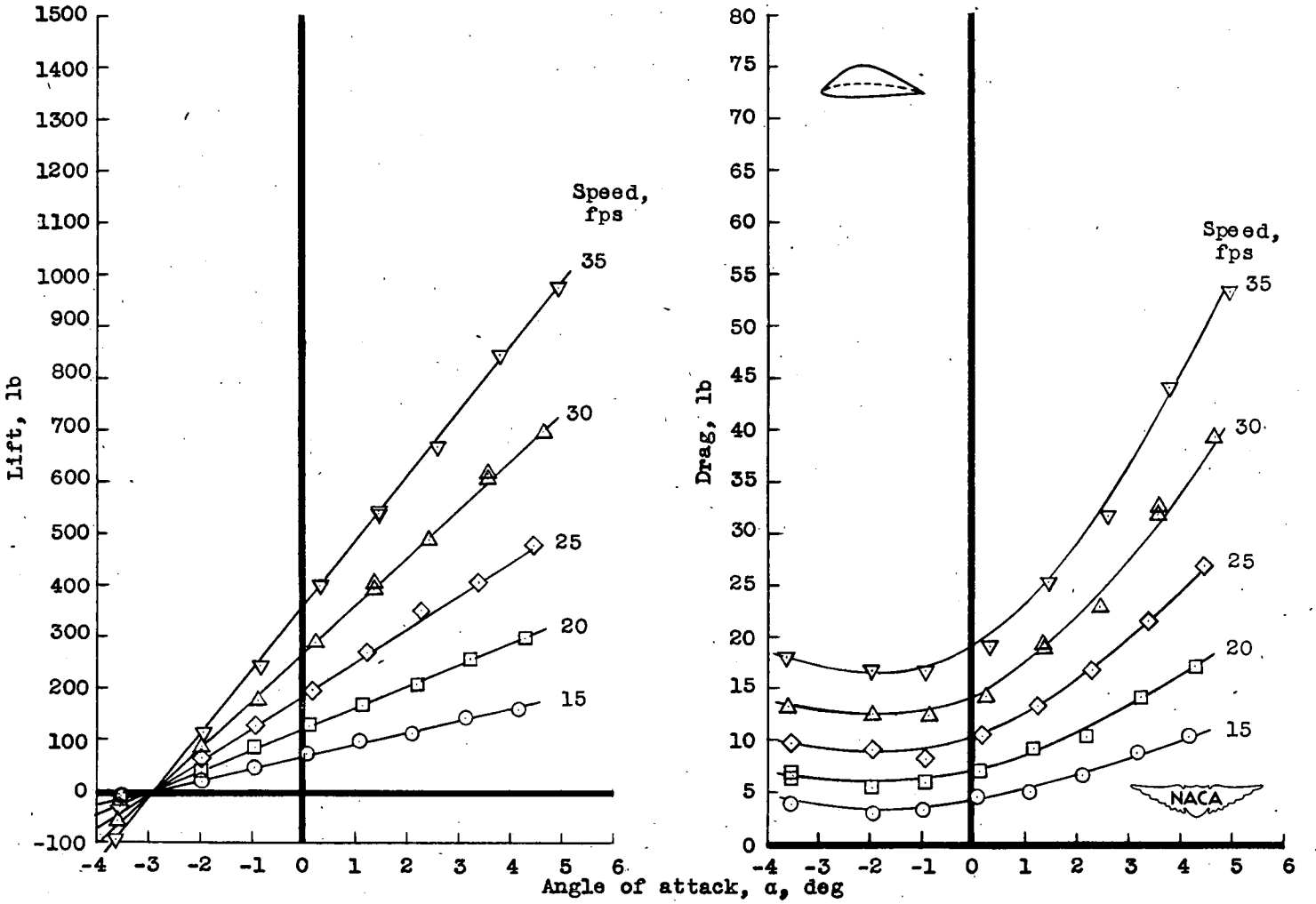

(a) Depth, 0.5 chord.

Figure 8.- Lift and drag of hydrofoil with end plate A.

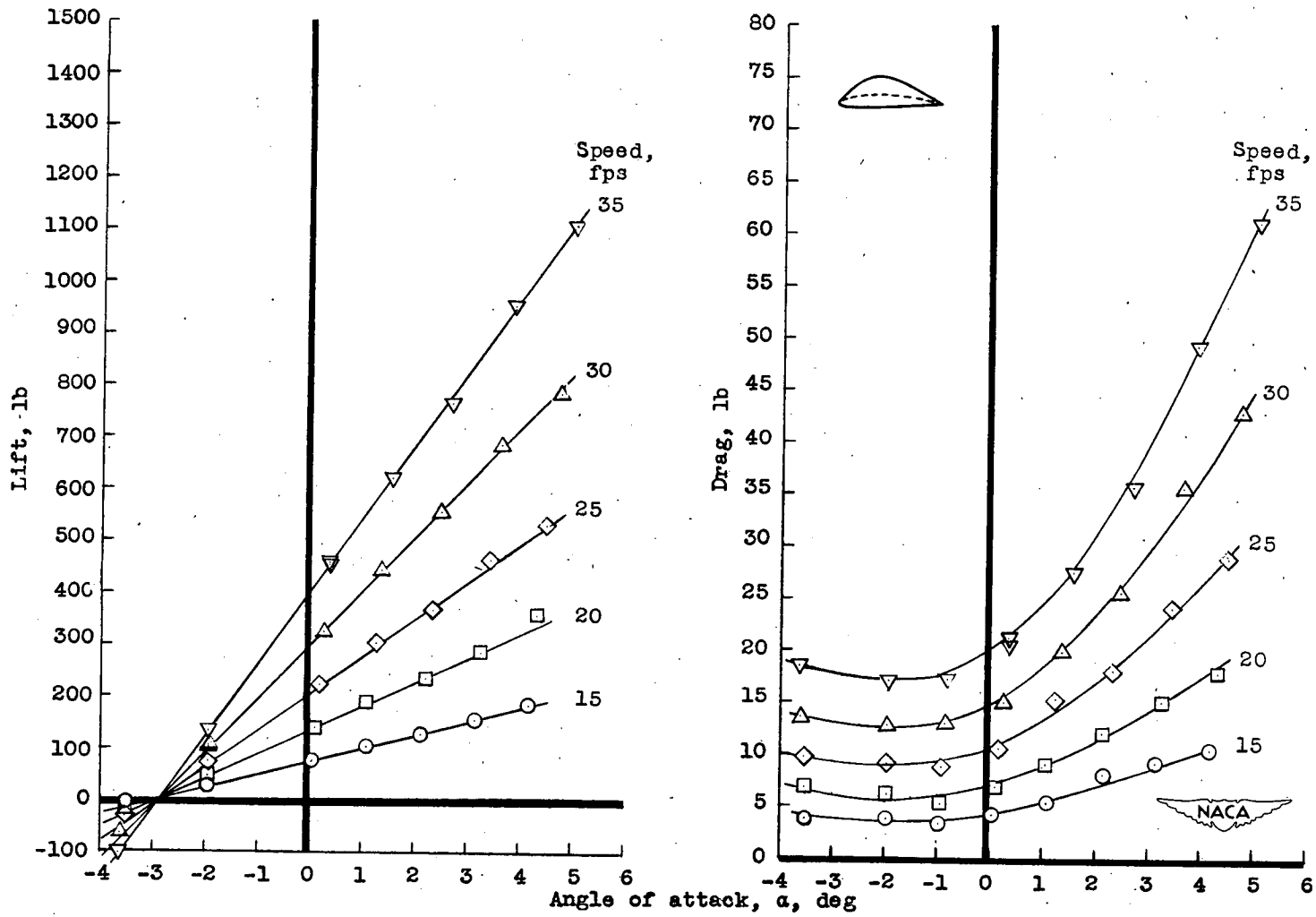

(b) Depth, 1.0 chord.

Figure 8.- Continued.

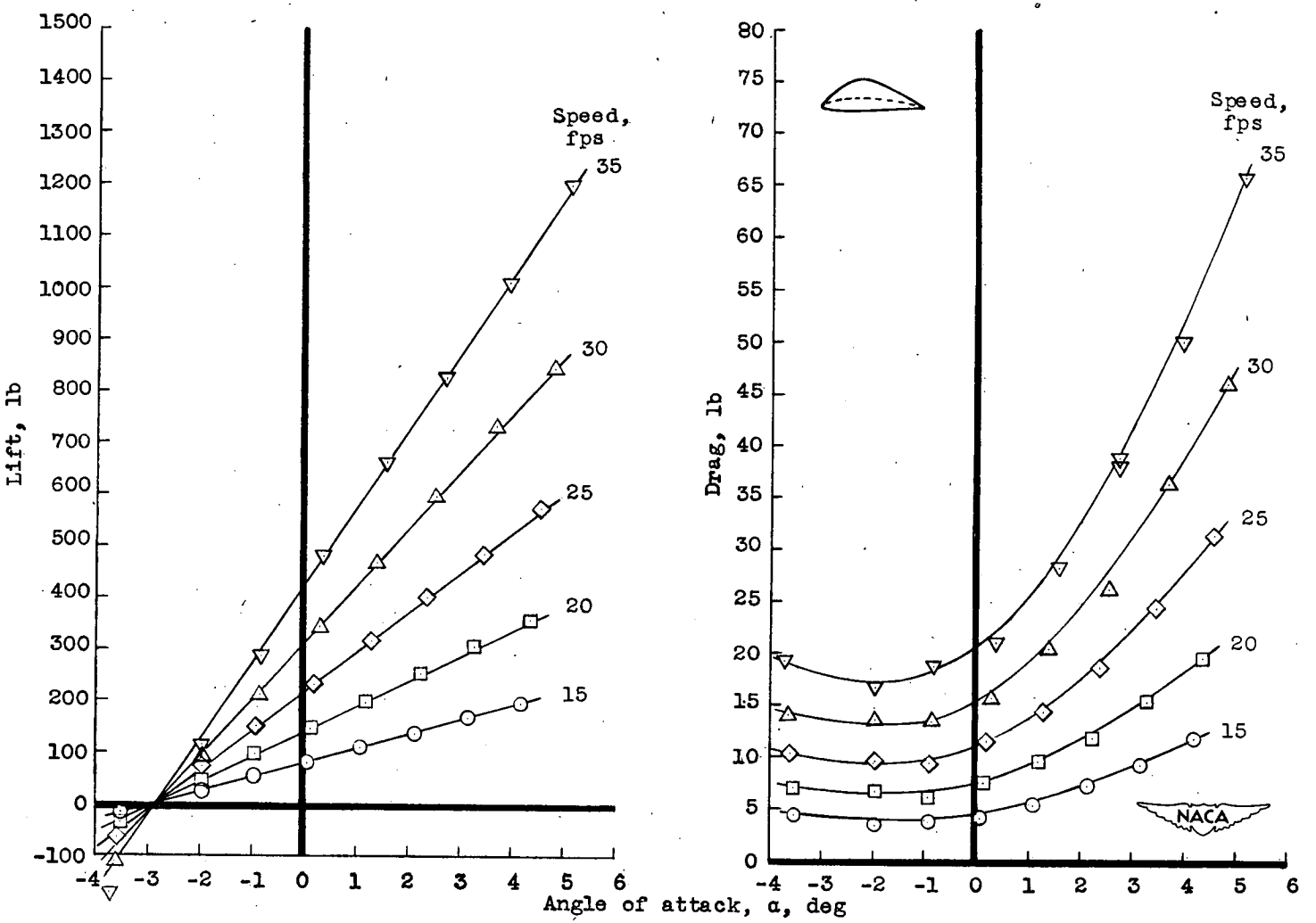

(c) Depth, 2.0 chords.

Figure 8.- Continued.

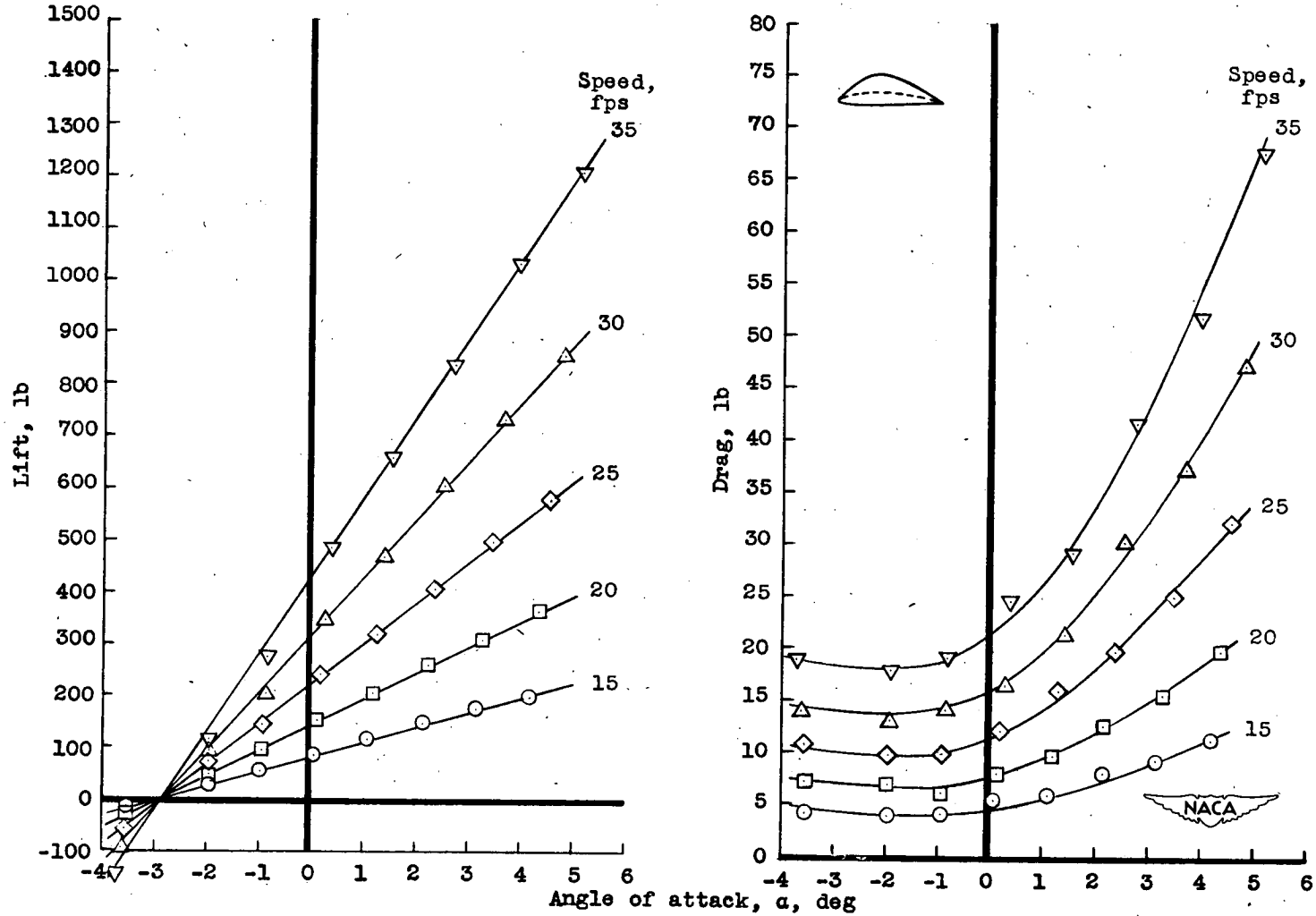

(d) Depth, 3.0 chords.

Figure 8.- Continued.

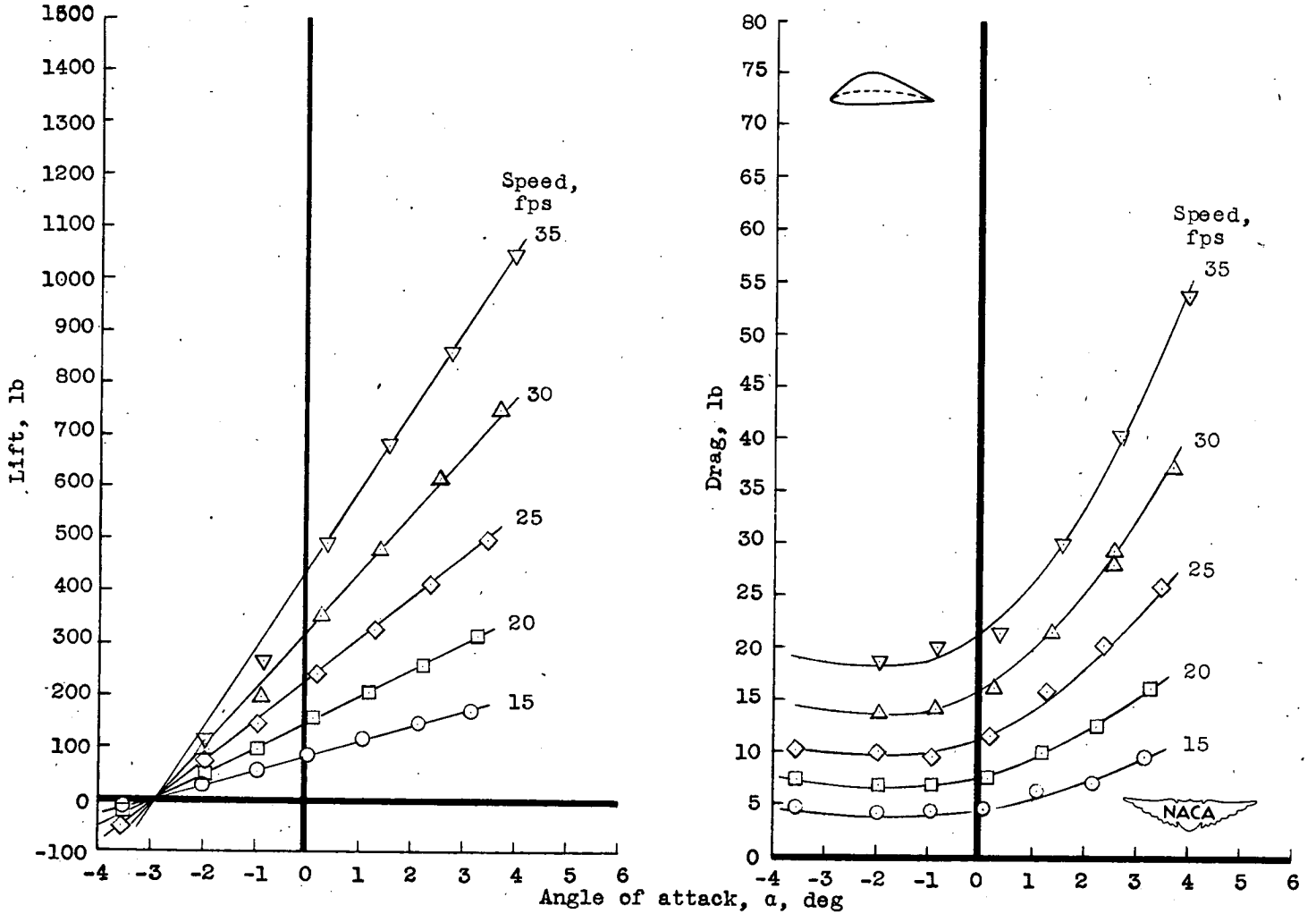

(e) Depth, 4.0 chords.

Figure 8.- Concluded.

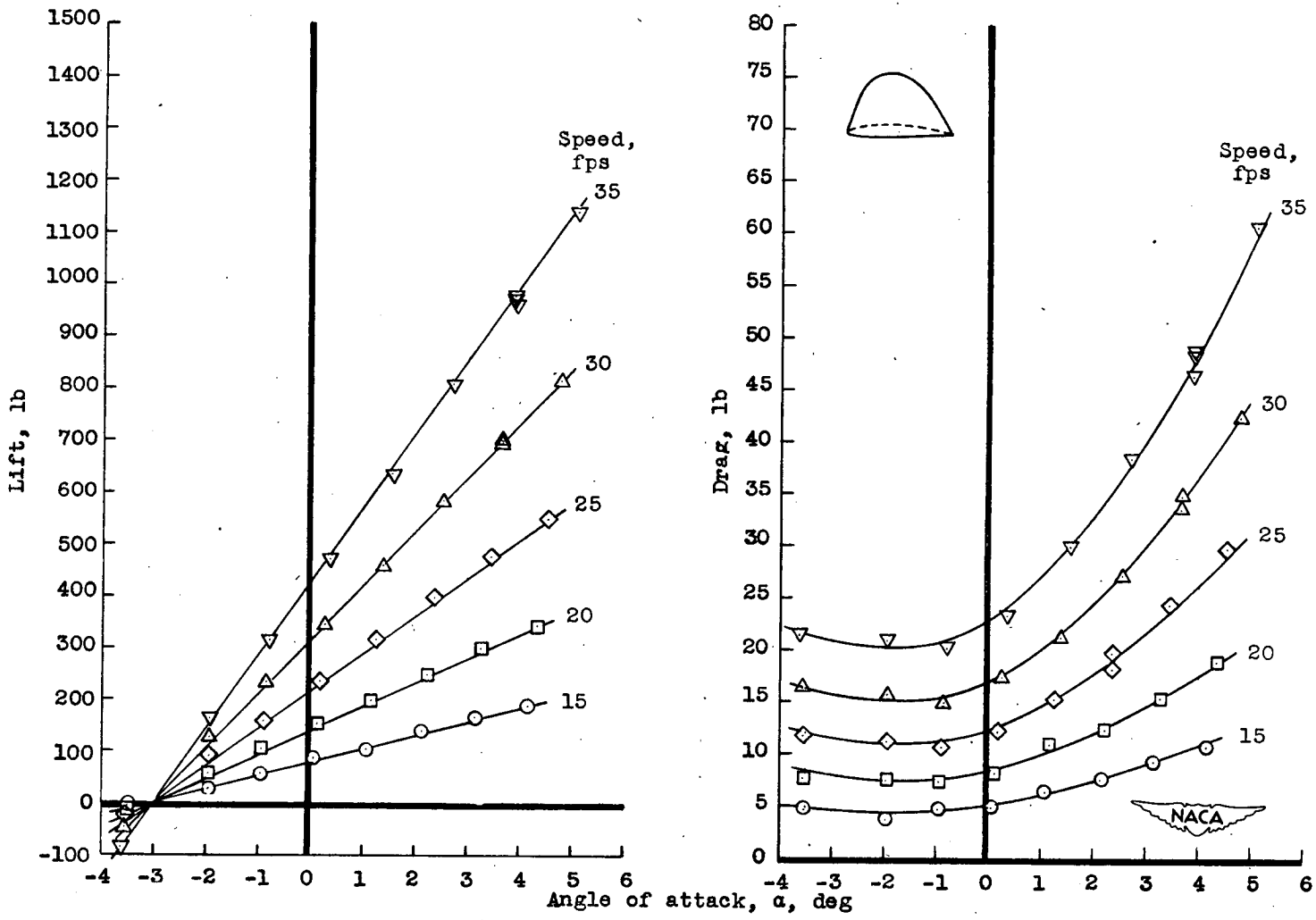

(a) Depth, 1.0 chord.

Figure 9.- Lift and drag of hydrofoil with end plate B.

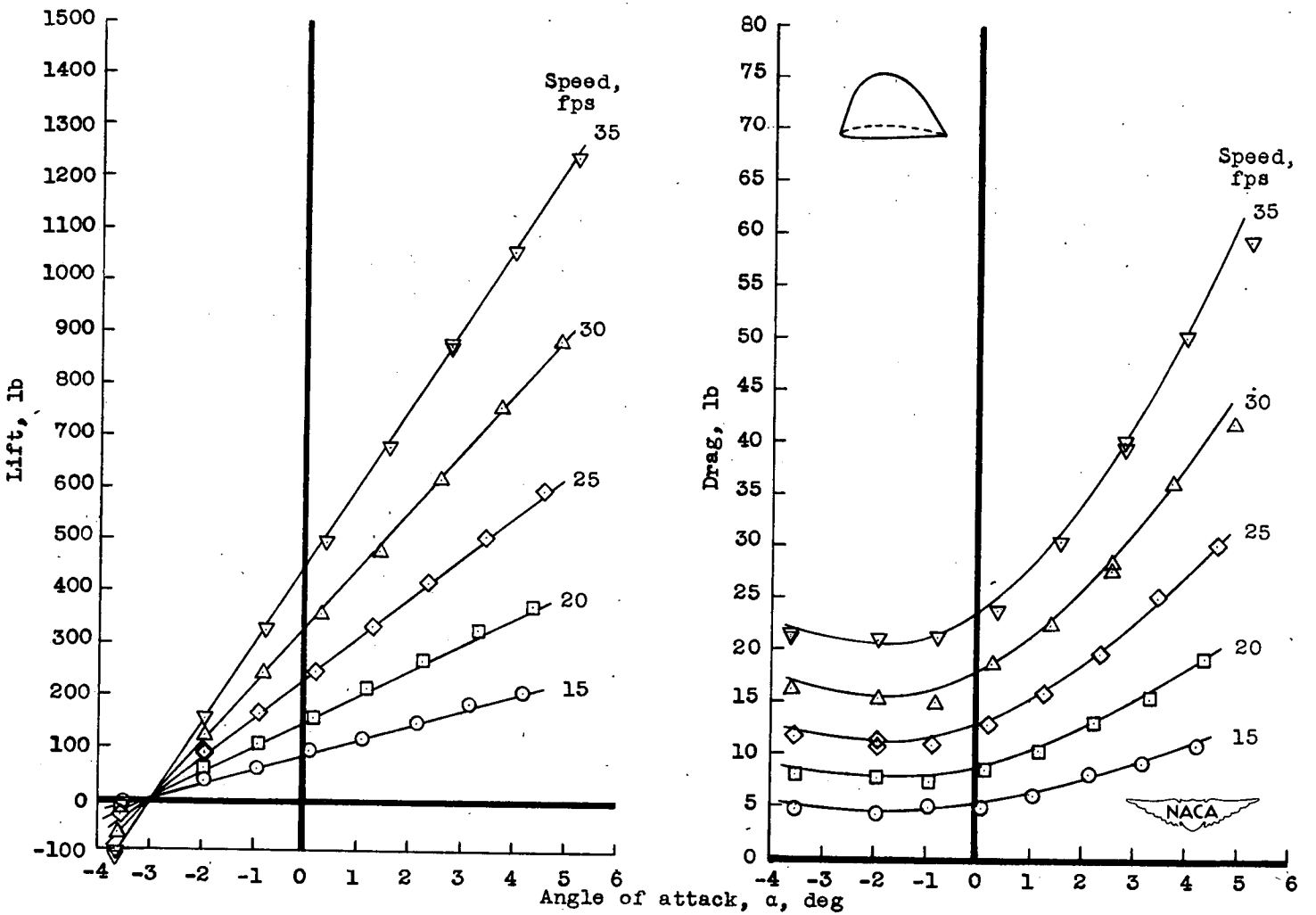

(b) Depth, 2.0 chords.

Figure 9.- Continued.

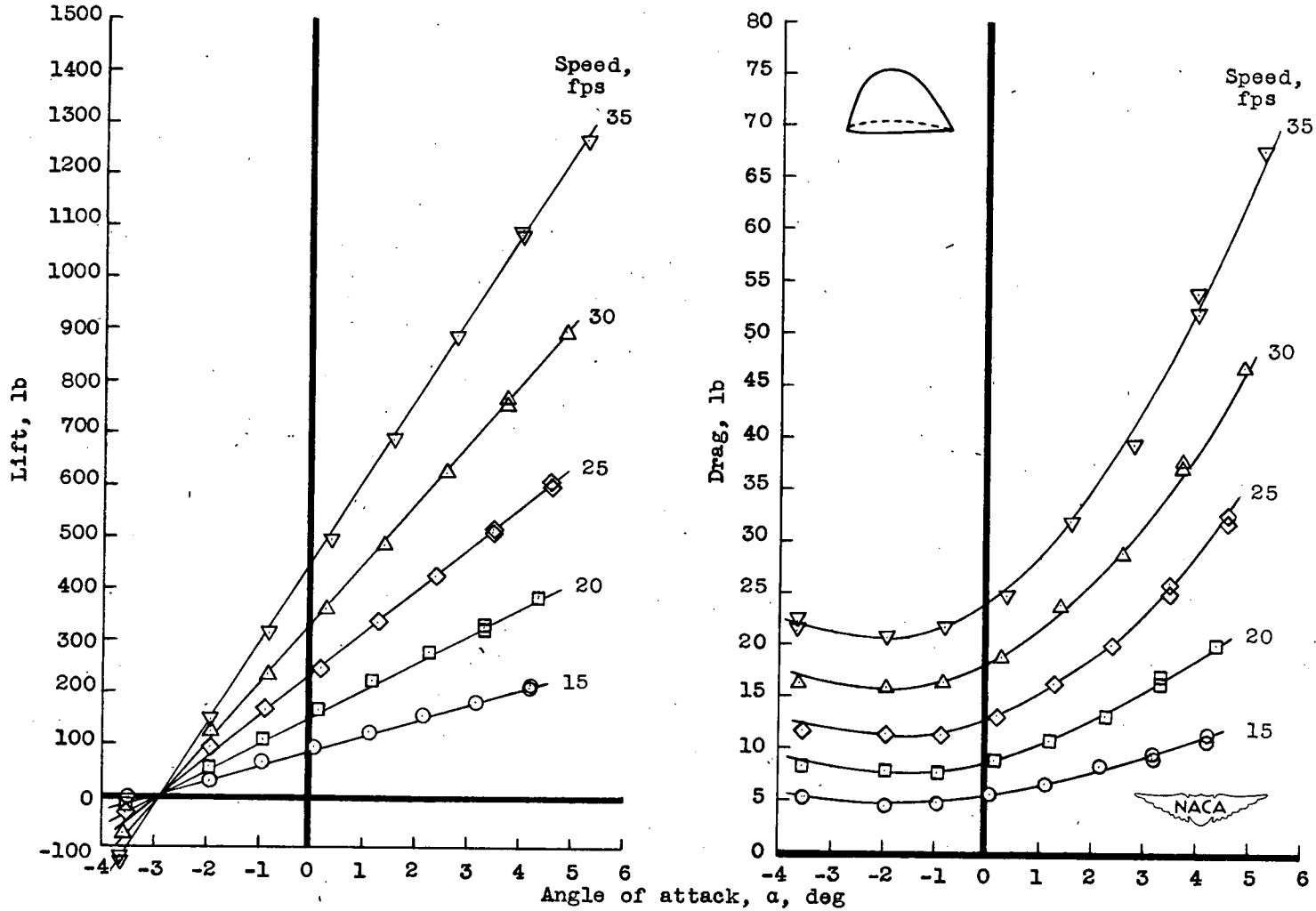

(c) Depth, 3.0 chords.

Figure 9.- Continued.

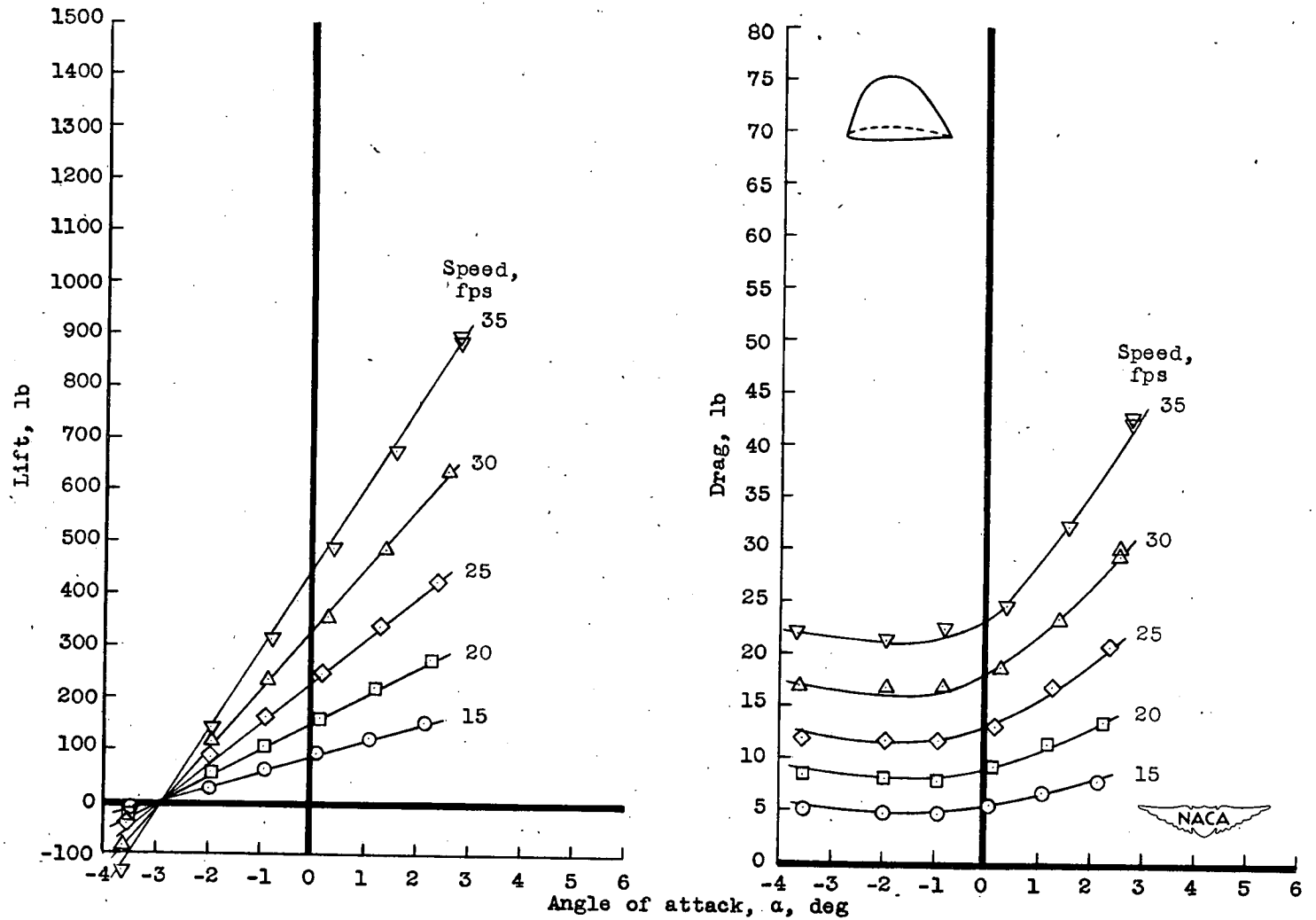

(d) Depth, 4.0 chords.

Figure 9.- Concluded.

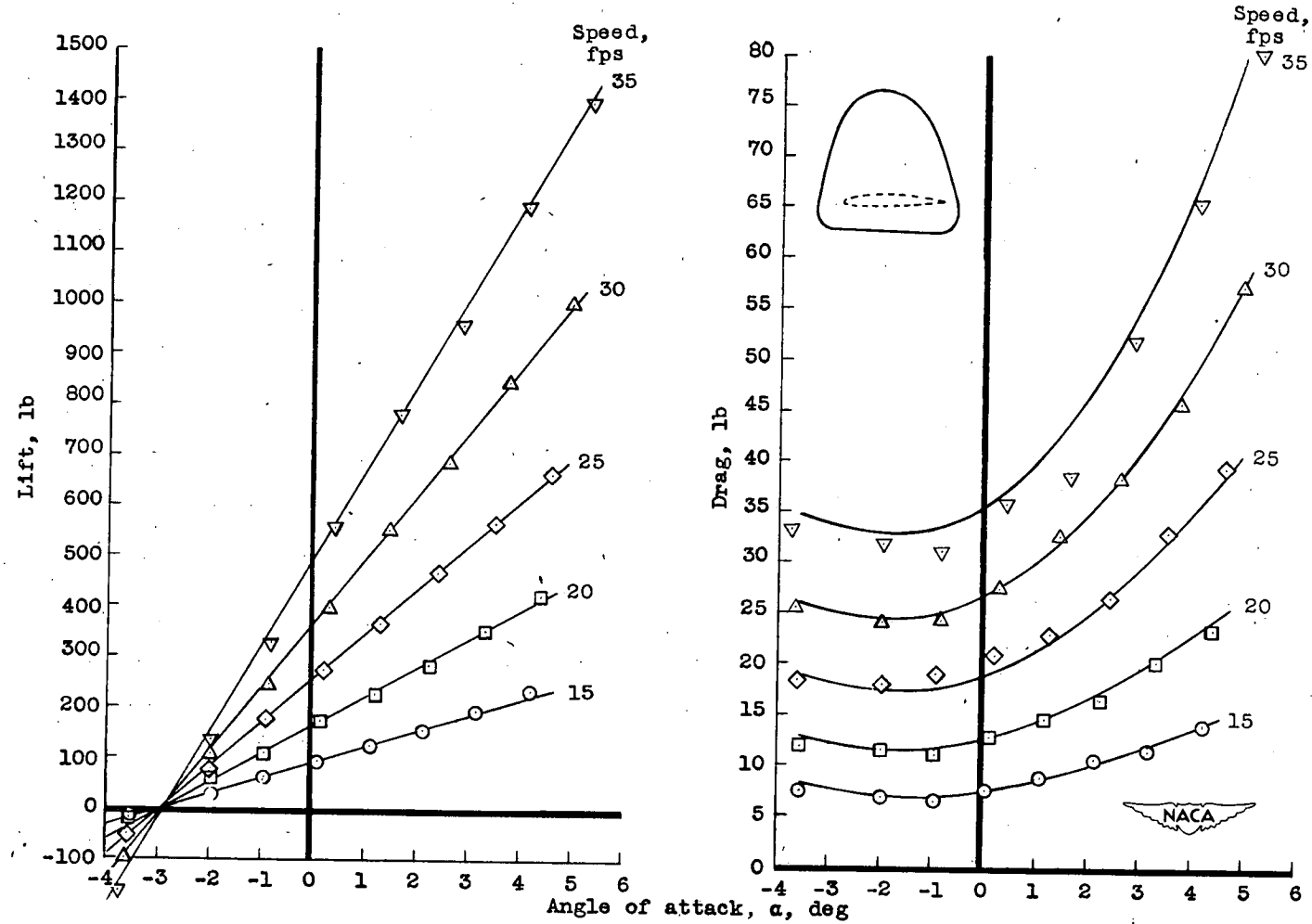

(a) Depth, 2.0 chords.

Figure 10.- Lift and drag of hydrofoil with end plate C.

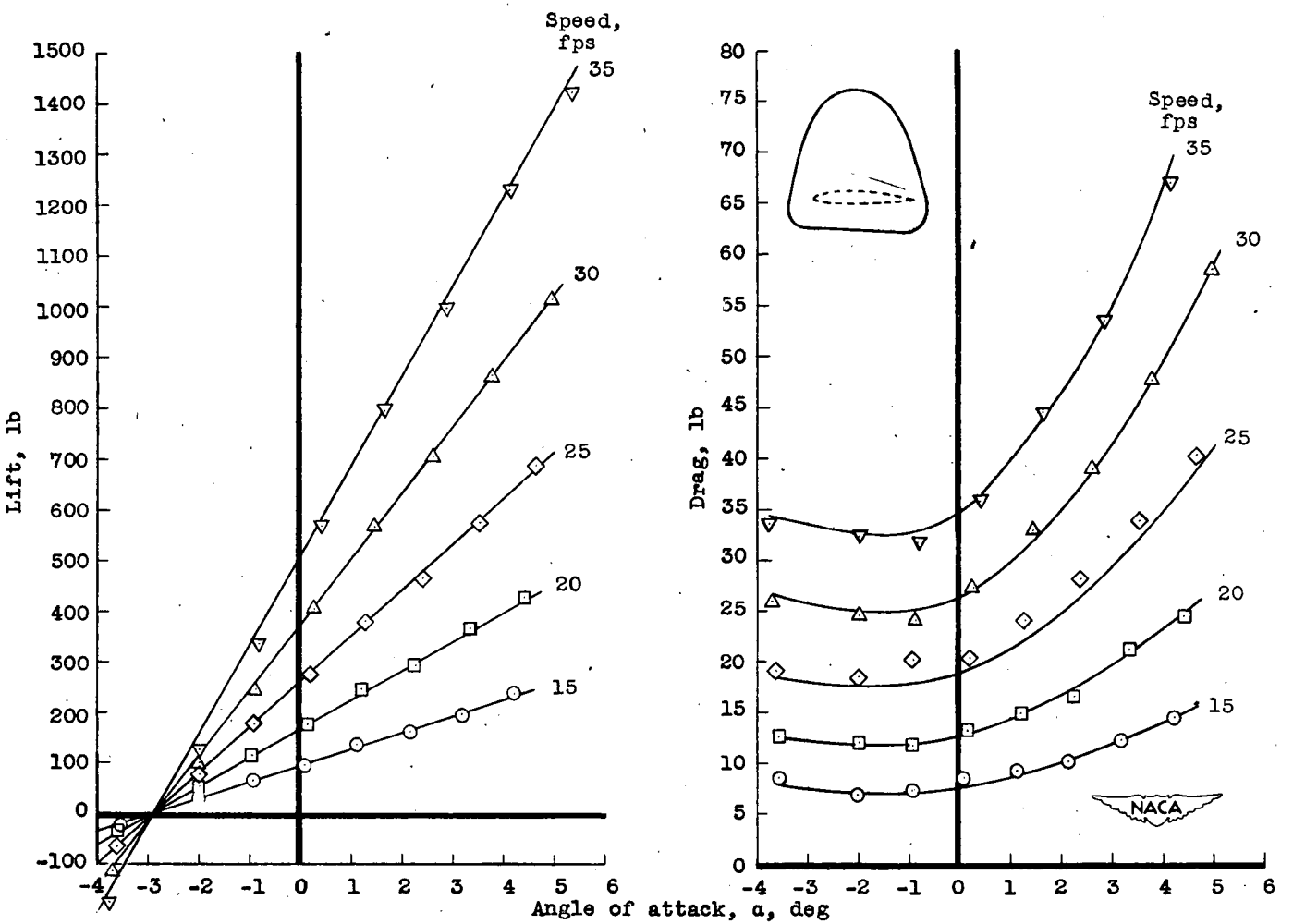

(b) Depth, 3.0 chords.

Figure 10.- Continued.

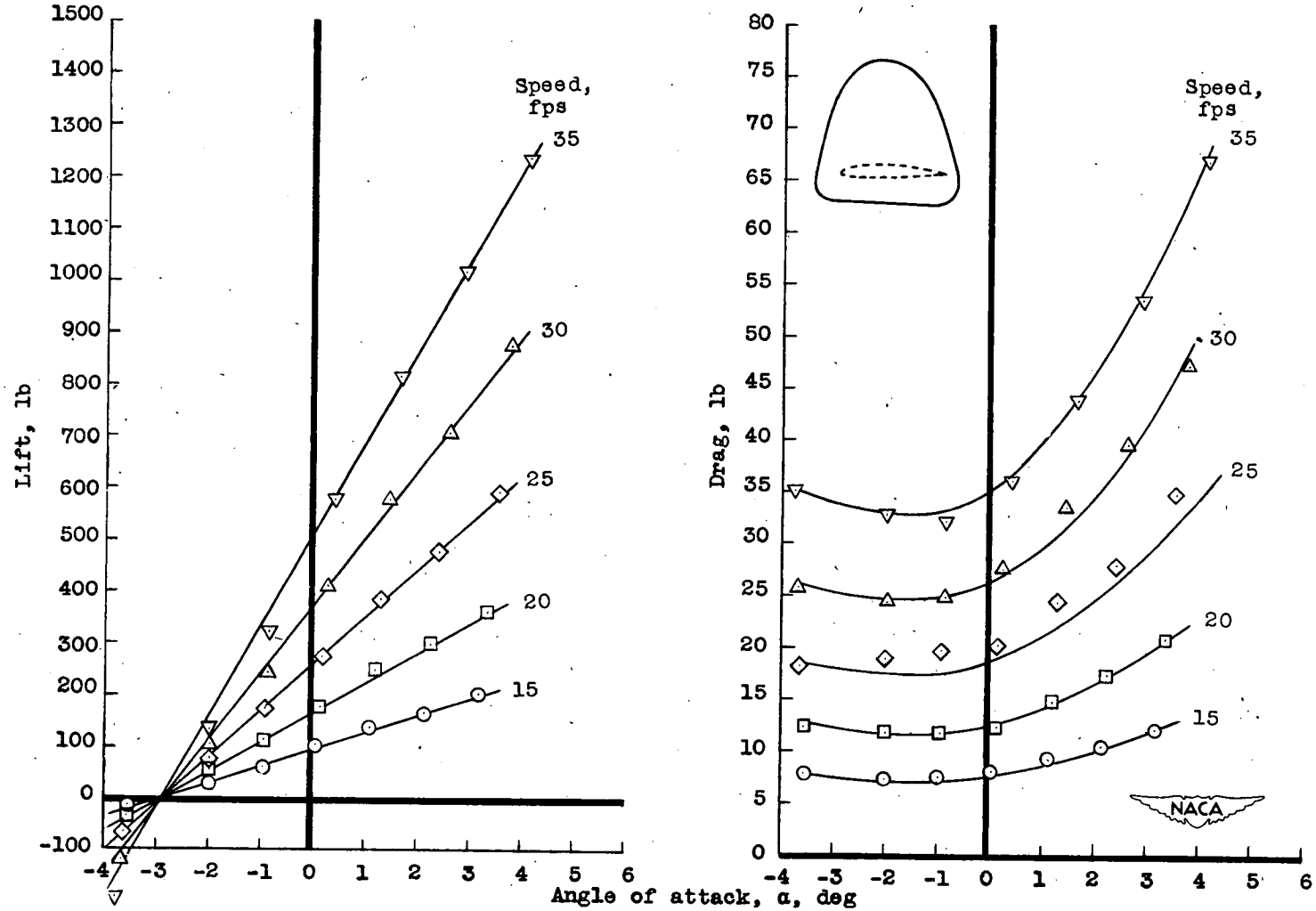

(c) Depth, 4.0 chords.

Figure 10.- Concluded.

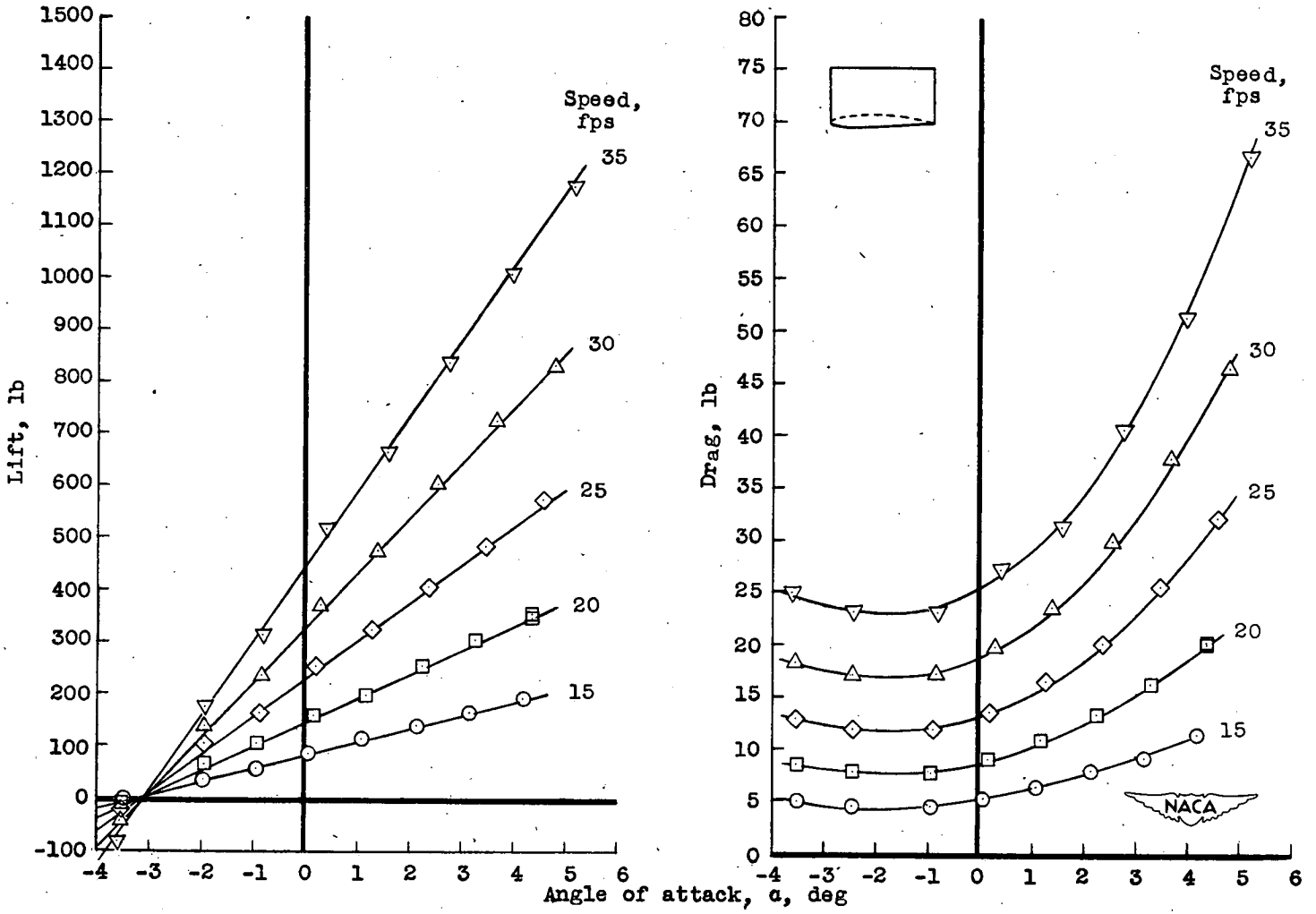

(a) Depth, 1.0 chord.

Figure 11.- Lift and drag of hydrofoil with end plate D.

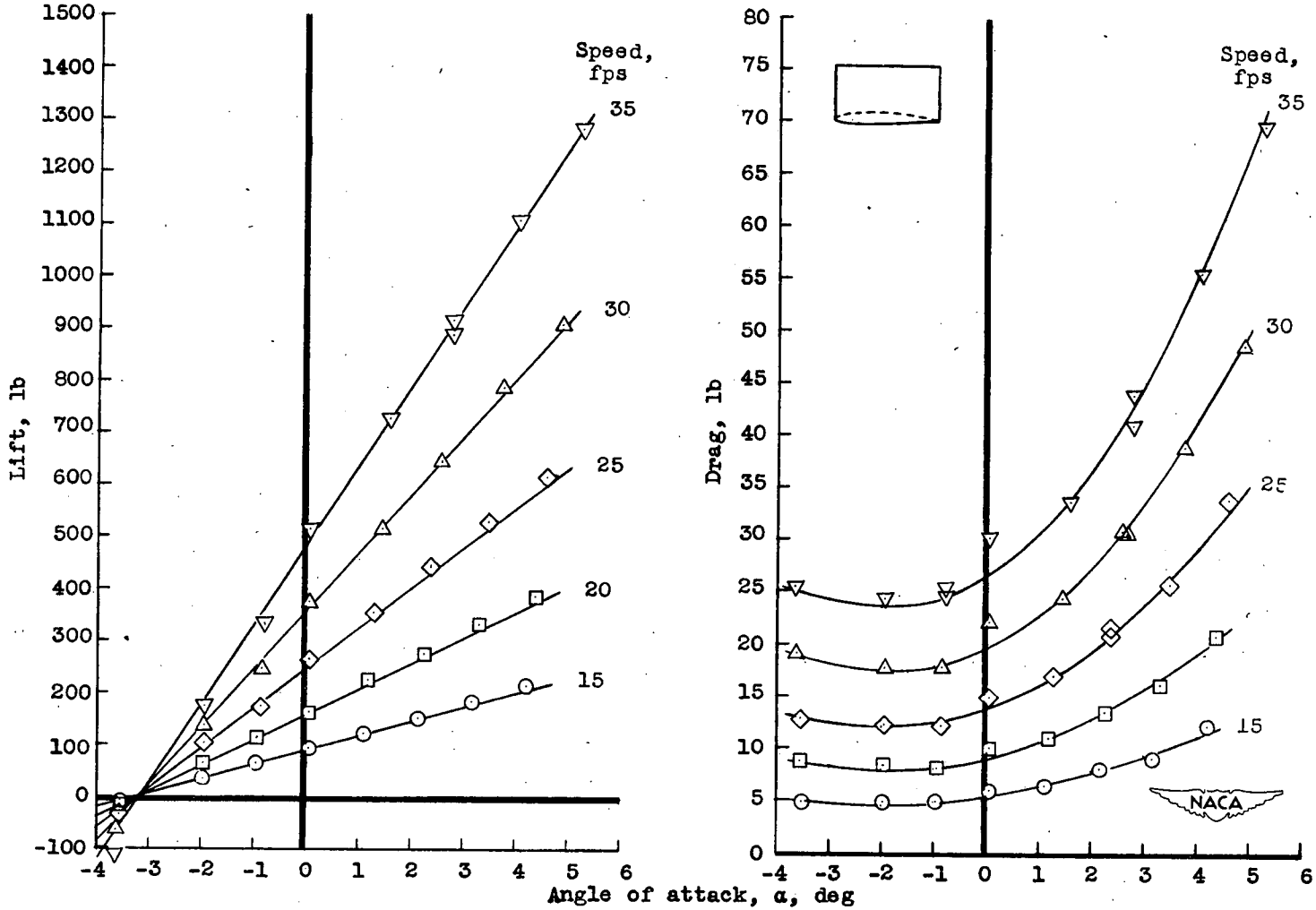

(b) Depth, 2.0 chords.

Figure 11.- Continued.

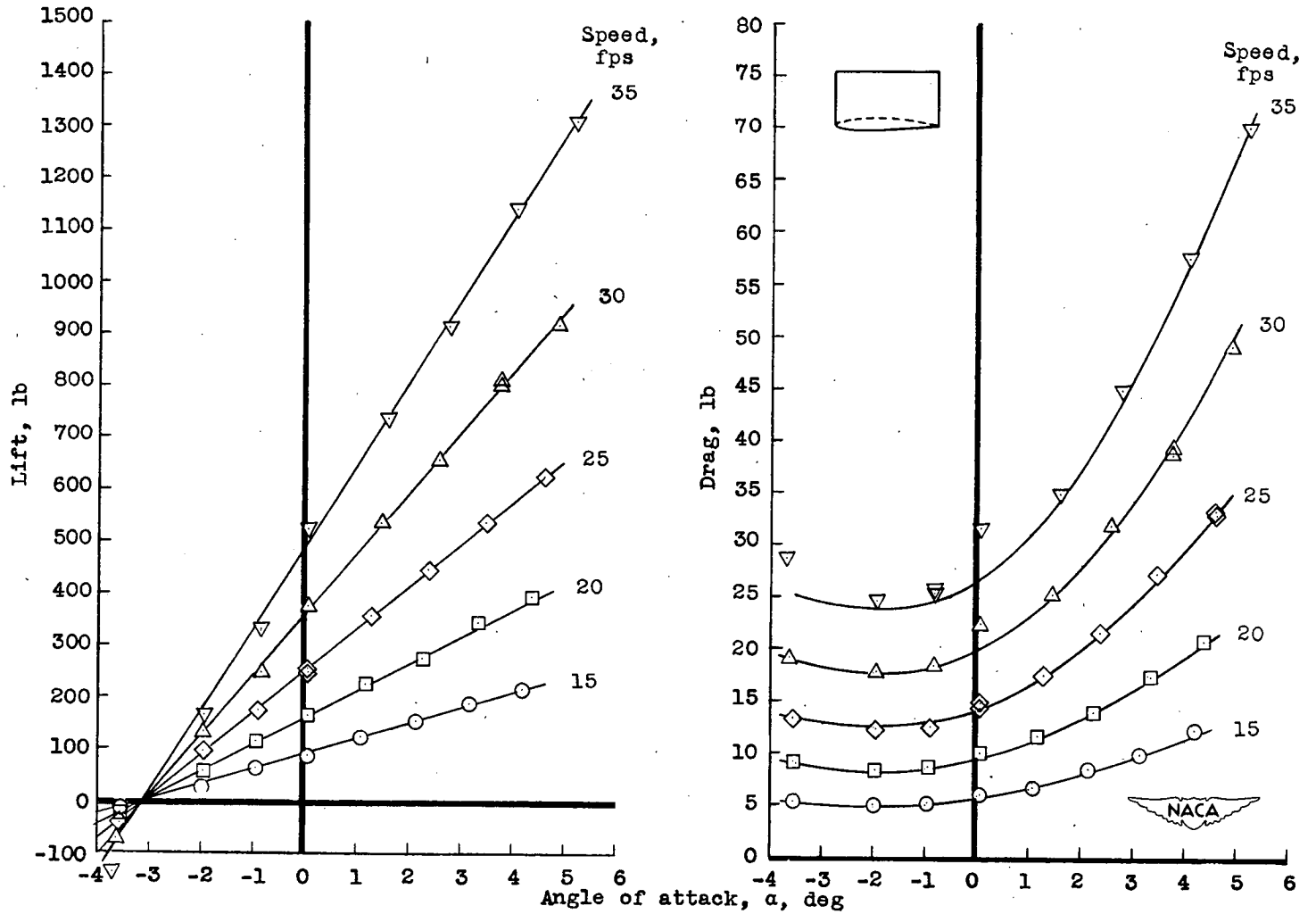

(c) Depth, 3.0 chords.

Figure 11.- Continued.

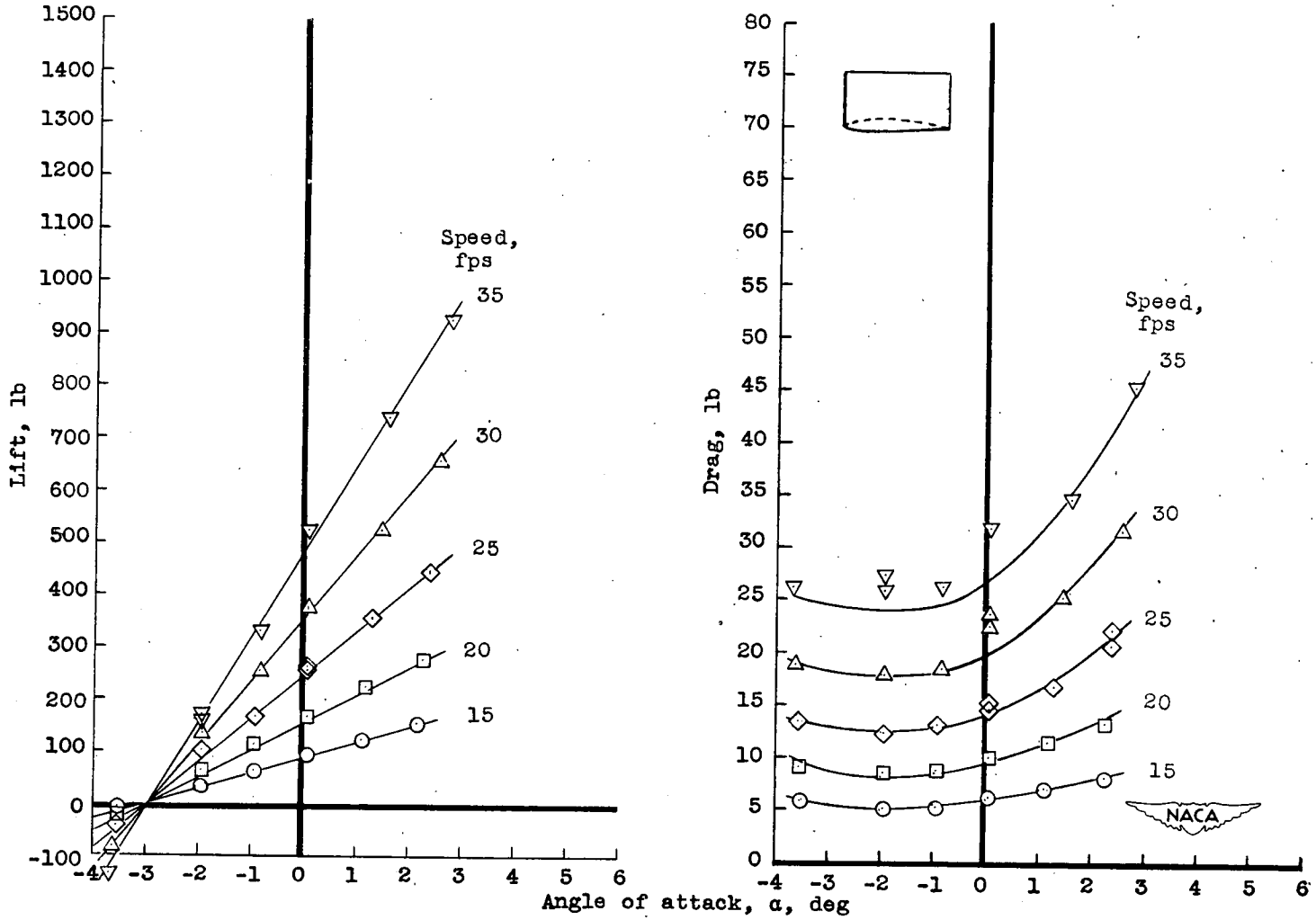

(d) Depth, 4.0 chords.

Figure 11.- Concluded.

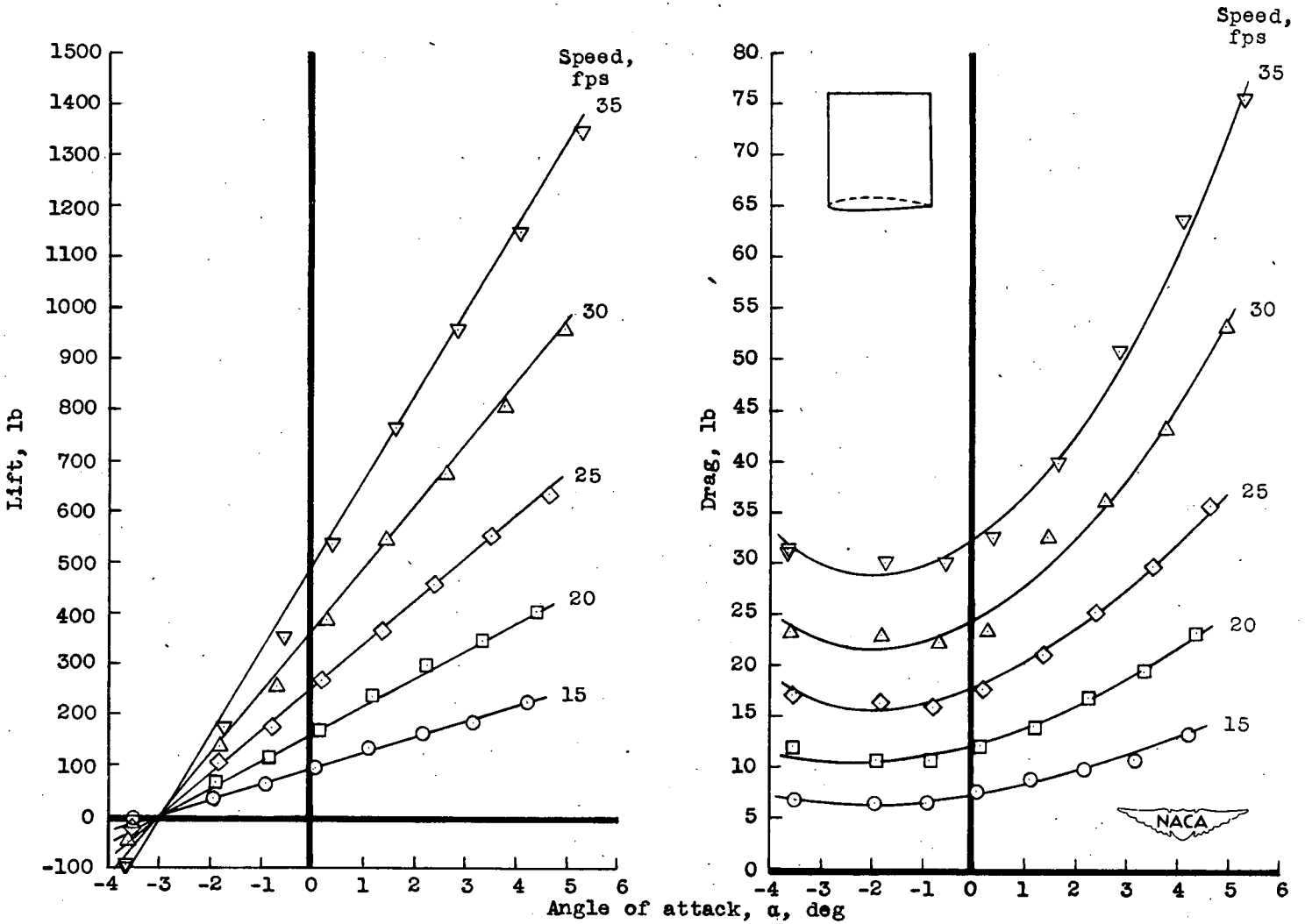

(a) Depth, 2.0 chords.

Figure 12.- Lift and drag of hydrofoil with end plate E.

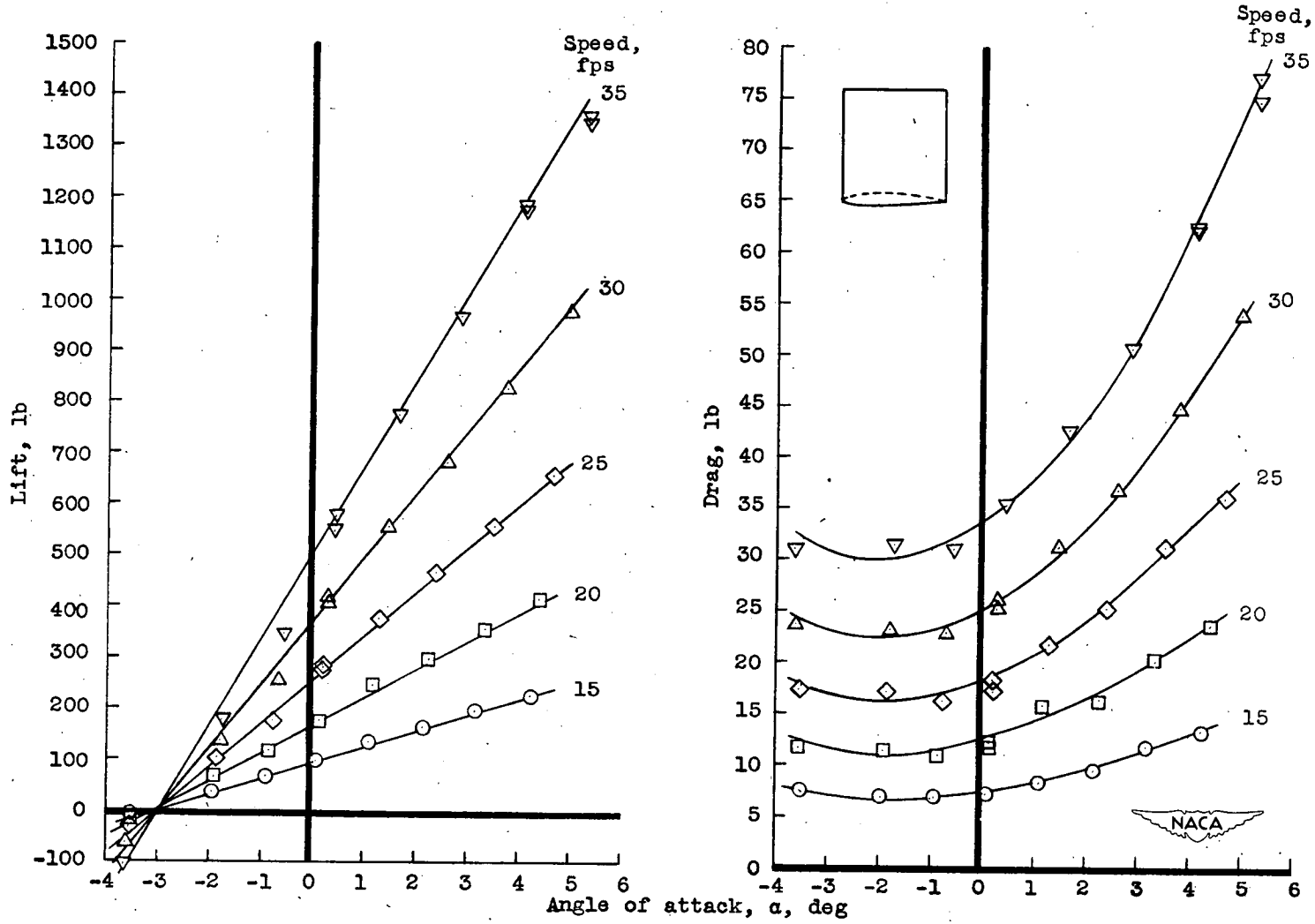

(b) Depth, 3.0 chords.

Figure 12.- Continued.

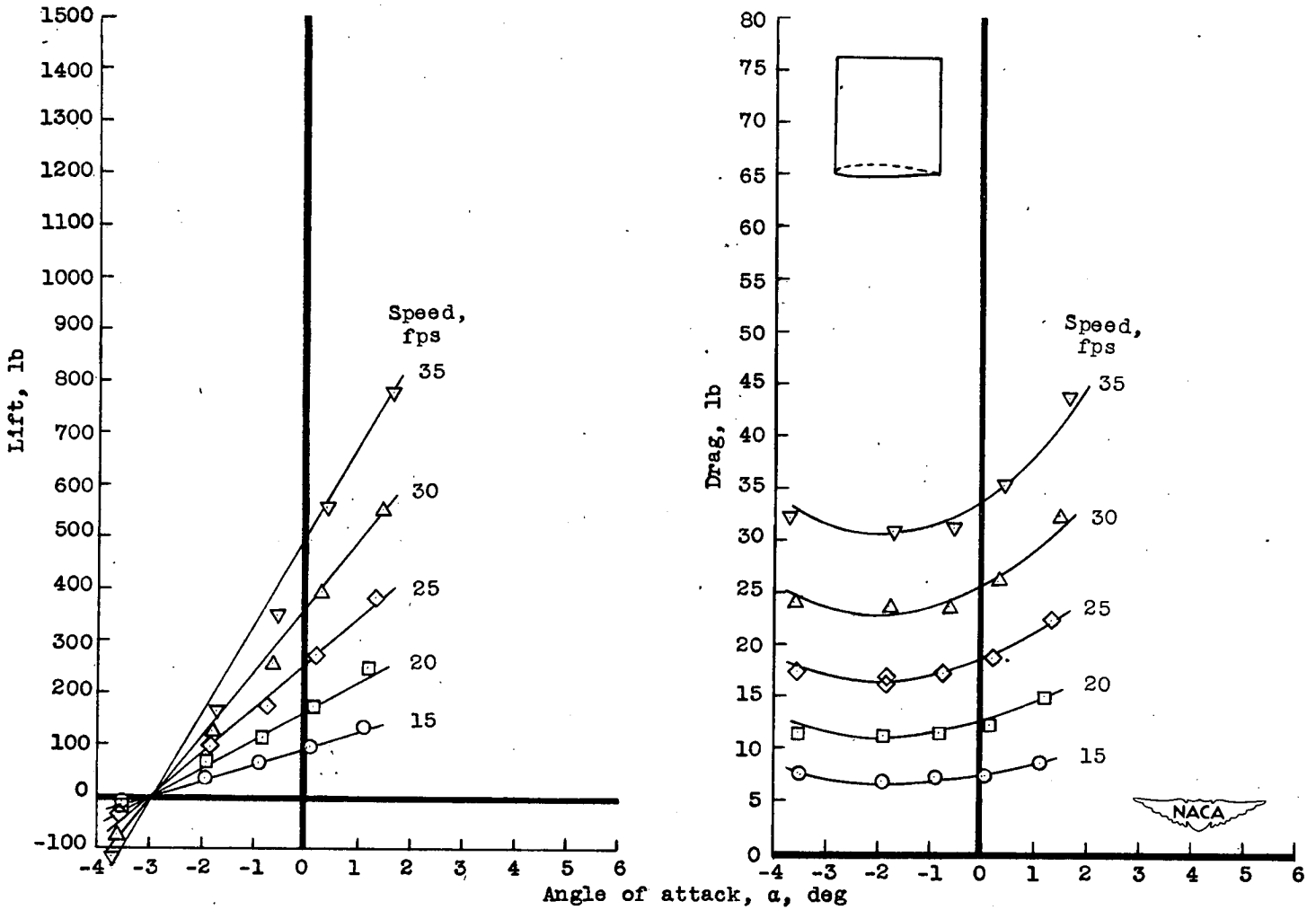

(c) Depth, 4.0 chords.

Figure 12.- Concluded.

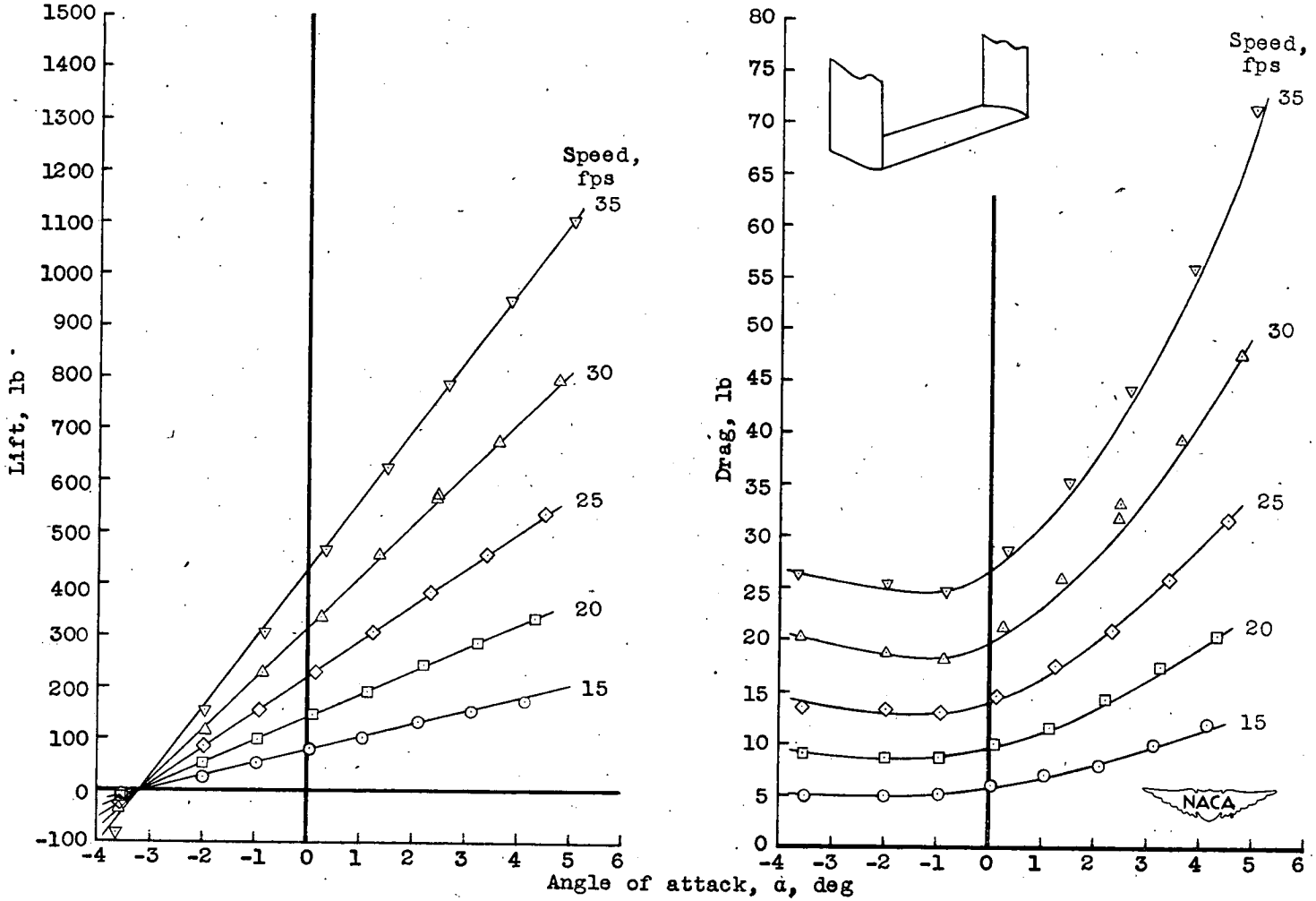

(a) Depth, 0.61 chord.

Figure 13.- Lift and drag of hydrofoil with end struts.

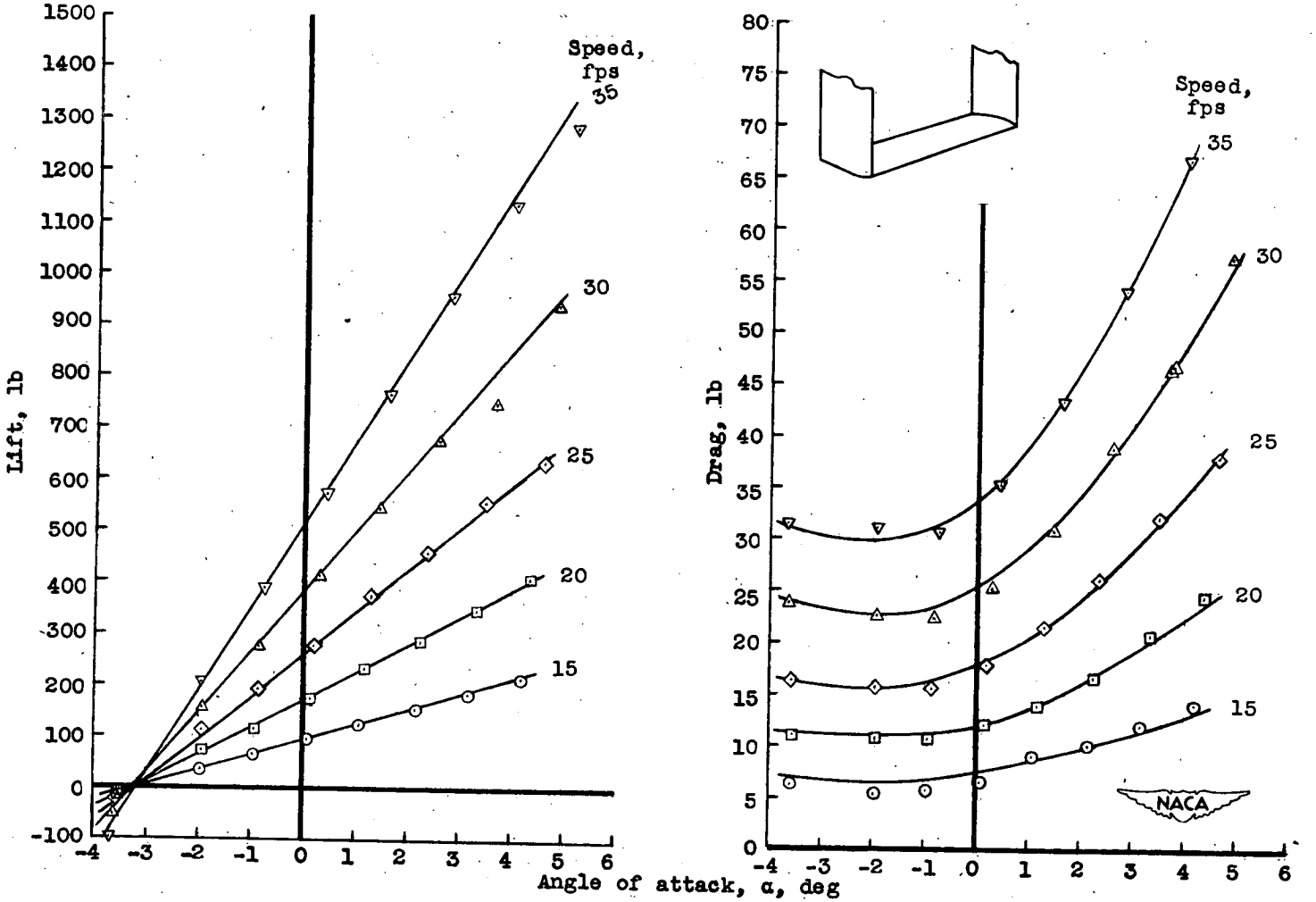

(b) Depth, 1.41 chords.

Figure 13.- Continued.

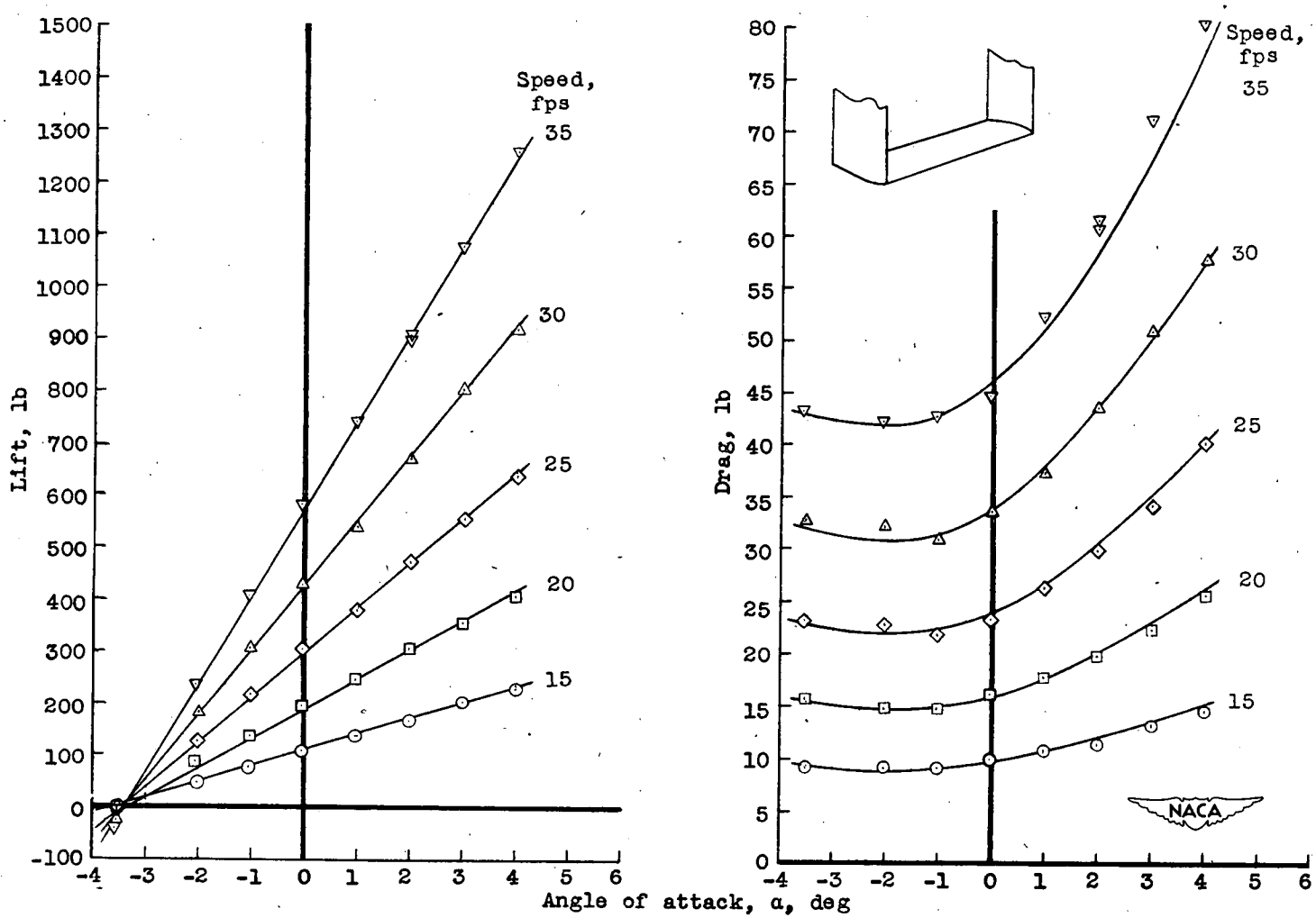

(c) Depth, 2.54 chords.

Figure 13.- Continued.

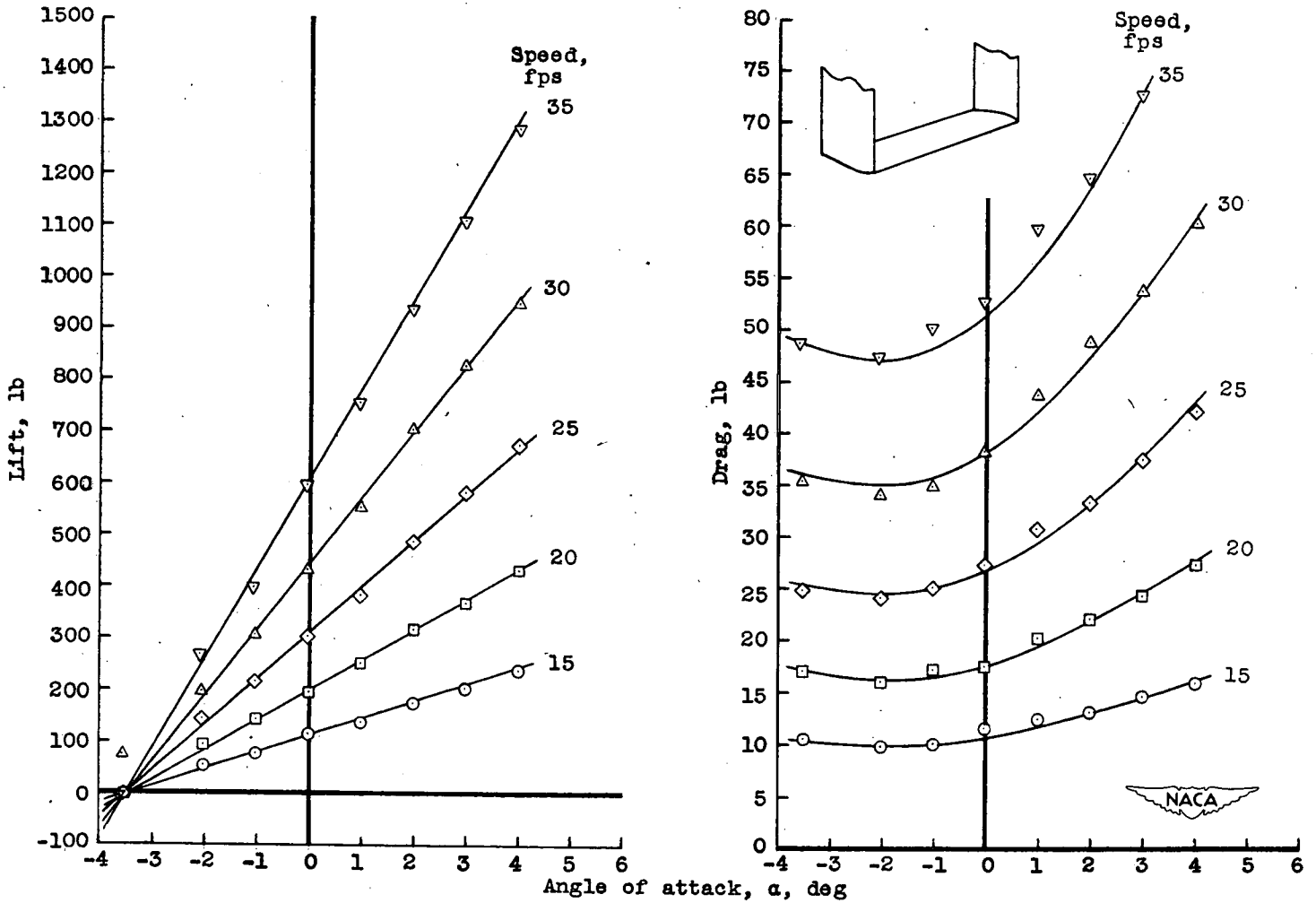

(d) Depth, 3.73 chords.

Figure 13.- Concluded.

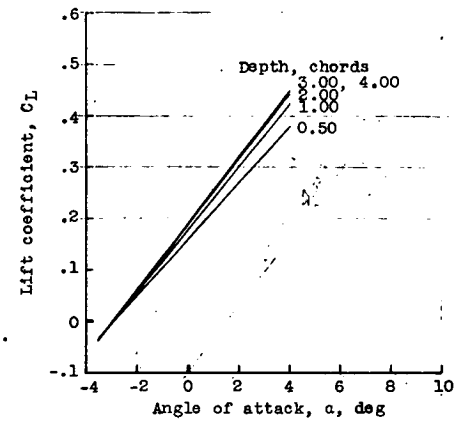

(a) Lift - all speeds.

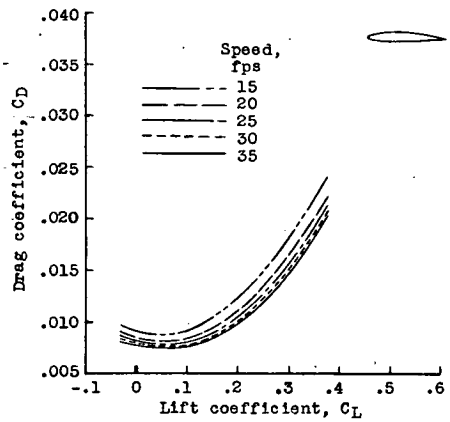

(b) Drag - depth, 0.50 chord.

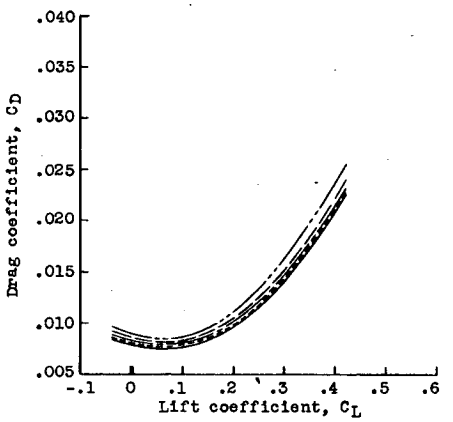

(c) Drag - depth, 1.00 chord.

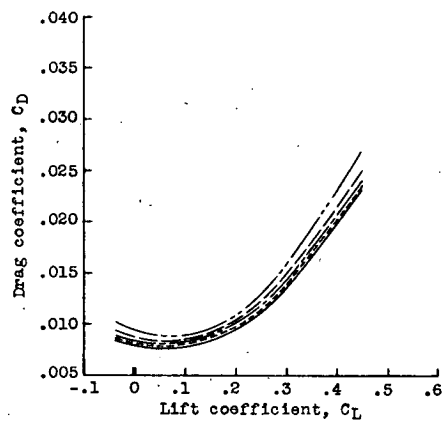

(d) Drag - depth, 2.00 chords.

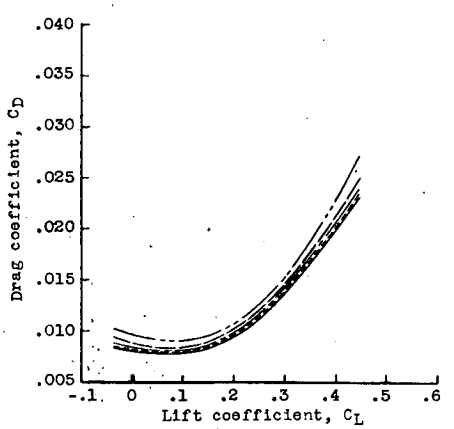

(e) Drag - depth, 3.00 chords.

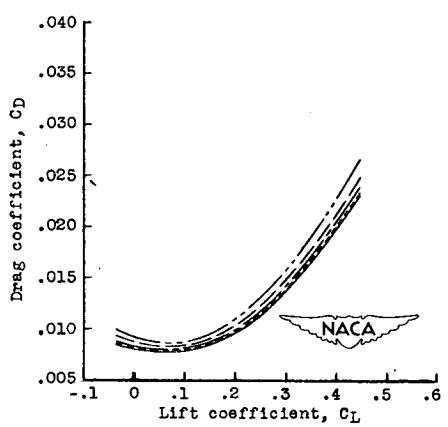

(f) Drag - depth, 4.00 chords.

Figure 14.- Lift and drag coefficients of the hydrofoil without end plates.

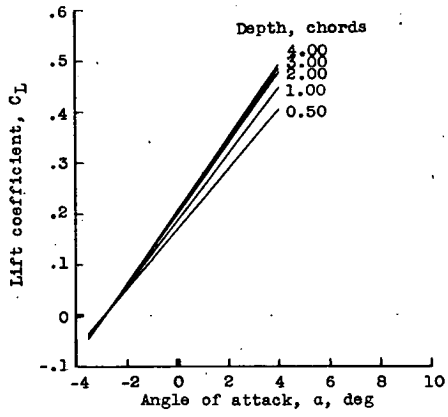

(a) Lift - all speeds.

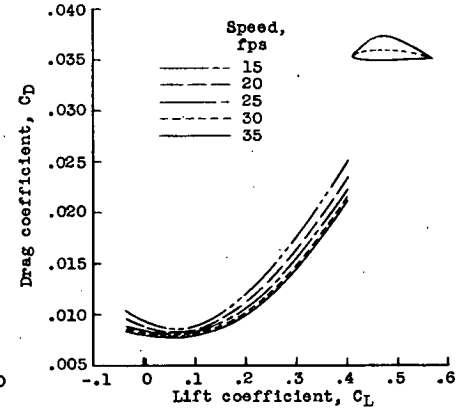

(b) Drag - depth, 0.50 chord.

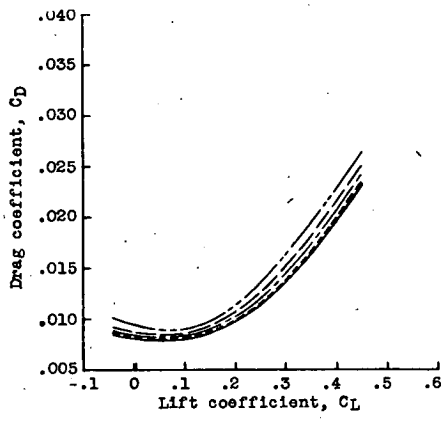

(c) Drag - depth, 1.00 chord.

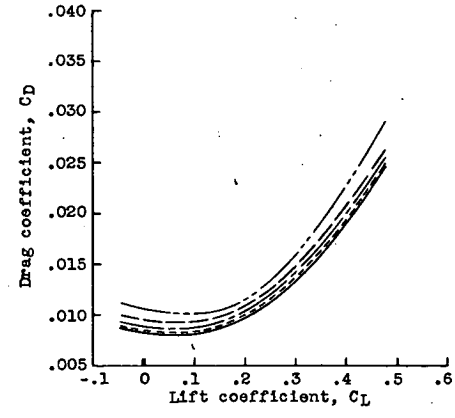

(d) Drag - depth, 2.00 chords.

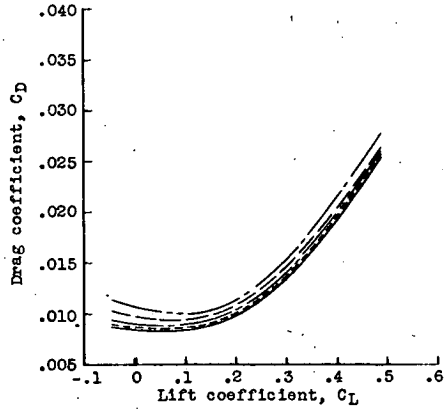

(e) Drag - depth, 3.00 chords.

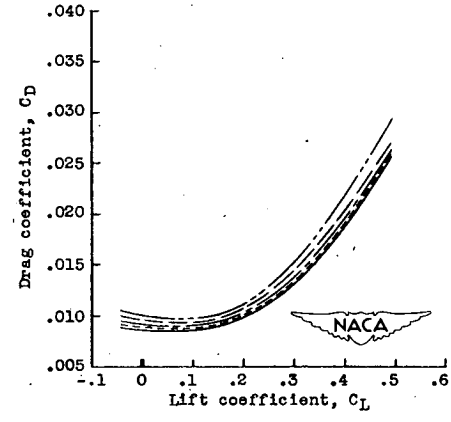

(f) Drag - depth, 4.00 chords.

Figure 15.- Lift and drag coefficients of the hydrofoil with end plate A.

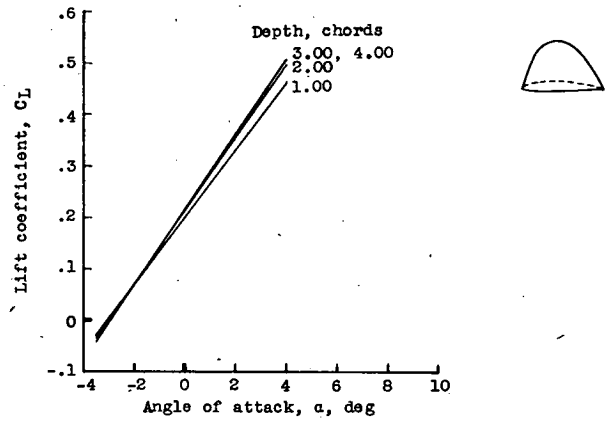

(a) Lift - all speeds.

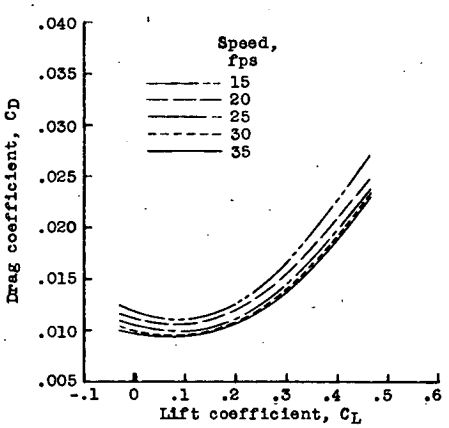

(b) Drag - depth, 1.00 chord.

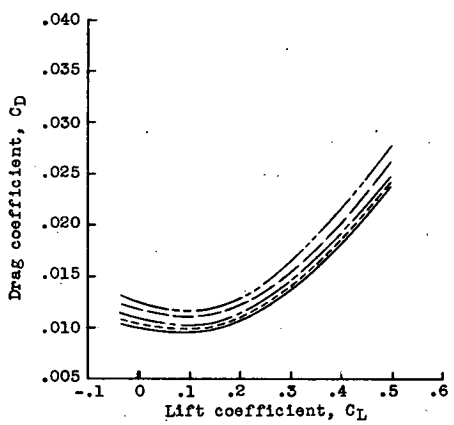

(c) Drag - depth, 2.00 chords.

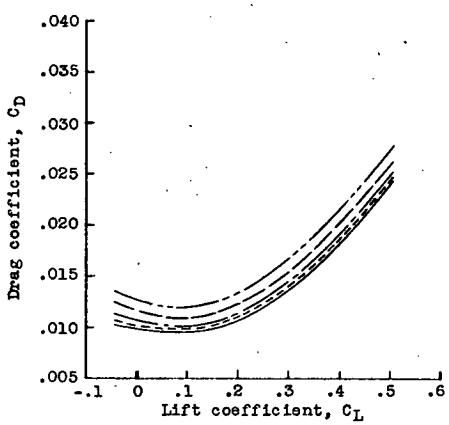

(d) Drag - depth, 3.00 chords.

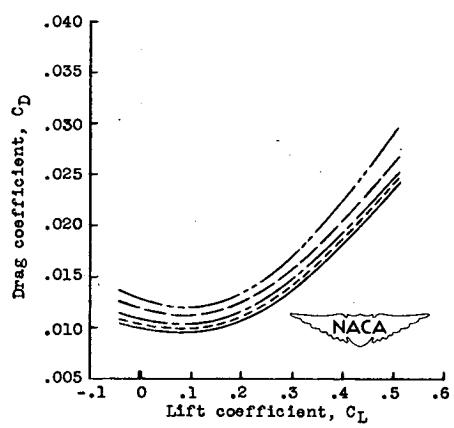

(e) Drag - depth, 4.00 chords.

Figure 16.- Lift and drag coefficients of the hydrofoil with end plate B.

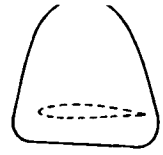

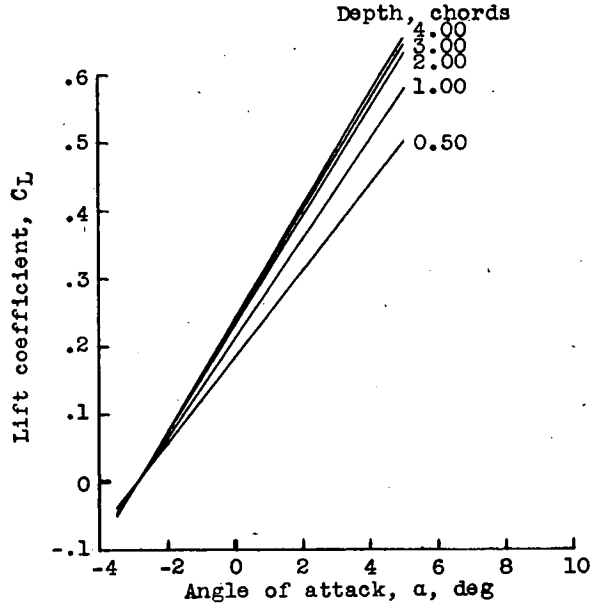

(a) Lift - all speeds.

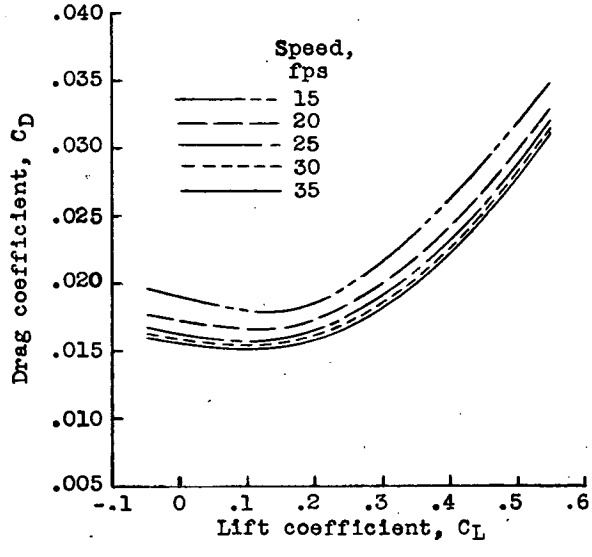

(b) Drag - depth, 2.00 chords.

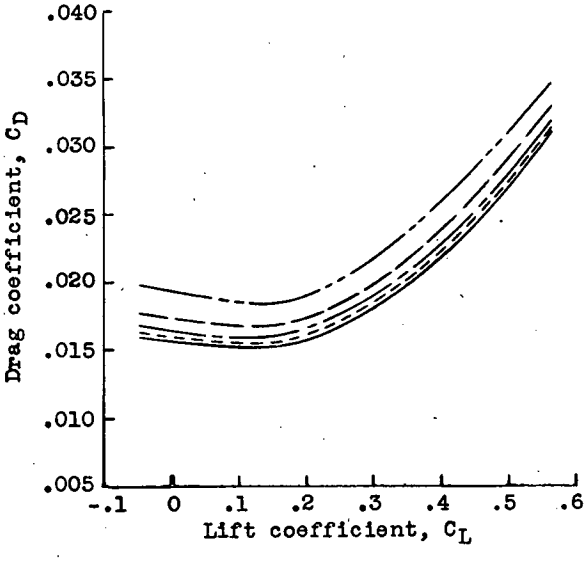

(c) Drag - depth, 3.00 chords.

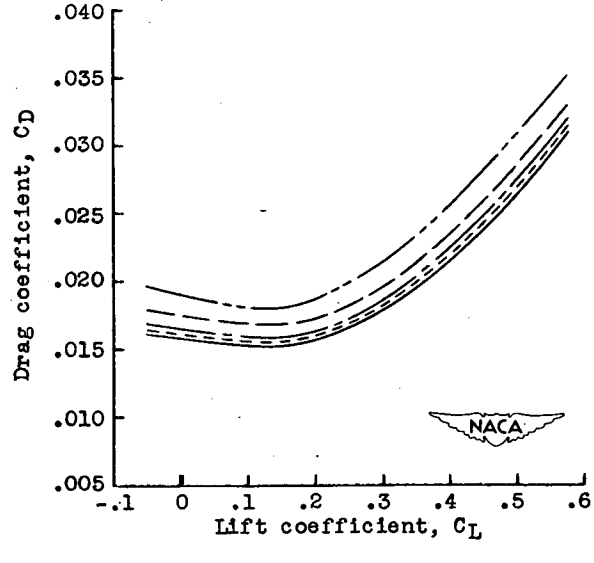

(d) Drag - depth, 4.00 chords.

Figure 17.- Lift and drag coefficients of the hydrofoil with end plate C.

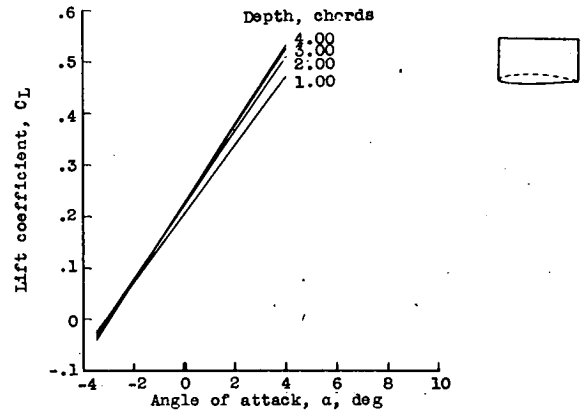

(a) Lift - all speeds.

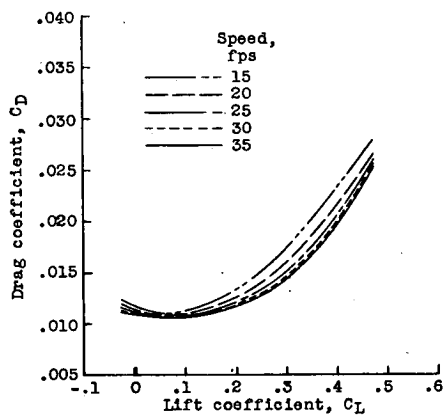

(b) Drag - depth, 1.00 chord.

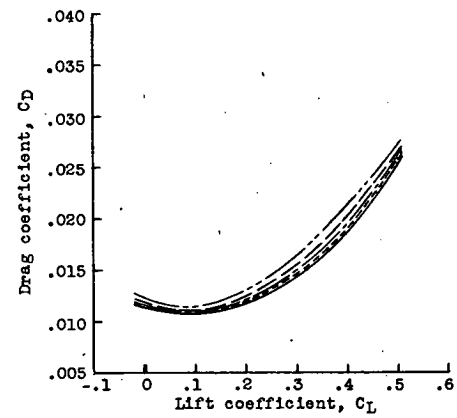

(c) Drag - depth, 2.00 chords.

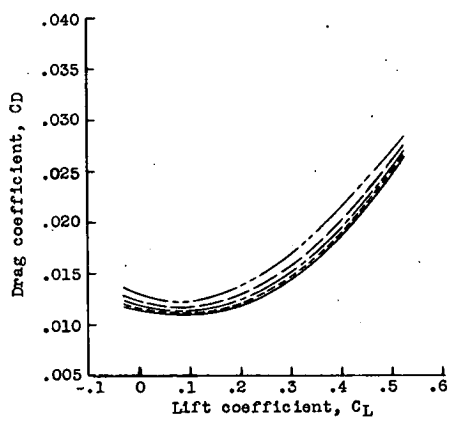

(d) Drag - depth, 3.00 chords.

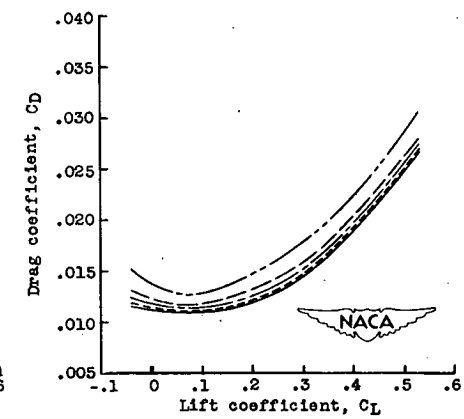

(e) Drag - depth, 4.00 chords.

Figure 18.- Lift and drag coefficients of the hydrofoil with end plate D.

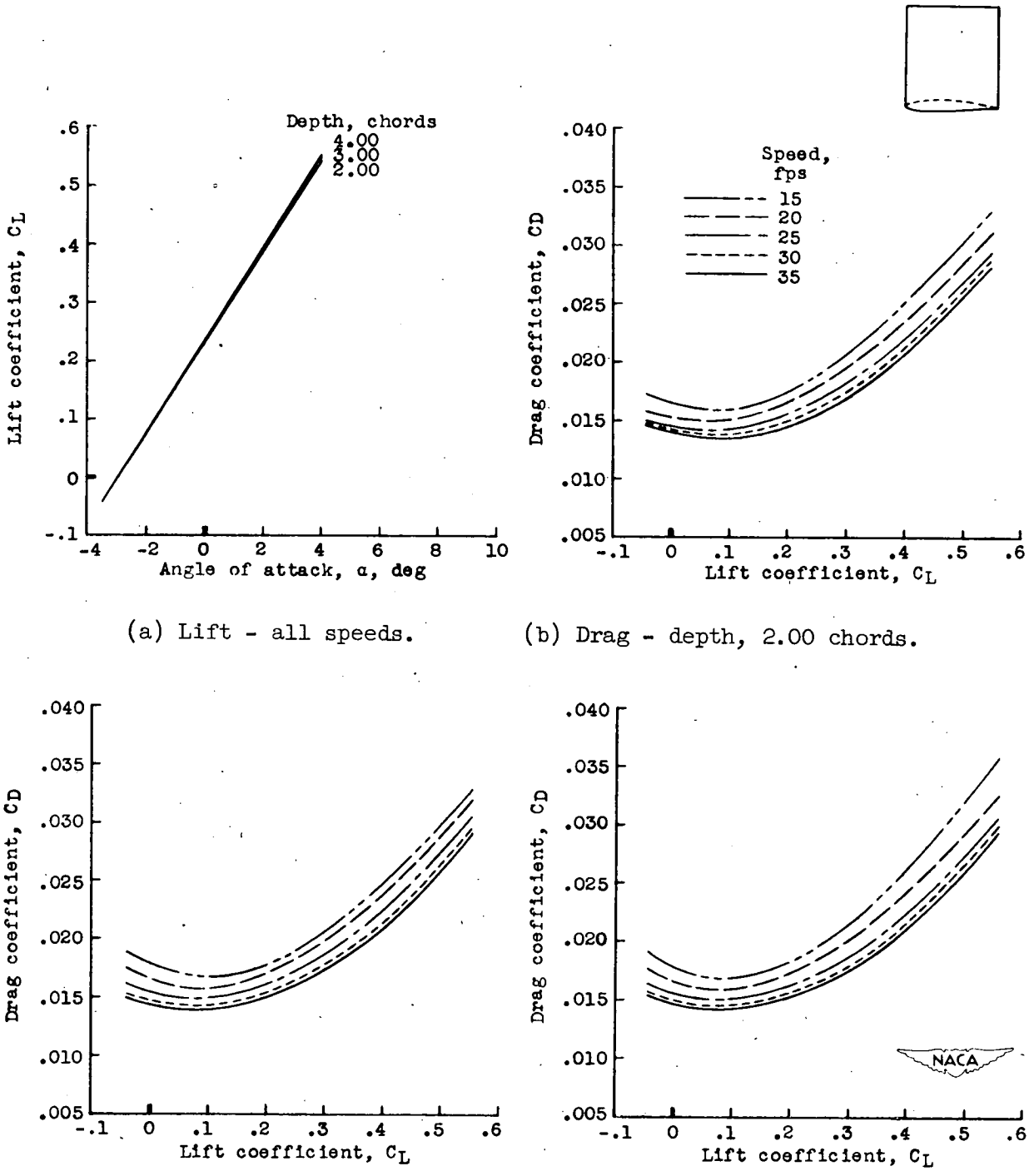

(a) Lift - all speeds.

(b) Drag - depth, 2.00 chords.

(c) Drag - depth, 3.00 chords.

(d) Drag - depth, 4.00 chords.

Figure 19.- Lift and drag coefficients of the hydrofoil with end plate E.

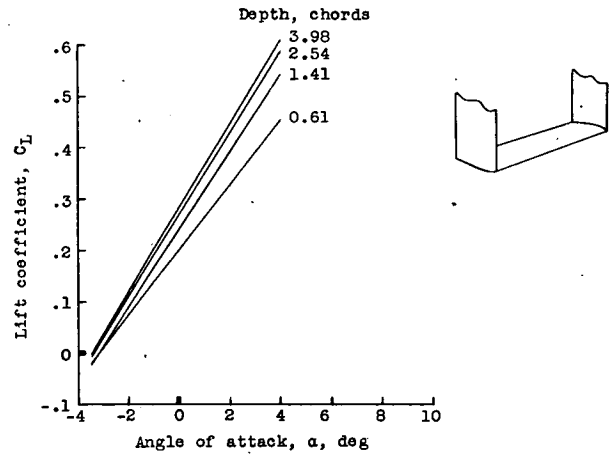

(a) Lift - all speeds.

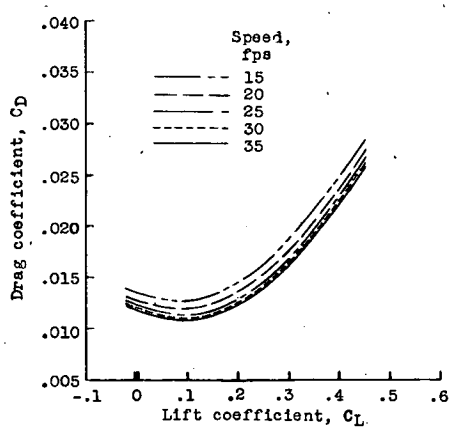

(b) Drag - depth, 0.61 chord.

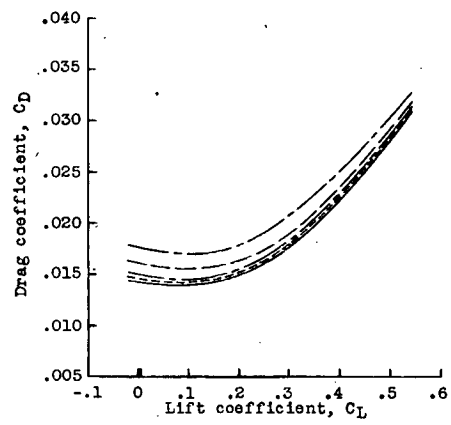

(c) Drag - depth, 1.41 chords.

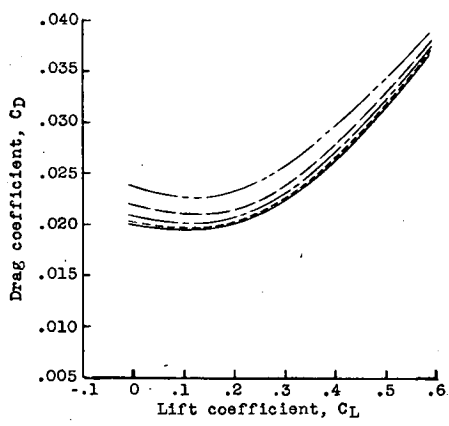

(d) Drag - depth, 2.54 chords.

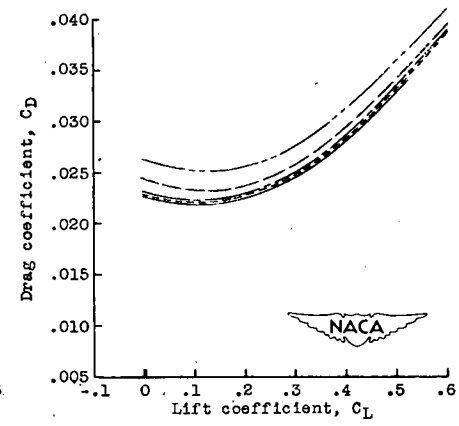

(e) Drag - depth, 3.98 chords.

Figure 20.- Lift and drag coefficients of the hydrofoil with end struts.

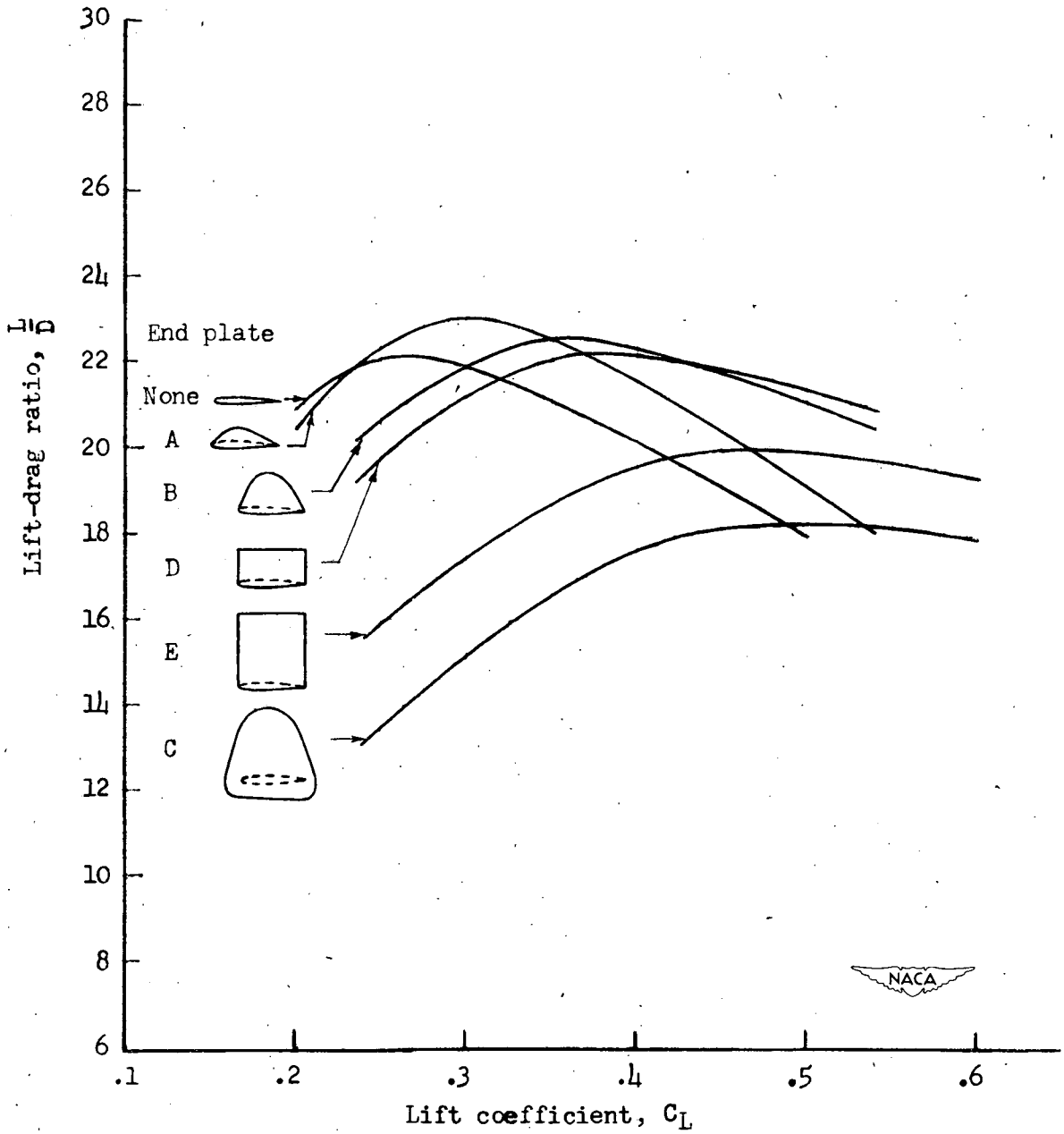

Figure 21.- Variation of lift-drag ratio with lift coefficient for the hydrofoil with and without end plates. Speed, 35 feet per second; depth, 4.0 chords.

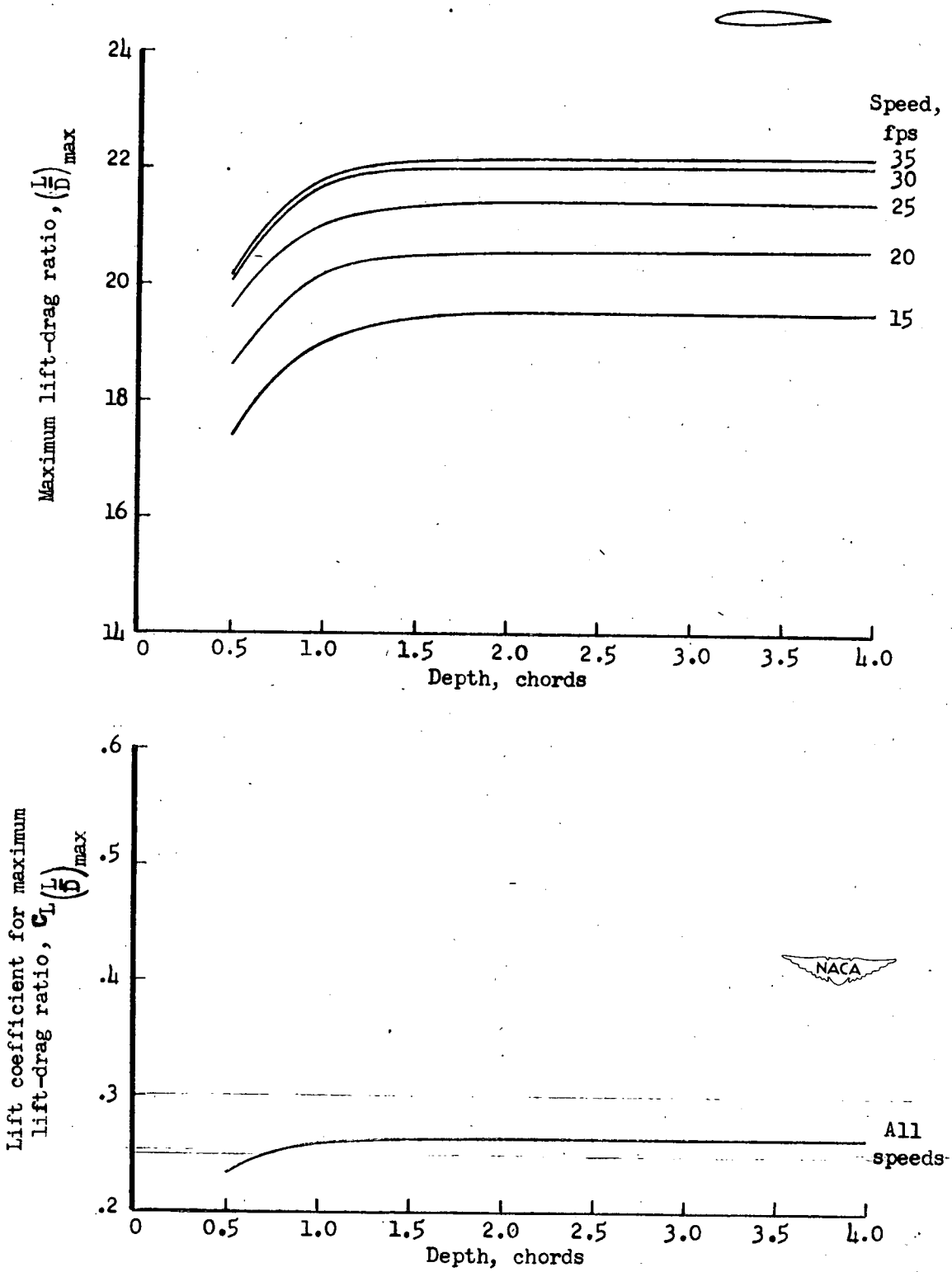

(a) No end plates.

Figure 22.- Variation of maximum lift-drag ratio and lift coefficient at which it occurs, with depth and speed.

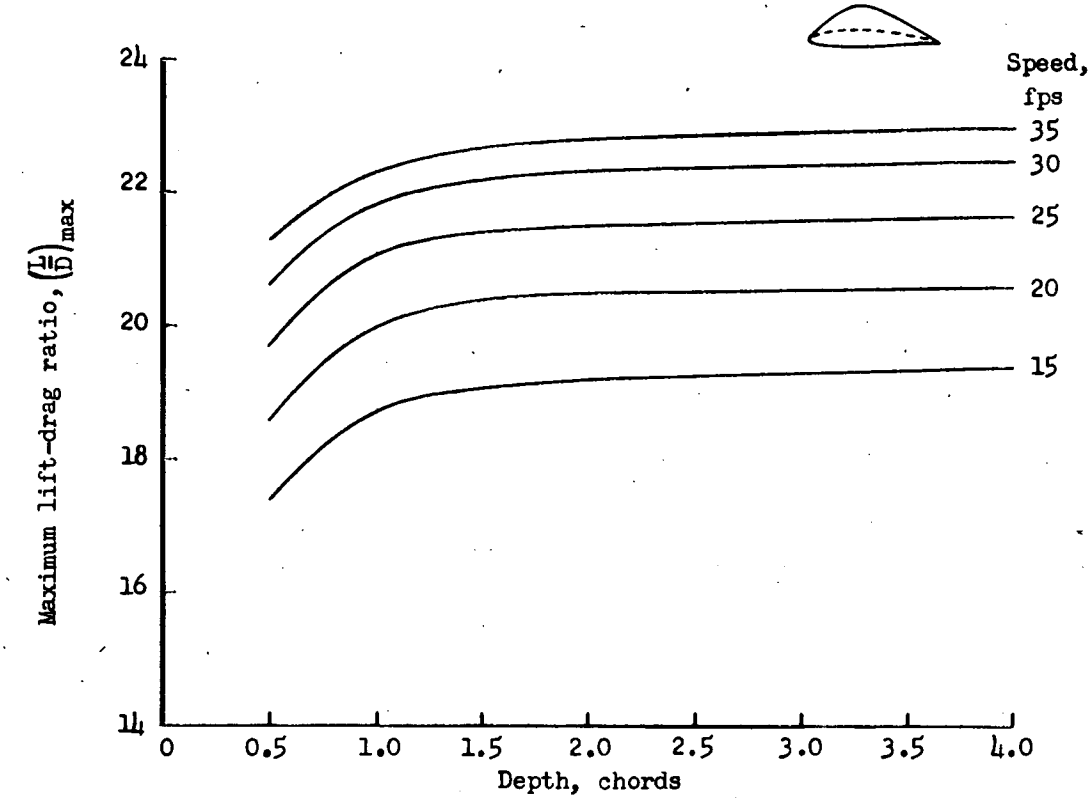

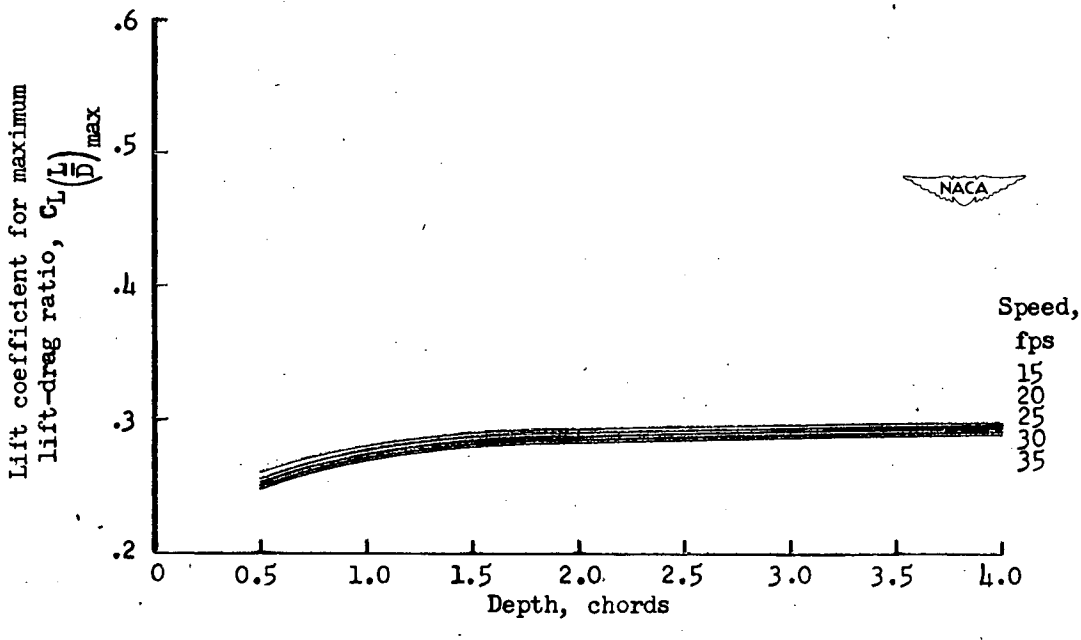

(b) End plate A.

Figure 22.- Continued.

[redacted]

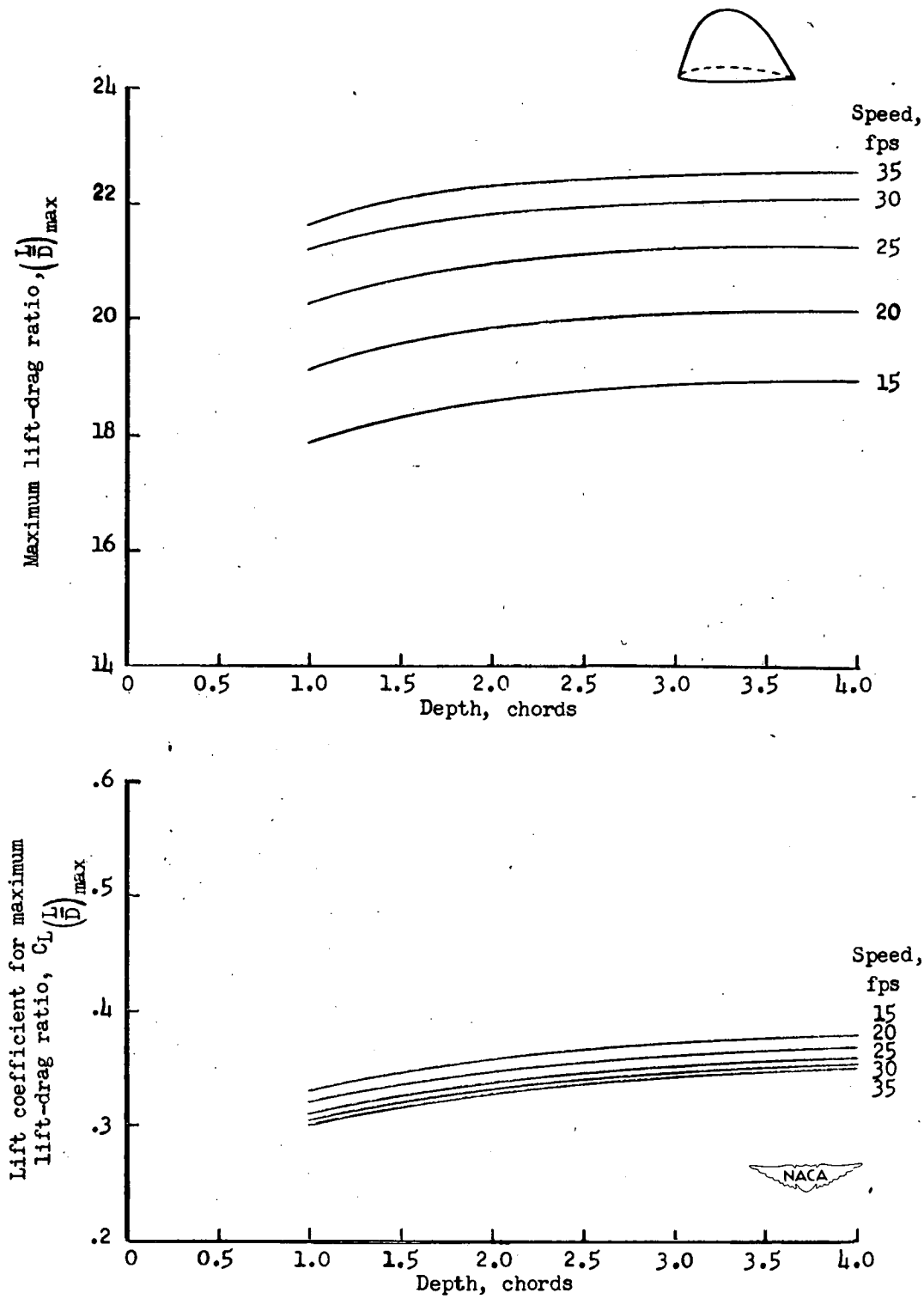

(c) End plate B.

Figure 22.- Continued.

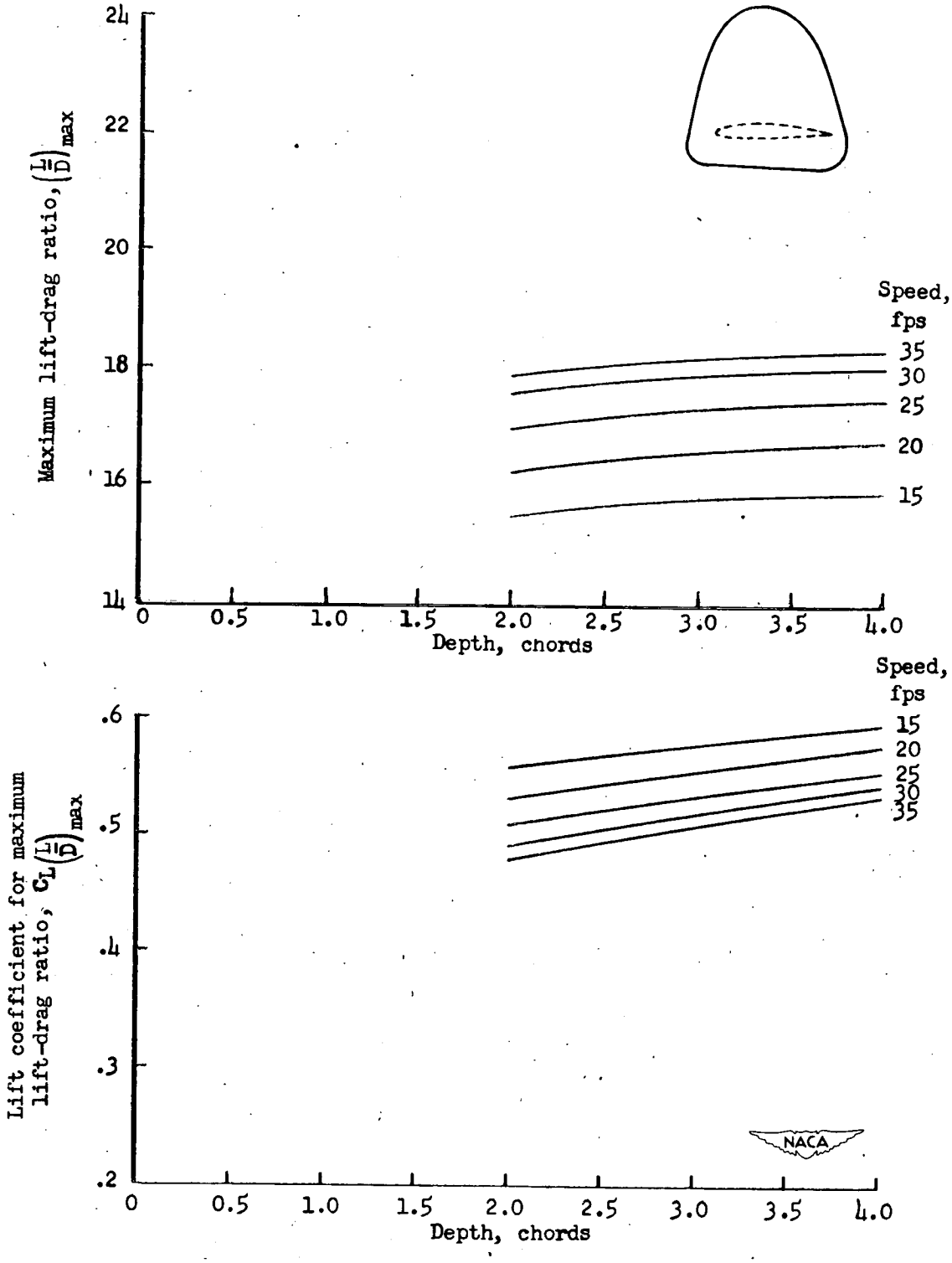

(d) End plate C.

Figure 22.- Continued.

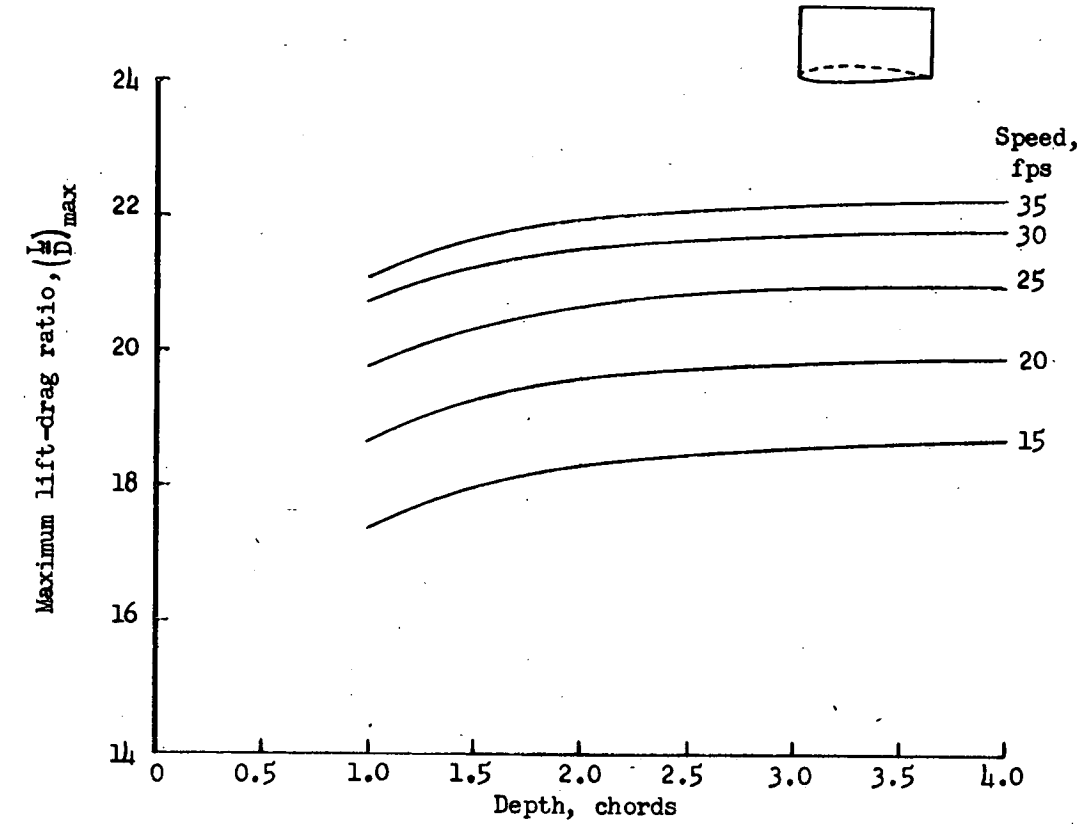

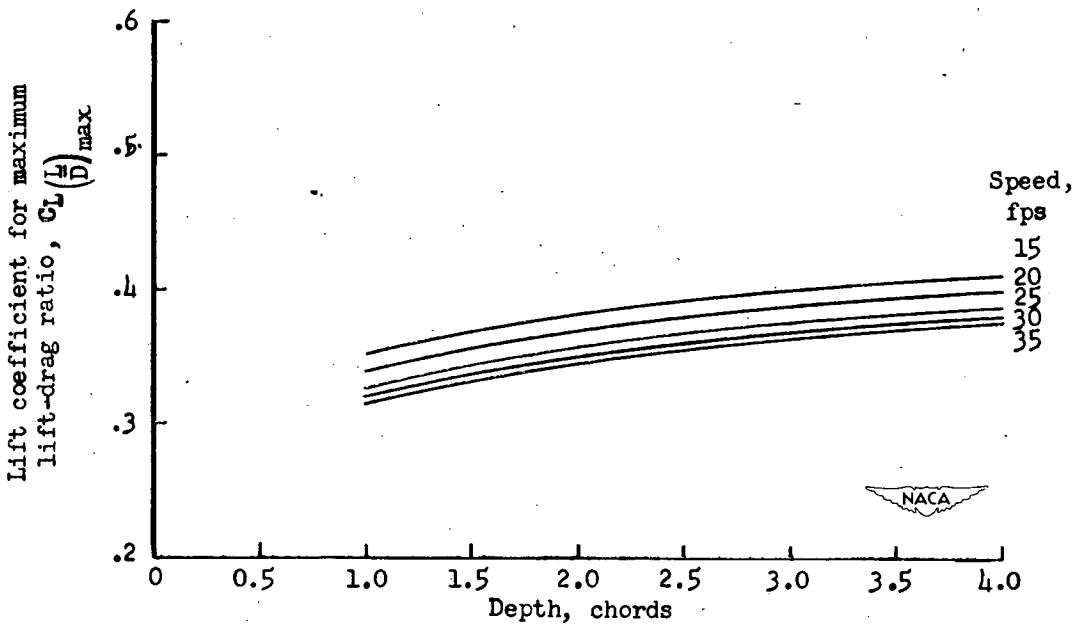

(e) End plate D.

Figure 22.- Continued.

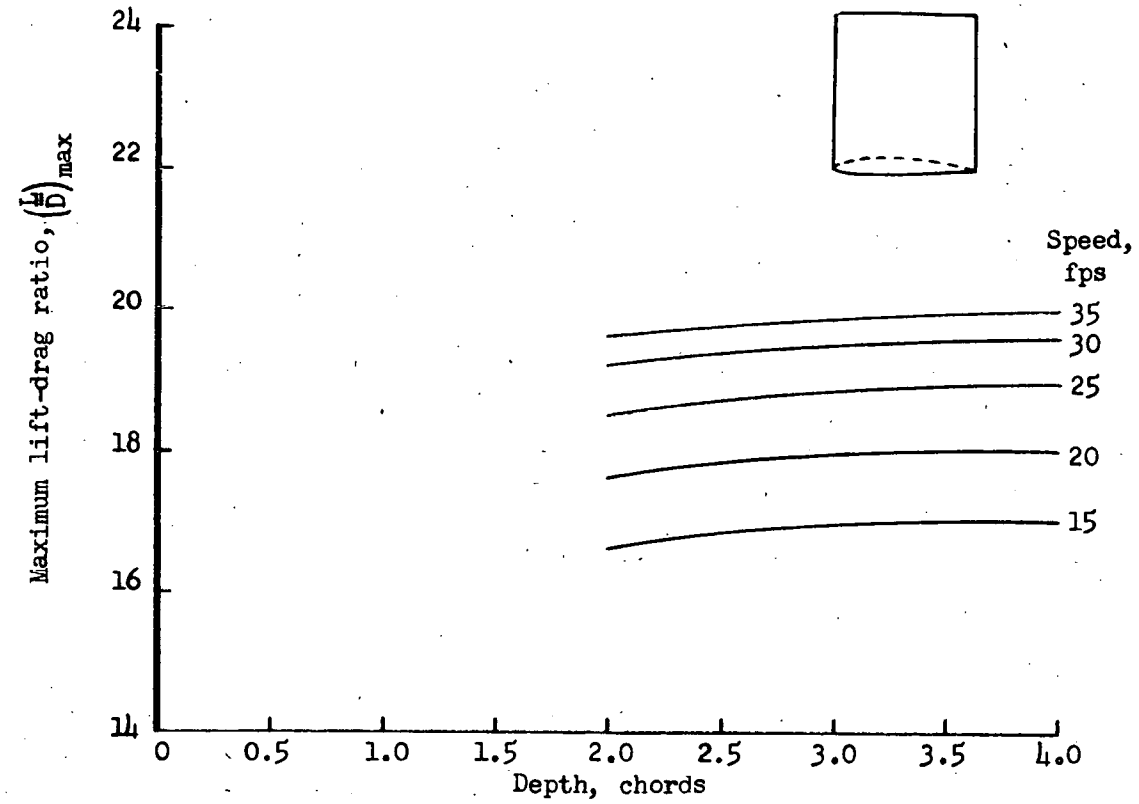

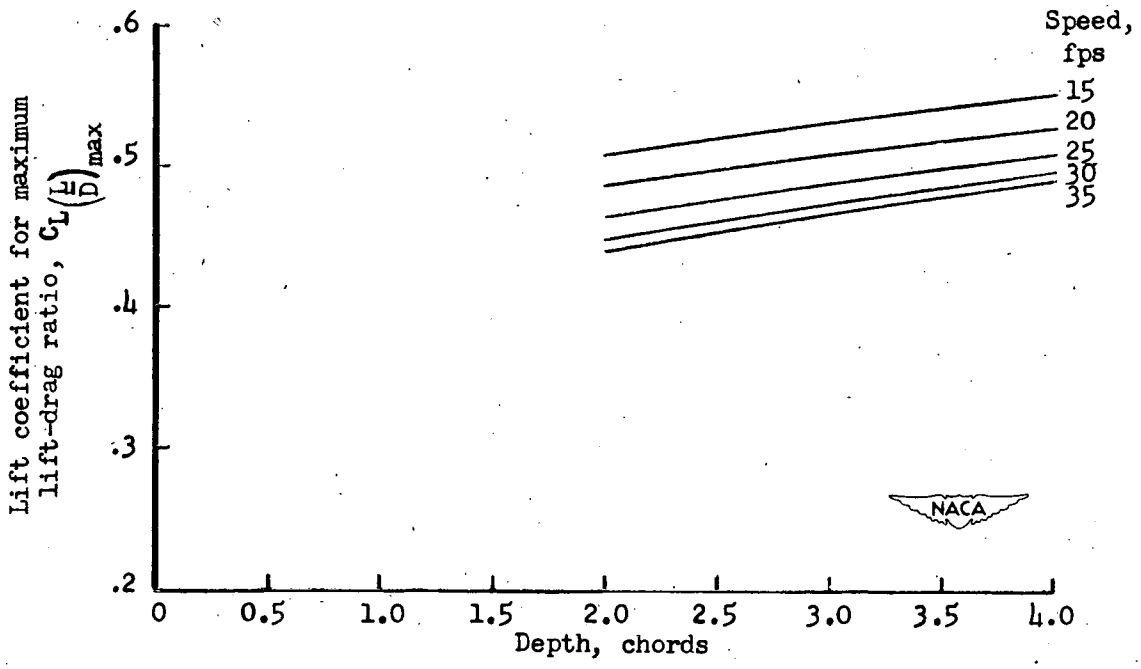

(f) End plate E.

Figure 22.- Concluded.

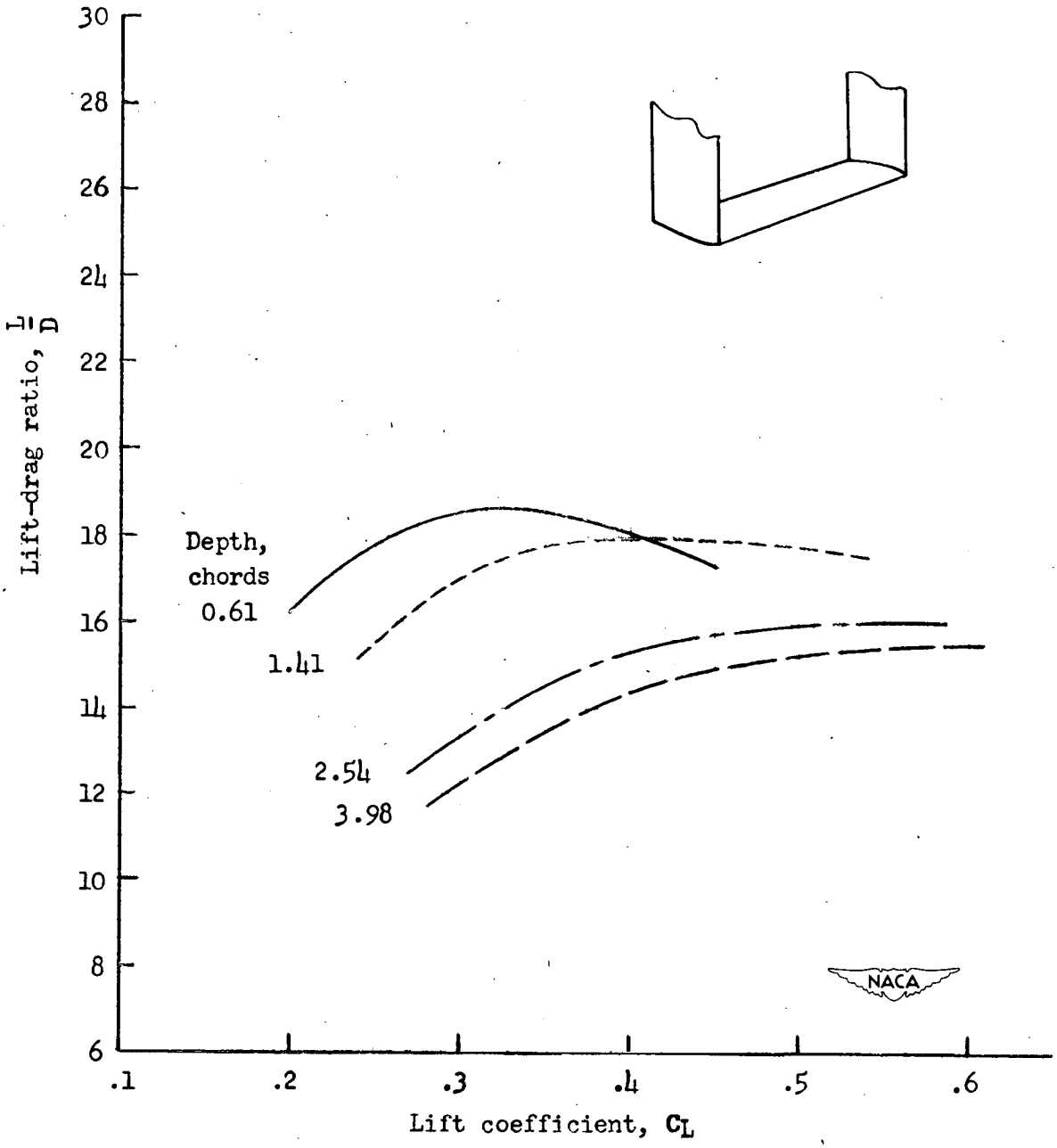

Figure 23.- Variation of lift-drag ratio with lift coefficient for the hydrofoil with end struts. Speed, 35 feet per second.

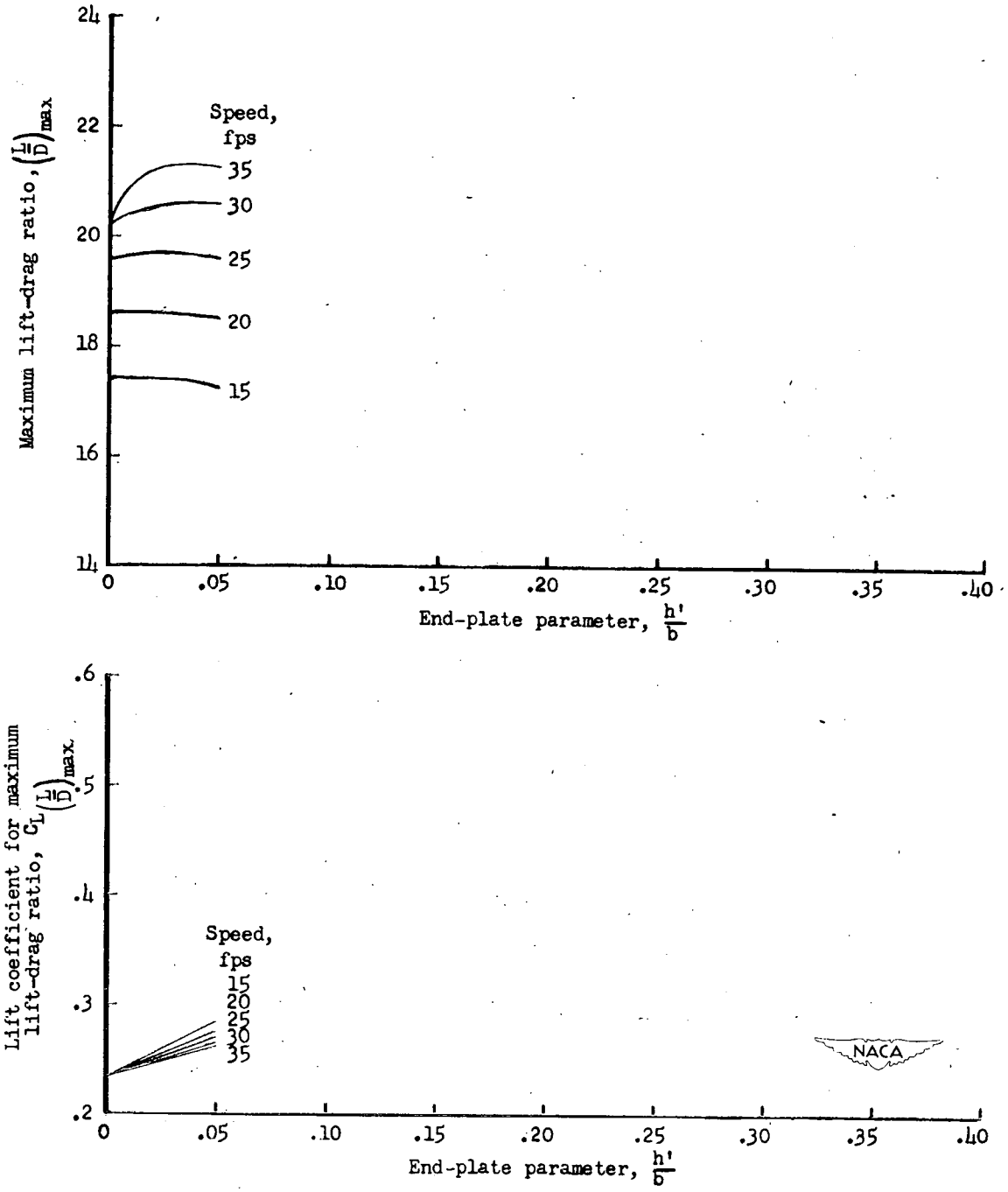

(a) Depth, 0.5 chord.

Figure 24.- Variation of maximum lift-drag ratio and the lift coefficient at which it occurs with speed and end-plate parameter h'/b.

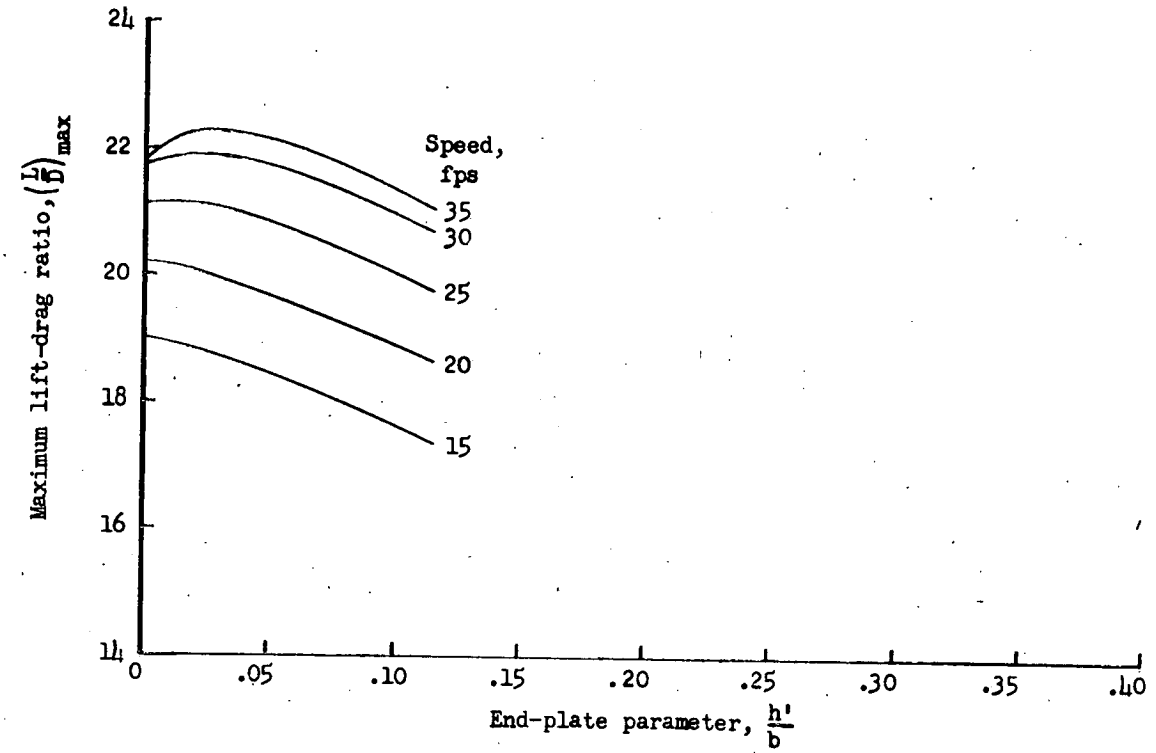

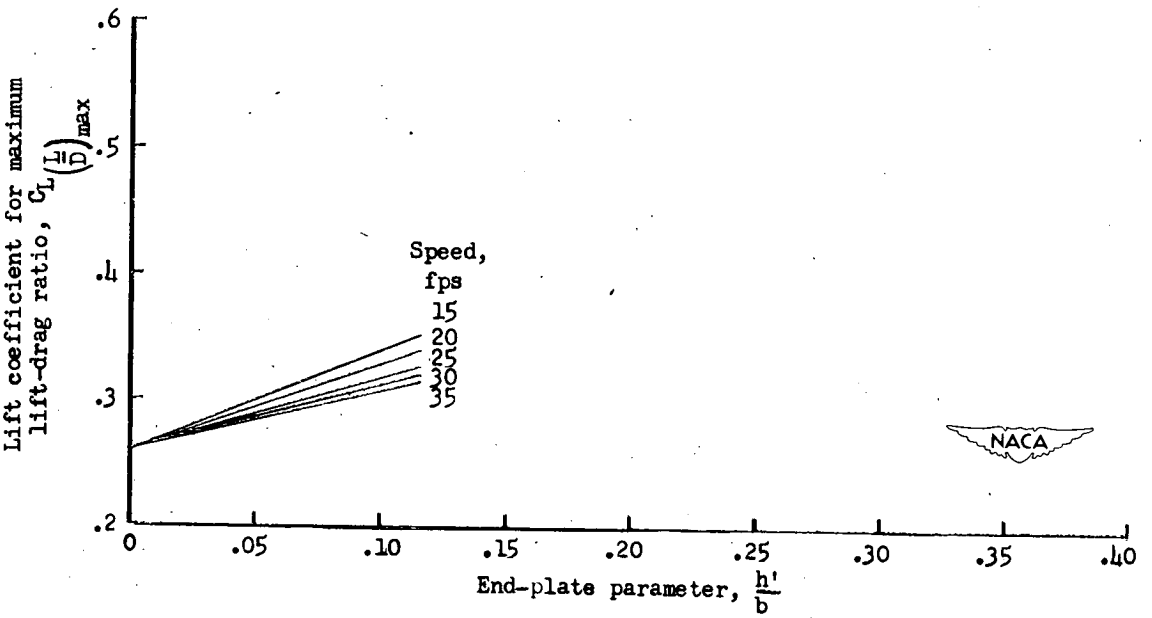

(b) Depth, 1.0 chord.

Figure 24.- Continued.

[redacted]

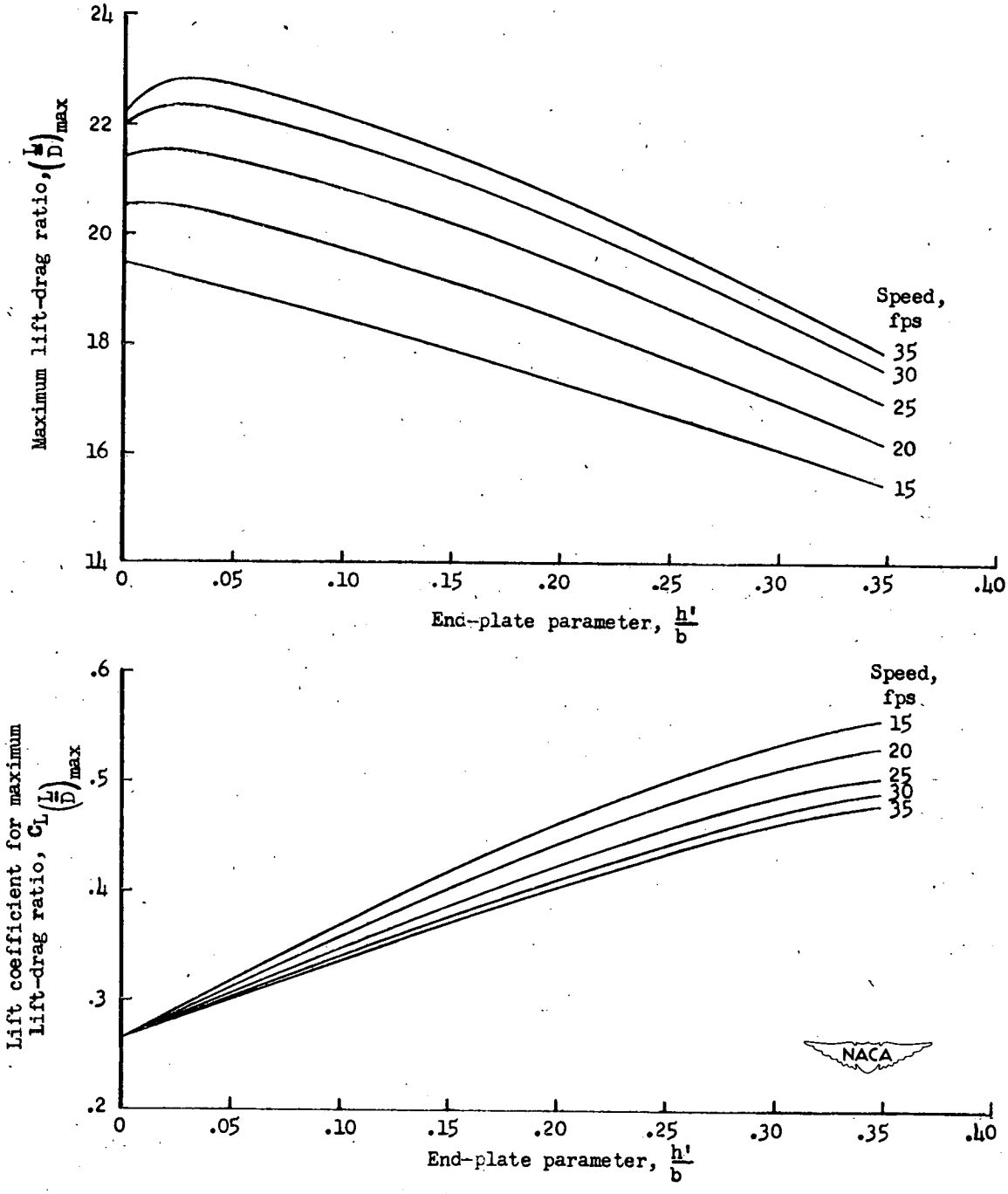

(c) Depth, 2.0 chords.

Figure 24.- Continued.

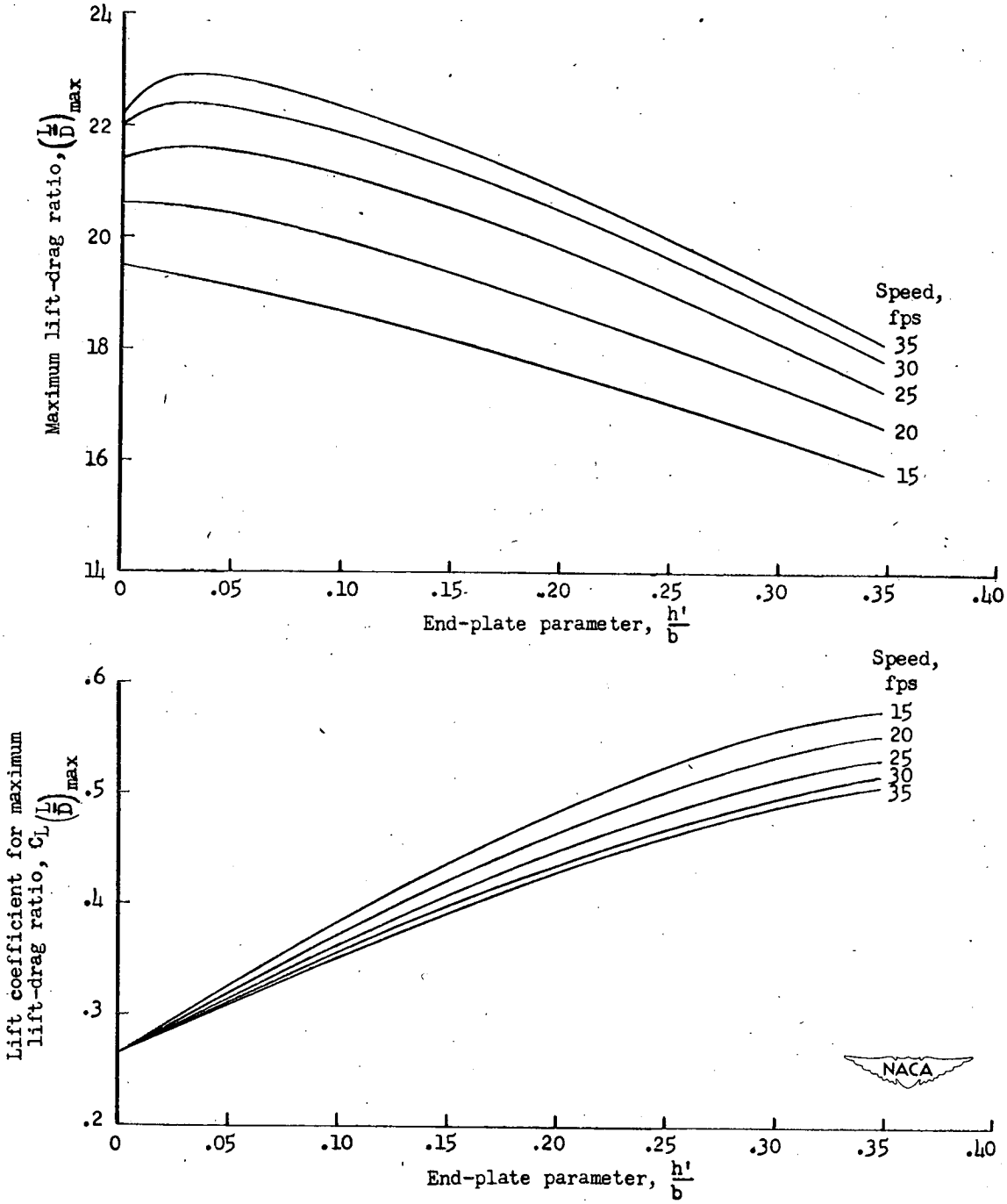

(d) Depth, 3.0 chords.

Figure 24.- Continued.

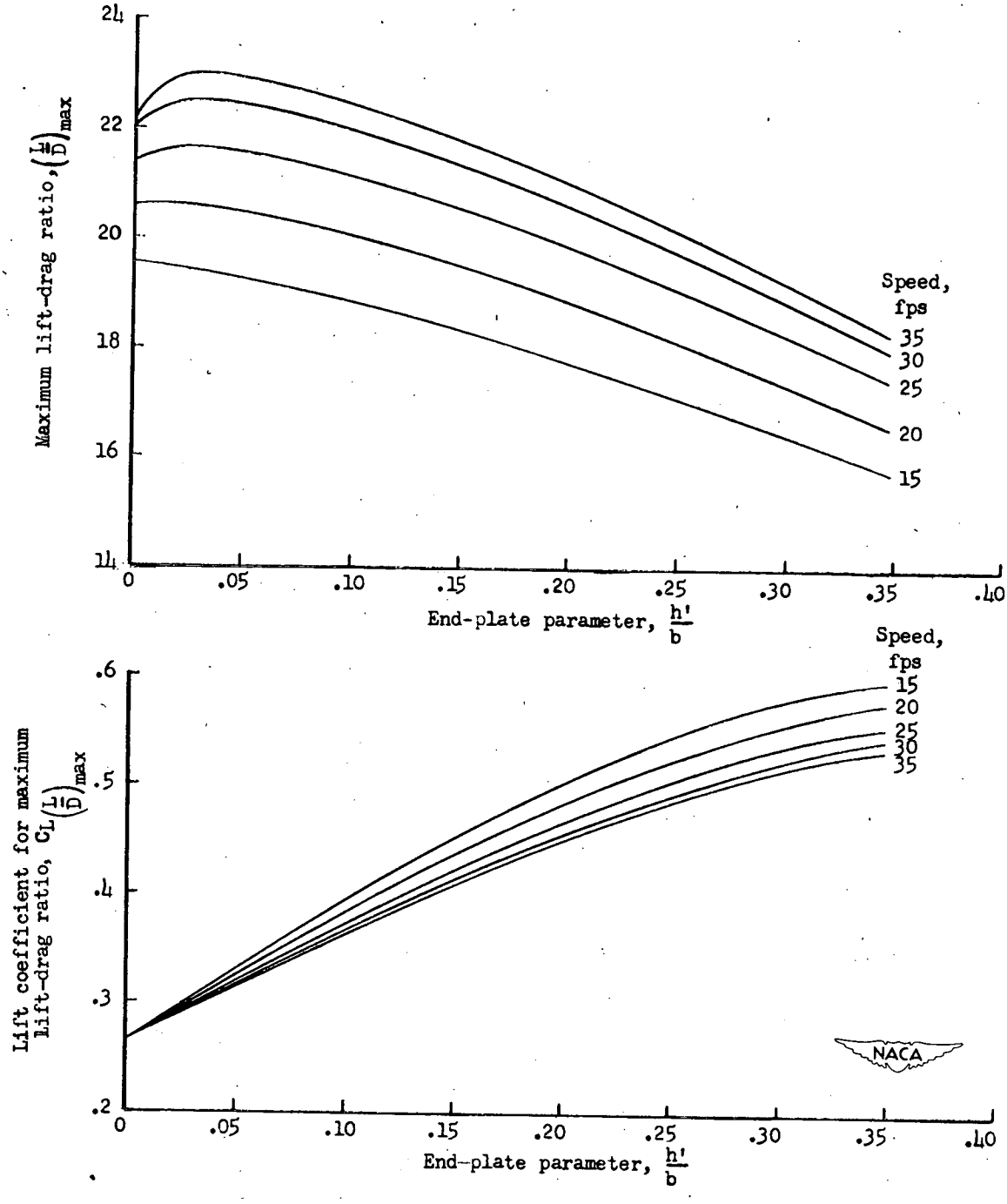

(e) Depth, 4.0 chords.

Figure 24.- Concluded.

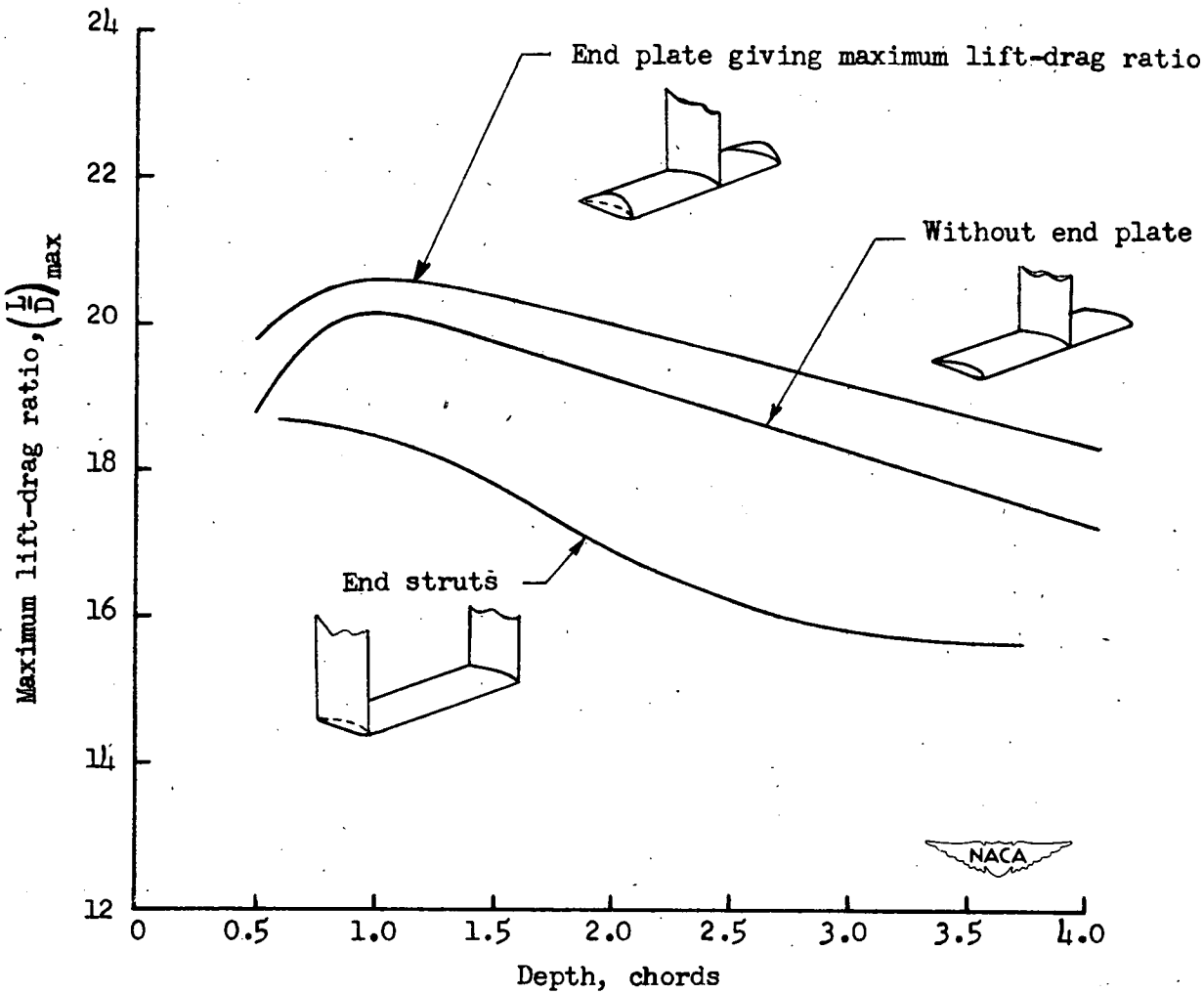

Figure 25.- Comparison of maximum lift-drag ratios. Speed, 35 feet per second.

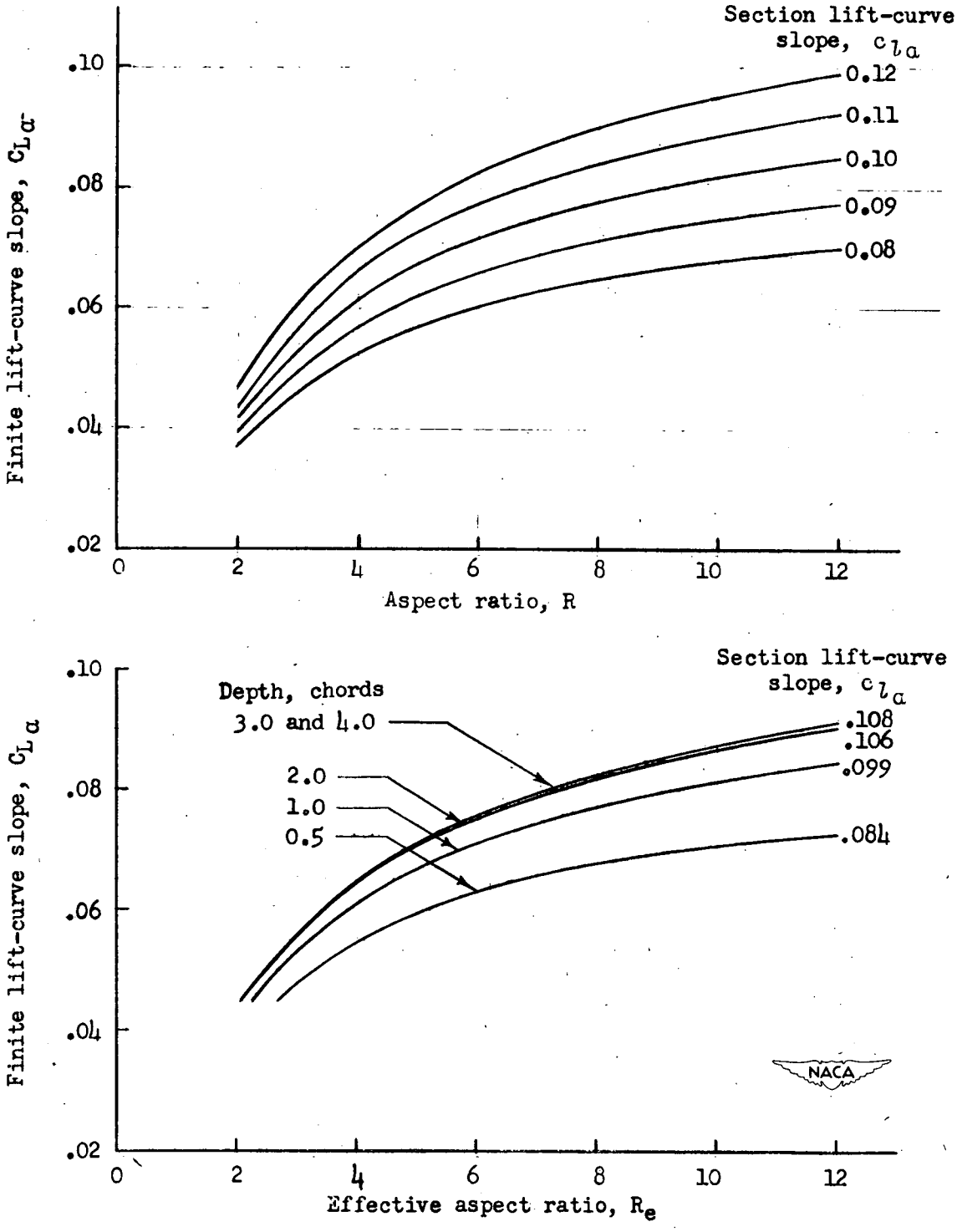

Figure 26.- Charts based on lifting-surface theory showing relation of lift-curve slope and aspect ratio.

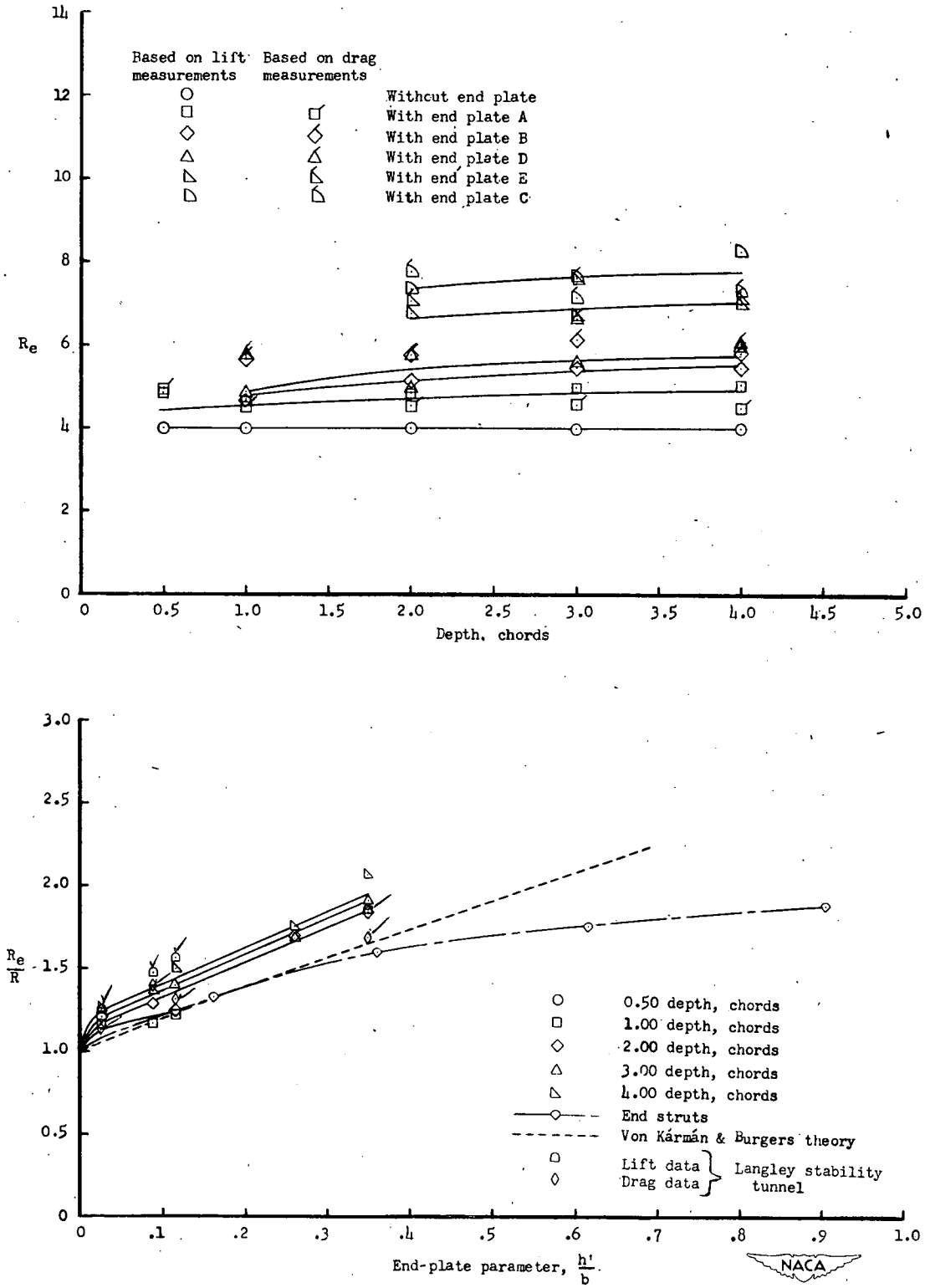

Figure 27.- Variation of effective aspect ratio with end-plate parameter h'/b and depth of submersion.

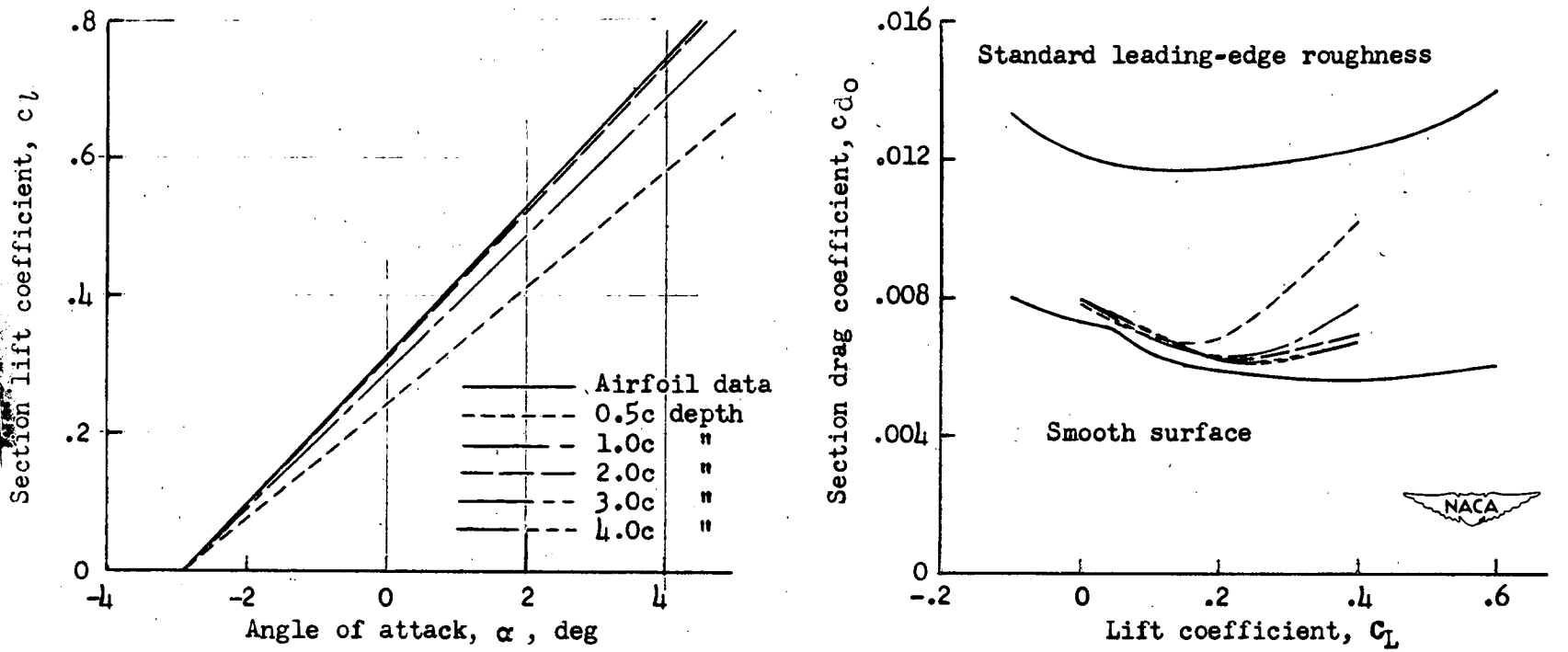

Figure 28.- Lift and drag characteristics of NACA 64_1A412 hydrofoil converted to infinite aspect ratio compared at a Reynolds number of 2.0×10^6 with aerodynamic data for the NACA 64_1-412 section.

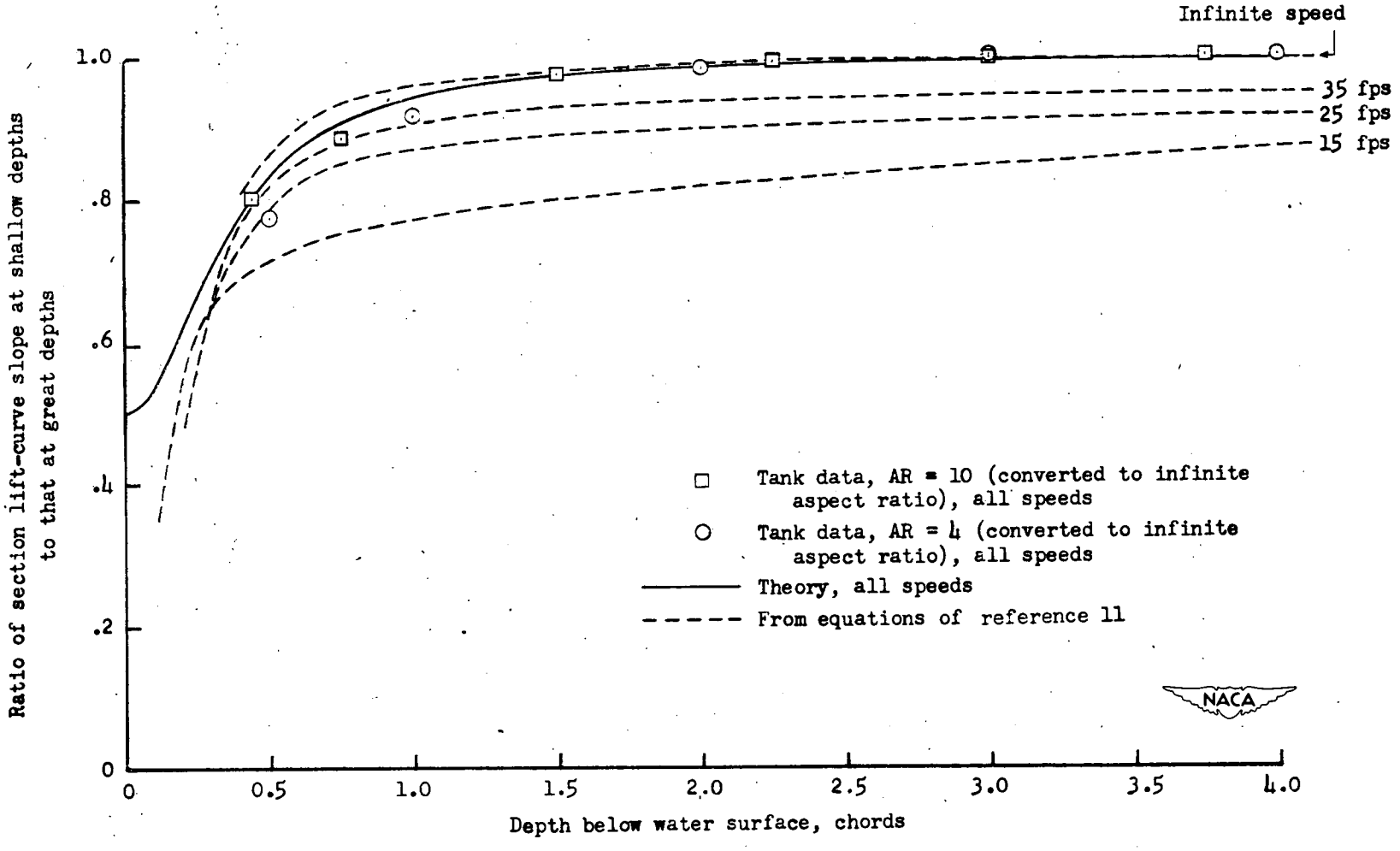

Figure 29.- Effect of depth on section lift-curve slope.